DOCTORAL THESIS

Mechanosynthesis of Hemicucurbiturils and Their Complexation: An Analytical Study

Tatsiana Jarg

Mechanosynthesis of Hemicucurbiturils and Their Complexation: An Analytical Study

TATSIANA JARG

TALLINN UNIVERSITY OF TECHNOLOGY
School of Science
Department of Chemistry and Biotechnology
This dissertation was accepted for the defence of the degree of Doctor of Philosophy in Chemistry on 19/09/2024

Supervisor: Prof. Riina Aav
                              Department of Chemistry and Biotechnology
                              Tallinn University of Technology
                              Tallinn, Estonia

Reviewed by: Assoc. Prof. Maria Kuhtinskaja
                              Department of Chemistry and Biotechnology
                              Tallinn University of Technology
                              Tallinn, Estonia

Opponents: Assist. Prof. Kaisa Helttunen
                              Department of Chemistry
                              University of Jyvaskyla
                              Jyväskylä, Finland

                              Prof. Ivo Leito
                              Institute of Chemistry
                              University of Tartu
                              Tartu, Estonia

Defence of the thesis: 17/10/2024, Tallinn

Declaration:
Hereby I declare that this doctoral thesis, my original investigation and achievement, submitted for the doctoral degree at Tallinn University of Technology has not been submitted for doctoral or equivalent academic degree.

Tatsiana Jarg

----
                                                                    signature

Jarg, T. (2024). *Mechanosynthesis of Hemicucurbiturils and Their Complexation: An Analytical Study* [TalTech Press]. https://doi.org/10.23658/taltech.57/2024

TALLINNA TEHNIKAÜLIKOOL
DOKTORITÖÖ
57/2024

Hemikukurbituriilide mehhanosünteesi ja nende komplekseerimise analüüs

TATSIANA JARG

Contents

List of Publications

The list of author's publications, on the basis of which the thesis has been prepared:

I   T. Dalidovich, K. A. Mishra, **T. Shalima**, M. Kudrjašova, D. G. Kananovich, R. Aav. Mechanochemical Synthesis of Amides with Uronium-Based Coupling Reagents: A Method for Hexa-amidation of Biotin[6]uril. *ACS Sustainable Chemistry & Engineering*, **2020**, 8, 41, 15703–15715.

II   **T. Shalima**, K. A. Mishra, S. Kaabel, L. Ustrnul, S. Bartkova, K. Tõnsuaadu, I. Heinmaa, R. Aav. Cyclohexanohemicucurbit[8]uril Inclusion Complexes with Heterocycles and Selective Extraction of Sulfur Compounds from Water. *Frontiers in Chemistry*, **2021**, 9:786746.

III E. Suut-Tuule[‡], **T. Jarg**[‡], P. Tikker, K.-M. Lootus, J. Martõnova, R. Reitalu, L. Ustrnul, J. S. Ward, V. Rjabovs, K. Shubin, J. V. Nallaparaju, M. Vendelin, S. Preis, M. Öeren, K. Rissanen, D. Kananovich, R. Aav. Mechanochemically Driven Covalent Self-Assembly of a Chiral Mono-Biotinylated Hemicucurbit[8]uril. *Cell Reports Physical Science*, **2024**, 5, 102161.

Note: [‡] – shared first authorship. The family name Shalima was changed to Jarg in 2022.

Author's Contribution to the Publications

Contributions to the papers in this thesis are:

I   The author was responsible for mass-spectrometric characterization of amidation products, chromatographic method development and analysis of the biotin[6]uril hexa-amidation reaction mixtures. The author participated in the compilation of supporting material and preparation of the manuscript.

II   The author was responsible for the solid-phase extraction and a part of solution- and solid-state binding studies. The author had a significant role in the compilation of the supporting material and preparation of the manuscript.

III The author was responsible for chromatographic and mass-spectrometric analysis during development of mono-biotinylated hemicucurbit[8]uril solid-state synthesis, mechanistic studies, anion binding in solution studies, immobilization of the macrocycle on silica material and its application in perchlorate removal experiments. The author had a significant role in the compilation of the supporting material and preparation of the manuscript.

Other Publications by the Author (Not Discussed in This Thesis)

1. J. Parve, M. Kudryašova, **T. Shalima**, L. Villo, I. Liblikas, I. Reile, T. Pehk, N. Gathergood, R. Aav, L. Vares, O. Parve. A Scalable Lipase-catalyzed Synthesis of (R)-4-(Acyloxy)pentanoic Acids from Racemic γ-Valerolactone. *ACS Sustain Chem Eng*, **2021**, 9 (4), 1494–1499.

2. A. Kooli, **T. Shalima**, E. Lopušanskaja, A. Paju, M. Lopp. Selective C-alkylation of substituted naphthols under non-aqueous conditions. *Tetrahedron*, **2021**, 95, 13227.

3. M. Sharma, S. Hussain, **T. Shalima**, R. Aav, R. Bhat. Valorization of Seabuckthorn Pomace to Obtain Bioactive Carotenoids: An Innovative Approach of Using Green Extraction Techniques (Ultrasonic and Microwave-Assisted Extractions) Synergized With Green Solvents (Edible Oils). *Ind Crops Prod*, **2022**, 175, 114257.

4. T. Dalidovich, J. V. Nallaparaju, **T. Shalima**, R. Aav, D. G. Kananovich. Mechanochemical Nucleophilic Substitution of Alcohols via Isouronium Intermediates. *ChemSusChem*, **2022**, 15 (3), e202102286.

5. K. Hunt, A. G. Sosa, **T. Shalima**, U. Maran, R. Vilu, T. Kanger. Synthesis of 6 '-galactosyllactose, a deviant human milk oligosaccharide, with the aid of Candida antarctica lipase-B. *RSC Org. Biomol. Chem.* , **2022**, 20, 4724–4735.

6. J. Parve, M. Kudryashova, **T. Shalima**, L. Villo, M. Ferschel, A. Niidu, I. Liblikas, I. Reile, R. Aav, N. Gathergood, L. Vares, T. Pehk, O. Parve. Stereoselective Synthesis of γ-(Acyloxy)Carboxylic Acids and γ-Lactones Features the Switch of Stereopreference of CalB Along Sodium γ-Hydroxycarboxylate Homologues. *EurJOC*, **2022**, 26 (3).

7. J. V. Nallaparaju, T. Nikonovich, **T. Jarg**, D. Merzhyievskyi, R. Aav, D. G. Kananovich. Mechanochemistry-Amended Barbier Reaction as Expedient Alternative to Grignard Synthesis. *Angew. Chem. Int. Ed.*, **2023**, 62 (39) e202305775.

8. S. Hussain, M. Sharma, **T. Jarg**, R. Aav, R. Bhat. Natural Pigments (Anthocyanins and Chlorophyll) and Antioxidants Profiling of European Red and Green Gooseberry (Ribes uva-crispa L.) Extracted Using Green Techniques (UAE-Citric Acid-Mediated Extraction). *CRFS*, **2023**, 366, 91–100.

9. A. Krech, V. Yakimchyk, **T. Jarg**, D. G. Kananovich, M. Ošeka. Ring-Opening Coupling Reaction of Cyclopropanols with Electrophilic Alkenes Enabled by Decatungstate as Photoredox Catalyst. *Adv. Synth. Catal.*, **2024**, 7, 100629.

10. M. Laktsevich-Iskryk, A. Krech, M. Fokin, M. Kimm, **T. Jarg**, T. Noël, M. Ošeka. Telescoped Synthesis of Vicinal Diamines via Ring-Opening of Electrochemically Generated Aziridines in Flow. *J. Flow Chem.*, **2024**, 14 (1) 139–147.

11. J. V. Nallaparaju, R. Saatsi, D. Merzhyievskyi, **T. Jarg**, R. Aav, D. G. Kananovich. Mechanochemical Birch Reduction with Low Reactive Alkaline Earth Metals. *Angew. Chem. Int. Ed.*, **2024**, 63, e202319449.

12. T. Nikonovich, **T. Jarg**, J. Martõnova, A. Kudrjašov, D. Merzhyievskyi, M. Kudrjašova, F. Gallou, R. Aav, D. G. Kananovich. Protecting-Group-Free Mechanosynthesis of Amides from Hydroxycarboxylic Acids: Application to the Synthesis of Imatinib. *RCS Mechanochem.*, **2024**, 1, 189.

Introduction

The lock-and-key principle formulated by Emil Fischer in 1894[1] states that selective molecular recognition and the subsequent reactions occur only on condition that the enzyme (the lock) and the substrate (the key) possess complementary geometries. This concept has profoundly influenced modern host-guest chemistry, which relies on the structural compatibility between substrates and receptors. The discovery of crown ethers and their complexes with alkali metals by Charles Pedersen in 1967[2] sparked interest in macrocycles as functional supramolecular hosts. Twenty years later, in 1987 Charles Pedersen along with Donald Cram and Jean-Marie Lehn were awarded a Noble Prize in Chemistry.[3] This topic has evolved further and has been recognized with another Nobel Prize in 2016 received by Jean-Pierre Sauvage, Fraser Stoddart and Bernard Feringa for design and synthesis of molecular machines.[4]

Up to date, certain families of macrocycles, such as cyclodextrins, calixarenes, and cucurbiturils, have received enormous attention and have been extensively studied by many research groups around the globe. Structural diversity makes macrocyclic cavitands perfect candidates for molecular recognition with applications in sensing,[5,6] drug delivery,[7–9] sequestration of toxins,[10] capture of pollutants,[11] etc. At the same time, synthetic versatility of macrocycles promotes design of their functionalized derivatives as well as novel receptor molecules with "custom" features, which allows to enhance supramolecular capabilities. For example, fine structural tuning can result in responsive macrocycles[12] bearing properties that can be switched on and off by external stimuli such as light, pH, redox, and provide controllable binding via changing parameters of the system.

Further research is essential for developing sustainable synthesis of macrocylic receptors and discovering new applications. This thesis advances the field by introducing analytical approaches to the mechanosynthesis of chiral hemicucurbiturils and conducting host-guest studies of the new cavitands. Mechanochemistry, a rapidly evolving environmentally friendly alternative to solution-based synthesis, utilizes mechanical energy to drive chemical transformations, thereby reducing or eliminating the need for bulk solvents. However, synthesizing complex molecules still demands significant effort to develop effective analytical tools for monitoring the processes occurring in these reactions.

This dissertation begins with an overview of the progress in hemicucurbituril chemistry, covering common synthetic strategies and methods for analyzing complex mixtures of macrocycles and intermediates both in solution and in the solid state. The applications of hemicucurbiturils are then discussed, with a focus on their anion-binding properties and ability to form complexes with neutral guests.

The results presented in this thesis encompass development of analytical methods using high-performance liquid chromatography coupled with mass spectrometry and their application in monitoring mechanosynthesis of hemicucurbiturils, as well as host-guest binding studies of the new host compounds. The developed procedures were employed to monitor solid-state formation of biotin[6]uril hexa-amide (**Publication I**) and mono-biotinylated hemicucurbit[8]uril (**Publication III**). The latter represented a particulary intriguing example of a macrocycle assembly from different building blocks, involving numerous intermediates, and thus posed significant challenges for both analysis and mechanistic understanding. Furthermore, the properties of hemicucurbit[8]uril receptors and their potential applications were explored through host-guest studies with

small neutral heterocycles (**Publication II**) and a number of anions (**Publication III**), including those found as environmental pollutants.

In addition to the publications discussed in the thesis, the results of this study have been presented at several international conferences in Estonia, Latvia, Lithuania, Portugal, Italy and Iceland.

Abbreviations

AJS-ESI	Agilent jet stream electrospray ionization
APCI-MS	atmospheric pressure chemical ionization mass spectrometry
APS	3-aminopropyl silica gel
ATD	arrival time distribution
Bio[*n*]	biotin[*n*]uril
BU[*n*]	bambus[*n*]uril
CB	cucurbituril
CD	cyclodextrin
CE	collision energy
CPMAS ssNMR	cross-polarization magic-angle spinning solid-state nuclear magnetic resonance
cycHC[*n*]	cyclohexanohemicucurbit[*n*]uril
DCC	dynamic covalent chemistry
DCL	dynamic covalent library
DMSO	dimethylsulfoxide
DS	degree of substitution
EIC	extracted ion chromatogram
ER-CID	energy-resolved collision induced dissociation
ESI-MS	electrospray ionization mass spectrometry
HC	hemicucurbituril
HC[*n*]	unsubstituted hemicucurbit[*n*]uril
HPLC	high-performance liquid chromatography
HRMS	high-resolution mass spectrometry
hybHC[*n*]	hybrid hemicucurbit[*n*]uril
IC	ion count
IMMS	ion-mobility mass spectrometry
IR	infrared
ITC	isothermal titration calorimetry
LAG	liquid-assisted grinding
LCD	lipidyl-cyclodextrin
LoD	limit of detection
LoQ	limit of quantitation
m/z	mass-to-charge
MALDI-TOF-MS	matrix-assisted laser desorption ionization time-of-flight mass spectrometry
mixHC[*n*]	mono-biotinylated hemicucurbit[*n*]uril
MS	mass spectrometry
NMR	nuclear magnetic resonance
PEG	3,6,9-trioxadecyl (polyethylene glycol)
RP-HPLC	reversed-phase high-performance liquid chromatography
RSD	relative standard deviation

SC-XRD	single-crystal X-ray diffraction
SIM	selected ion monitoring
TLC	thin layer chromatography
TPM	triphenylmethane
UV-Vis	ultraviolet-visible
v/v	volume per volume
w/w	weight per weight

1 Literature Overview

1.1 Evolution of Hemicucurbiturils and Their Derivatives

Single-bridged hemicucurbiturils (HCs)[13] appeared as a sub-class of the cucurbituril (CB) family renowned for its host-guest chemistry.[14] In contrast to the rigid double-stranded CBs, HCs exhibit far greater conformational flexibility and are typically defined by a hydrophobic, electron-deficient cavity and electron-rich portals. Over the last two decades HC group has significantly expanded (Figure 1) and is currently represented by unsubstituted hemicucurbit[n]urils (HC[n]) and their substituted derivatives, which include cyclohexanohemicucurbit[n]urils (cycHC[n]), bambus[n]urils (BU[n]), biotin[n]urils (Bio[n]), and hybrid (hybHC[n]). The continuous development of new HC-type cavitands is driven by functionalization of the macrocycle which allows to modulate their host properties, such as solubility, binding, chirality, etc.
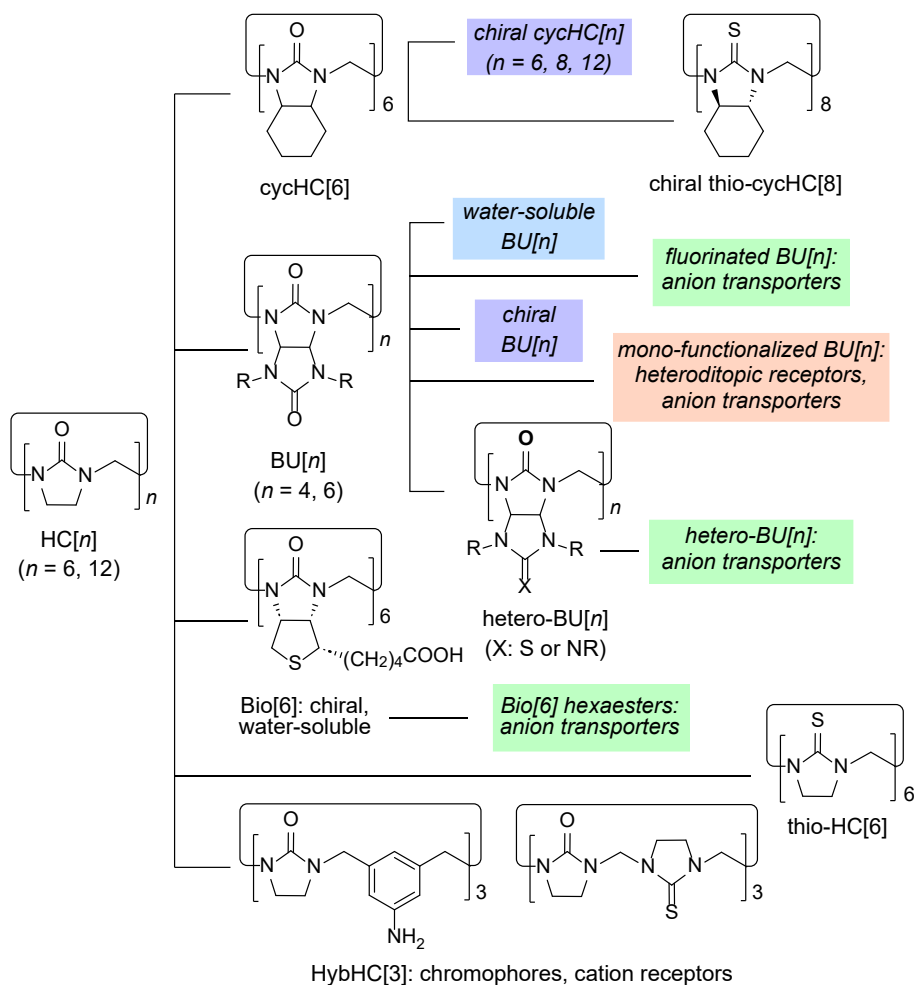

Figure 1. Overview of the trends in designing HC macrocyclic receptors.

1.1.1 Diverse Character of Hemicucurbiturils

The first HCs were discovered by Miyahara in 2004.[15] It was established, that condensation of ethyleneurea and formaldehyde in presence of HCl can be controlled by varying acid concentration and temperature, and result in either 6-membered HC[6] or twice larger HC[12]. The initial motivation for HCs synthesis was to obtain a novel receptor for binding metal cations realized through the cone orientation of carbonyl groups. However, single crystal X-ray diffraction (SC-XRD) analysis revealed a unique alternating conformation of the urea moieties[13,15] (Figure 2) which determines anion-binding properties of HCs.
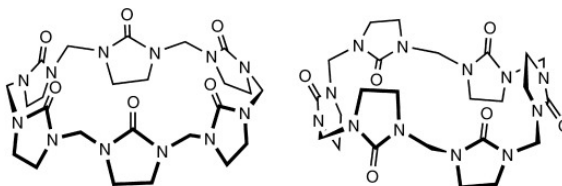

Figure 2. Expected cone (left) and confirmed alternate (right) conformations of urea monomers in HC[6]. Reprinted from ref. 15 with permission from John Wiley and Sons.

In 2024, Reany, Keinan and colleagues reported the synthesis of thio analogs of the unsubstituted HC[6].[16]

Cyclohexanohemicucurbit[n]urils

Condensation of ethyleneurea monomers bearing fused cyclohexane rings as bulky substituents was investigated by Wu and colleagues, who prepared the first substituted (*R,S*)-cycHC[6] in 2009.[17] The use of chiral (*S,S*)- and (*R,R*)-cyclohexaneurea monomers by Aav's group led to successful synthesis of (*S,S*)- and (*R,R*)-cycHC[6] (Figure 3), which became the first enantiomerically pure members of CB family in 2013.[18] Introduction of chirality into a macrocyclic receptor opens numerous possibilities for extended applications, such as enantiorecognition and chiral sensing. Modification of the ethylene urea with a norbornane ring in Šindelář's group in 2013 lead to formation of hexameric macrocycles.[19] Several years later another representative of 6-membered cyclohexane-substituted HC, the *inverted*-cycHC[6], was synthesized in Aav's group.[20]
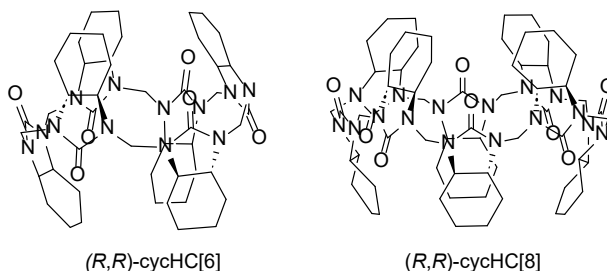

(*R,R*)-cycHC[6]   (*R,R*)-cycHC[8]

Figure 3. The structures of chiral cycHC[n] (n = 6, 8).

The search for higher homologs of (*R,R*)-cycHC[6] revealed the existence of larger cycHC[*n*] (*n* = 7–10) species, among which (*R,R*)-cycHC[8] was the most abundant side-product.[21] Deeper mechanistic studies of dynamic covalent chemistry (DCC) lead to

the efficient synthesis of cycHC[8],[22] which possesses a larger cavity compared to its hexameric homolog (Figure 3), thus being more appealing in terms of host-guest chemistry. Besides, even larger 12-membered macrocycle cycHC[12][23] was isolated, although in a very low 1% yield, impractical for further applications. In addition to being the first chiral HCs, cycHC[n] are also the first example of HCs prepared both in solution and in the solid state (Figure 3).[24]

Very recently, Reany, Keinan and co-workers reported the mechanosynthesis of cycHC[8] thio-analog prone to conformational adaptation upon binding anions.[16] Compared to the oxo-cycHC[8], thio-cycHC[8] proved to have higher association constants when encapsulating anionic guests due to the higher polarizability of thiourea.

Bambus[n]urils

BU[n] are a subclass of HCs first described by Šindelář and co-workers in 2010.[25] These macrocycles consist of glycoluril monomers with one urea moiety di-substituted with alkyl groups, linked by methylene bridges through the other urea. Hexameric methyl-substituted $Me_{12}BU[6]$ became the first representative of this subclass. Further, the scope of BU[n] macrocycles was expanded by replacing methyl substituents with propyl and benzyl groups, affording $Pro_mBU[n]$ and $Ben_mBU[n]$ (m = 2n, n = 4, 6).[26]

Next, Šindelář's group focused on development of water-soluble receptors, applicable for detection of anionic pollutants and anion transport in biological processes. The type of substituents on the macrocycle portals greatly affects receptor solubility and binding properties, which was demonstrated in the synthesis of water-soluble BU[n] decorated with 4-carboxybenzyl,[27] carboxyalkyl,[28] amino,[29] and 3,6,9-trioxadecyl (PEG)[30] groups.

Another milestone was the preparation of fluorinated BU[6]s in 2019, which act as efficient transmembrane anion transporters.[31] Notably, the presence of electron-withdrawing groups on the benzene substituents allows to fine-tune the binding properties of the receptor via the inductive effect.[32]

Selective mono-functionalization of the $Ben_{12}BU[6]$ scaffold resulted in versatile macrocycles bearing one carboxylic group suitable for further derivatization (Figure 4). Subsequent amide coupling with crown ethers delivered heteroditopic receptors merging the anion- and cation-binding properties of the two cavitands.[33,34] Remarkably, the efficiency of liquid-liquid extraction of alkali halides by the new conjugates significantly surpassed the performance of the equivalent mixture of BU[6] and crown ether, implying a cooperative effect in the binding of ion pairs.
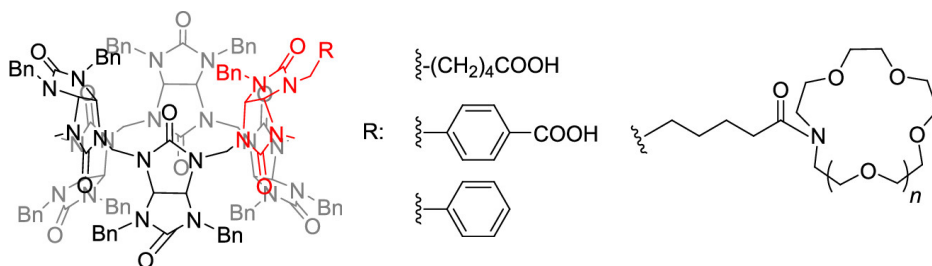

Figure 4. The structures of mono-functionalized BU[6]. Adapted from ref. 33 with permission from the American Chemical Society.

Decoration of BU[6] with chiral substituents provided cavitands suitable for enantiorecognition of chiral carboxylates.[35,36] More examples of enantiomerically pure BU[n] include orthogonally protected BU[n] which can be modified by various chiral

motifs,[37] and a mono-functionalized macrocycle prepared from the mixture of D-biotin and glycoluril urea monomers.[38]

Thio-analogs of BU[n], duo-functional semithio-bambus[n]urils (semithio-BU[n], n = 4, 6), were developed by Reany, Keinan, and colleagues in 2014.[39] Shortly after, the same group introduced semiaza-bambus[n]urils (semiazaBU[n], n = 4, 6).[40] Incorporation of sulfur atoms resulted in HCs suitable for encapsulation of anions as well as binding metal cations at their sulfur-edged portals. Lipophilic semithio-BU[6] and semiaza-BU[6] proved to act as efficient transmembrane chloride transporters.[41,42]

Biotin[n]urils

The similarity of naturally occurring biotin to the urea monomers previously used in preparation of HC[n] inspired Pittelkow and co-workers to study its macrocyclization with formaldehyde. In 2014 they described the synthesis of the first water-soluble HC – Bio[6].[43] The use of biotin provided chiral centers in the macrocycle and carboxylic acid functionalities, which granted solubility in polar solvents and could be used for further derivatization (Figure 5).
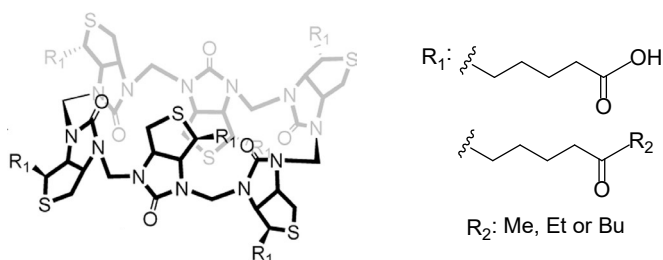

Figure 5. The structures of Bio[6] and corresponding alkyl ester derivatives. Adapted from ref. 44 with permission from the American Chemical Society.

Methyl-, ethyl- and butyl-esterification of Bio[6] produced a number of hydrophobic receptors capable of selective transmembrane transport of Cl⁻.[44] In addition, Pittelkow's group demonstrated that Bio[6] can be diastereoselectively oxidized in the sulfur position with a consequent effect on anion recognition properties of biotin-L-sulfoxide[n]urils and corresponding esters.[45]

Hybrid Hemicucurbit[n]urils

The scope of HC application can be expanded by introducing chromophores and functional groups suitable for derivatization. In 2014 Keinan, Pappo and co-workers described the synthesis of macrocycles composed of alternating thiourea monomer and phenol derivative, which they named multifarenes.[46] In 2019 Šindelář's team attempted to incorporate xylylene fragments into macrocyclic framework, producing BU[n] hybrid analogs based on alternating glycoluril and aromatic rings.[47] Alas, the major isolated product consisting of two repeating units was too small to accommodate anions. Liu and colleagues followed the fragment coupling strategy, previously used in multifarene preparation, to assemble macrocycles from urea monomers substituted with benzene derivatives. In 2021 they presented a new amino-benzene containing hybHC (Figure 1), suitable for binding metal cations.[48] Insertion of aromatic rings improved the optical properties of the macrocycle, and amino groups can participate in complex formation via coordination and hydrogen bonds, as well as be utilized for further modification.[49]

Combination of glycoluril, ethyleneurea, and aromatic group resulted in a photoresponsive multi-hybHC[6], also applicable for complexation with metal cations.[50]

The same coupling method was applied in the synthesis of thio-hybHC[6]s in 2022.[51] Liu's group were the first to use commercially available ethylene thiourea to prepare HC, however, the attempts to obtain all-thio-hybHC[6] were unsuccessful both via condensation of the monomers and fragment coupling. Nevertheless, the latter approach allowed the construction of macrocycles containing up to 3 thio-motifs.

1.1.2 Synthetic Approaches to Hemicucurbiturils

The two most common strategies toward the synthesis of HCs include their assembly from starting monomers and post-modification of the existing macrocyclic framework.

Typically, HCs are prepared via acid-catalyzed condensation of *N,N'*-dialkylurea monomers with formaldehyde[13] following the principles of DCC.[52] The building blocks react with each other using reversable reactions to produce a mixture of oligomers – dynamic covalent library (DCL) (Figure 6). In the presence of acid, protonation of the urea nitrogen initiates the attack on the electrophilic carbon of the formaldehyde, leading to the elimination of water and creation of a reactive iminium intermediate. The latter swiftly reacts with a nitrogen atom of another available monomer, resulting in the formation of an acylaminal linkage after deprotonation. Continuous formation of such methylene bridges produces linear oligomers, but the process is reversible due to the hydrolysis of the acylaminal linkage in acidic medium. Consequently, instead of the infinite chain growth a rich DCL of various oligomerization products is formed. The presence of diverse HC intermediates was evidenced by Pittelkow's[43] and Aav's[22,24] groups during analysis of reaction mixture composition.
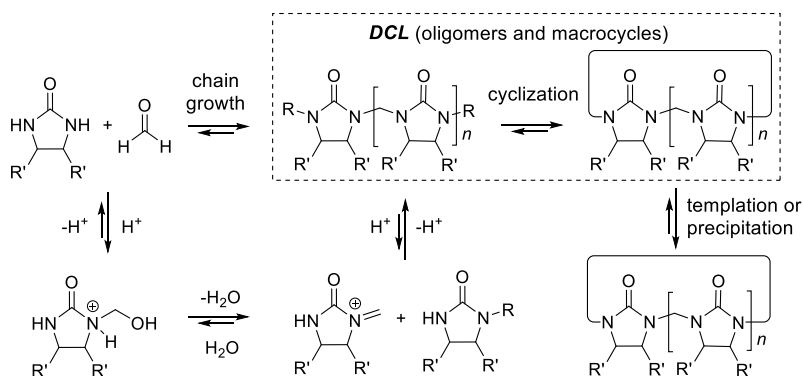
Figure 6. Formation of oligomers and macrocycles via dynamic reversible acylaminal linkages between urea monomers.

The equilibrium between chain growth, cyclization and stabilization of the macrocyclic product can be efficiently controlled by kinetic or thermodynamic parameters.[52] Macrocycle assembly requires optimal preorganization of the linear oligomers and efficient ring closure, and is therefore extremely sensitive to external stimuli, such as the amount and nature of the acid, concentration of the reagents, temperature and presence of template. The combination of favourable conditions allows to shift the chain-cycle equilibrium towards the formation of products, and anion templation proved to be an efficient tool in the synthesis of various receptors.[13,53,54] In addition to conventional

synthesis in solution, HCs can be assembled in the solid state via mechanochemistry[16,24] according to the same DCC principles.

Development of new macrocycles using post-modification approach has been exemplified by BU[n] amide coupling with crown ethers and other moieties,[33,34] alkylation of the orthogonally protected BU[n],[37] synthesis of semiaza-BU[6] from semithio-BU[6],[40] and Bio[6] esterification and oxidation.[44,45] Derivatization of the macrocycles requires the presence of functional groups that would allow for further modifications, however, the embedded substituents may also hamper macrocyclization and considerably influence the solubility and binding properties of the receptor. Although post-functionalization is an attractive approach in design of new macrocyclic receptors, it might be challenging to perform and result in a mixture of fully- and underfunctionalized products.

1.2 Analysis of Hemicucurbituril Formation in Solution and Solid State

Traditionally, thin layer chromatography (TLC) and nuclear magnetic resonance (NMR) spectroscopy are the most common tools utilized in a synthetic laboratory for analysis of reaction mixtures. TLC is a rapid routine technique used to separate the crude mixtures and monitor the reaction progress, however, it has limited resolution and sensitivity. NMR, on the other hand, is a powerful method able to provide detailed structural characterization of the sample as well as quantify the organic components of the probe. Yet, its application is severely restricted in case of complex mixtures which result in poor resolution of the signals. In these instances, alternative approaches, such as chromatographic separation methods, are required to obtain reliable data. Transition from solution-based synthesis of macrocycles to mechanochemistry is accompanied by additional complications for analysis, which is discussed in chapter 1.2.2 in more detail.

1.2.1 Separation and Identification of Hemicucurbiturils and Intermediates from Solution-Based Synthesis

Ever since the first attempts to synthesize HCs, there has been an urge for separation of products during analysis of crude reaction mixtures. The formation of HC[6] and HC[12] was observed with the aid of gel permeation chromatography with refractometry detection (Figure 7), followed by electrospray ionization mass spectrometry (ESI-MS) identification.[15]
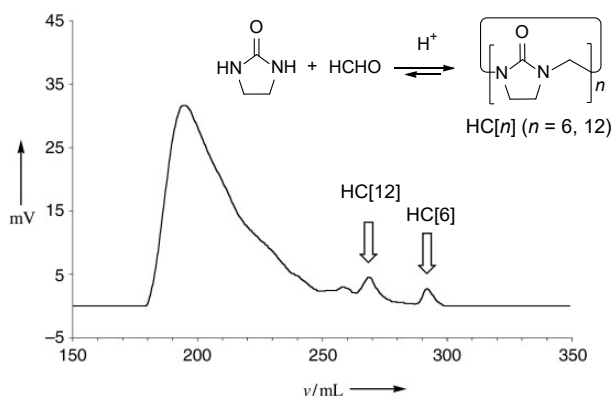

Figure 7. Chromatogram of the HC[n] crude reaction mixture. Adapted from ref. 15 with permission from John Wiley and Sons.

Identifying analytes in novel reactions is often a daunting task. To overcome this challenge, coupling various analytical techniques, such as high-performance liquid chromatography (HPLC) and mass spectrometry (MS), offers a powerful solution that significantly enhances the effectiveness of the analysis. HPLC-MS was employed by Pittelkow and co-workers to monitor the synthesis of Bio[6] and corresponding esters,[43,44] as well as to estimate diastereoselectivity during Bio[6] oxidation.[45] Due to the presence of carboxylic groups, Bio[6] and its intermediates are water-soluble and therefore well compatible with reversed-phase liquid chromatography (RP-HPLC). The chromatographic separation of the Bio[6] crude mixtures was performed on Dionex Acclaim RSLC 120 C18 (100 × 2.1 mm, 2.2 µm) column using 0.1% formic acid in water and 0.1% formic acid in acetonitrile under gradient elution. The signals were followed by UV-Vis diode array detector at 209 nm and ESI-MS. Calibration curves obtained for biotin, dimer and hexamer (Bio[6]) revealed that the UV response is directly proportional to the number of monomeric units in the analyte, which was further used in the quantitative analysis of oligomers at different stages of Bio[6] formation (Figure 8). The collected data provided a mechanistic insight: based on the changes in the oligomeric content it was suggested, that the macrocycle formation is likely to proceed via condensation of three dimers.[43]
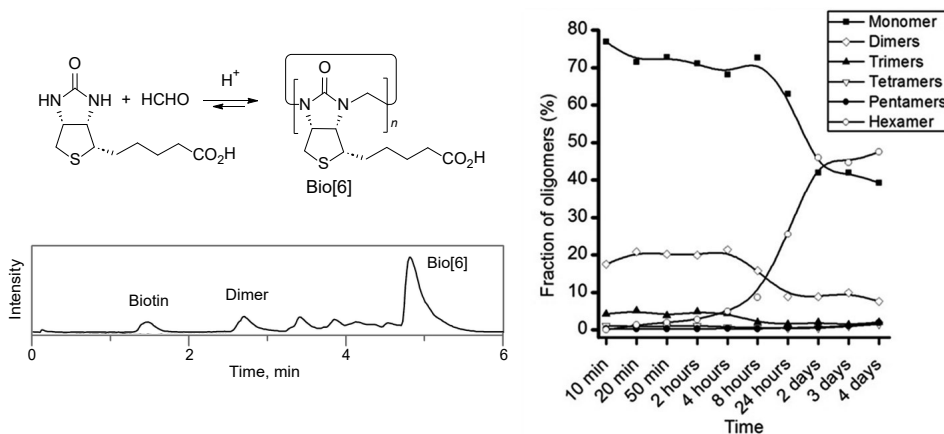

Figure 8. Quantitative analysis of oligomers during Bio[6] synthesis (note: hexamer = macrocycle). Adapted from ref. 43 with permission from the Royal Chemical Society.

Successful separation of the analytes allows to observe even trace levels of by-products, which may boost a whole new direction for research. The latter was the case in Aav's group during HPLC-MS analysis of (*R*,*R*)-cycHC[6] crude reaction mixture, which revealed the new homologs[21] and encouraged template-controlled selective synthesis of larger macrocycles.[22,23] Despite low solubility of cycHC[*n*] in water and acetonitrile, it was demonstrated that their solutions containing chlorinated solvent were compatible with RP-HPLC without risks of precipitation. A quantitative procedure was developed and successfully applied for analysis of cycHC[*n*] and HC[*n*] homologs and diastereomers.[55] Chromatographic separation was performed on Kinetex C18 column (2.1 × 100 mm, 2.6 µm) using water : acetonitrile and water with 0.1% trifluoracetic acid : acetonitrile as mobile phase in a gradient mode and monitoring the signals by UV and MS detectors. In contrast to Pittelkow's results for Bio[6],[43] UV absorbance of cycHC[*n*] macrocycles and oligomers did not correlate with the number of monomeric units,

therefore, each analyte required an individual calibration curve for quantitation. The proposed methodology was used for analysis of cycHC[*n*] crude mixtures (Figure 9) and HC[*n*] stability studies.
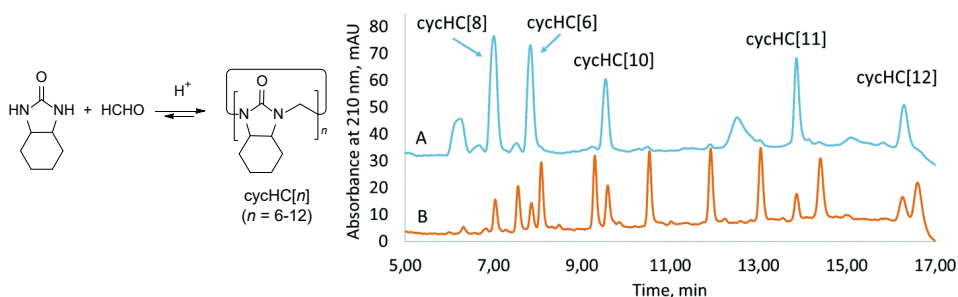

Figure 9. HPLC-UV chromatograms of cycHC[n] crude mixture (A) and isolated oligomers (B). Adapted from ref. 55 with permission from the Royal Chemical Society.

Šindelář's group used HPLC-MS to study the BU[*n*] analogs containing glycoluril and aromatic units. The crude mixture was purified using preparative RP-HPLC, and the main fraction was analyzed employing Gemini NX-C18 (4.6 × 100 mm, 3 µm) column and water : methanol mobile phase used in a gradient mode. The analytes were detected by atmospheric pressure chemical ionization mass spectrometry (APCI-MS) operated in scan mode.[47] Extracted ion chromatogram (EIC) showed two closely eluted peaks corresponding to [M+H]$^+$ of the 2-membered product, assigned as the diastereomers, accompanied by several peaks identified as protonated 3- and 4-membered by-products. In addition, prior to purification the crude mixture was characterized by matrix-assisted laser desorption ionization time-of-flight mass spectrometry (MALDI-TOF-MS), which revealed the presence of 2- to 5-membered products.[47] Developing chromatographic methods is often a complex and time-intensive process. However, when chromatographic separation is not feasible, MS alone can still yield crucial insights into the sample's composition, offering a valuable alternative for analysis. Šindelář and colleagues have extensively utilized MALDI-TOF-MS for analysis of reaction mixtures. Thus, MALDI-TOF-MS analysis of norHC[6] allowed to detect traces of norHC[*n*] homologs (*n* = 4, 5, 7, 8).[19] The same technique was applied for challenging crude mixtures of mono-functionalized BU[*n*][33,34,38] to confirm the formation of the target macrocycle and observe the by-products. Selective mono-functionalization via statistically driven condensation is extremely difficult due to formation of di- and tri-substituted side-products, which Šindelář and co-workers attempted to minimize by using excessive amount of non-modified glycoluril monomers.[33,34] The latest work, however, demonstrated that condensation between biotin and 2,4-dibenzylglycouril results in just two products – mono-functionalized macrocycle and homomeric Bn$_{12}$BU[6], even when the monomers are taken in 1:5 stoichiometric ratio. Another synthetic challenge was related to biotin oxidation in some reactions, which was also discovered with the aid of MALDI-TOF-MS.[38]

1.2.2 Analysis of Mechanochemical Reactions

Mechanochemistry has gained recognition as a technique for organic synthesis, which allows solvent-free reactions between solids by direct absorption of mechanical energy.[56,57] In contrast to the earliest solid-state reactions performed by primitive manual grinding of the reactants in a mortar with a pestle,[58] modern mechanosynthesis

utilizes various ball mills and twin-screw extruders, which allows to shorten reaction time considerably. Mechanochemical reactions proceed under neat or solvent-assisted conditions, where minute amounts of liquid is added to accelerate or enable chemical transformations. The amount of solvent used in liquid-assisted grinding (LAG) is expressed as liquid-to-solid ratio η (μl/mg),[59] and typically does not exceed 2 μl/mg.[57] Compared to traditional solution-based synthesis, mechanochemistry is considered more sustainable and offers several important benefits, such as avoiding bulk solvents, mild conditions, simple set-up, reduced reaction times and enhanced selectivity.

Mechanochemistry has been utilized in the synthesis of different macrocycles, including construction of the macrocyclic core[16,24,60–64] and various derivatizations.[65–67] Analysis of solid-state reaction mixtures can be executed using two approaches: *in situ* monitoring and *ex situ* measurements[68,69] (Figure 10).

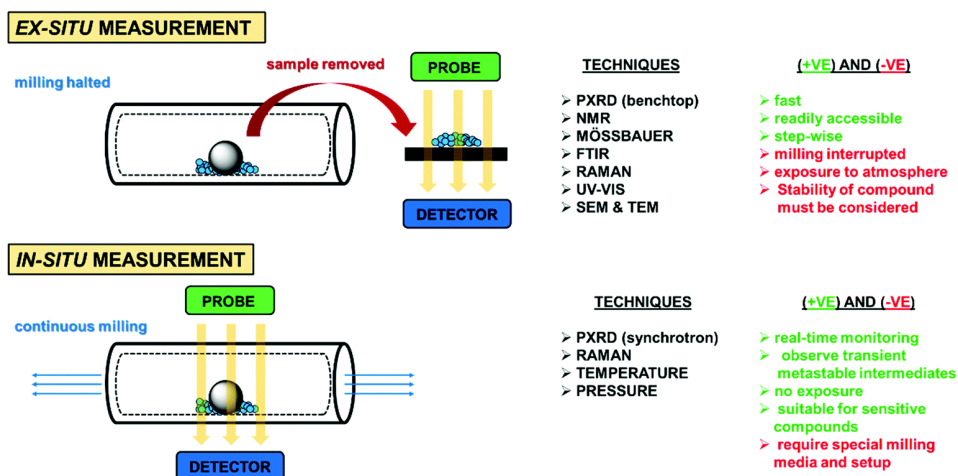*Figure 10. Comparison of in situ and ex situ characterization techniques for mechanochemical reactions. Reproduced from ref. 68 with permission from the Royal Chemical Society.*

Nowadays the most advanced techniques based on powder X-ray diffraction,[70] Raman,[71] X-ray absorption[72] and solid-state NMR[73] spectroscopies allow real-time *in situ* monitoring of reactions during milling, providing fundamental information on the mechanochemical transformations and kinetics. However, the application of these methods is limited as special equipment is required. Traditional *ex situ* analysis can be performed using any appropriate method, including widely implemented spectroscopic instruments (NMR, IR, UV-Vis), as well as chromatographic techniques coupled with various detectors. The limitations of *ex situ* methods are related to the forced interruption of the milling process and exposure of the reaction mixture to the atmosphere, besides, the stability of the compounds must be considered.

A key distinction between mechanochemical and solution-based synthesis lies in the homogeneity of reaction mixtures. In solution chemistry mass transfer is rarely a problem, as it can be efficiently handled by stirring. On the other hand, in ball-milled reactions this can be a difficult variable to control[56] and may have a dramatic effect on the reaction outcome, as well as analysis of the crude mixtures due to their inhomogeneity. The latter raises serious concerns during analysis of mechanochemical reactions. Even *in situ* techniques, which allow real-time monitoring, are to a certain

extent limited by specific region of the reaction vessel exposed to radiation,[74] while the homogeneous state can be attained at different rates. The same problem is expected during sampling for *ex situ* analysis, as the probe must sufficiently represent the composition of the whole mixture. In addition, the possibility of moisture absorption and evaporation of volatile components must be considered.

1.2.3 Determination of Macrocycles and Intermediates in Mechanosynthesis

Up to date, mechanochemical synthesis of macrocycles was investigated predominantly using *ex situ* analytical techniques. The choice of particular method depends on the specific reaction, composition of the crude mixture, properties of the compounds and the purpose of analysis. Whereas the formation of macrocyclic products can be characterized by NMR spectroscopy,[16,24,60] other analytical methods may serve as a feasible alternatives or complementary techniques, as showcased by several research groups.

Macrocycles containing highly conjugated π-π systems, such as porphyrins and phtalocyanines, are known for their characteristic and prominent UV-Vis absorption. Thus, UV-Vis spectrophotometry was applied by Hamilton's group to determine yields during solvent-free synthesis of porphyrins,[61] and Anaya-Plaza, Kaabel and co-workers used it in the kinetic studies of mechanochemical preparation of phtalocyanine (Figure 11).[64] In both cases, quantitation was based on calibration graphs following Lambert-Beer law.
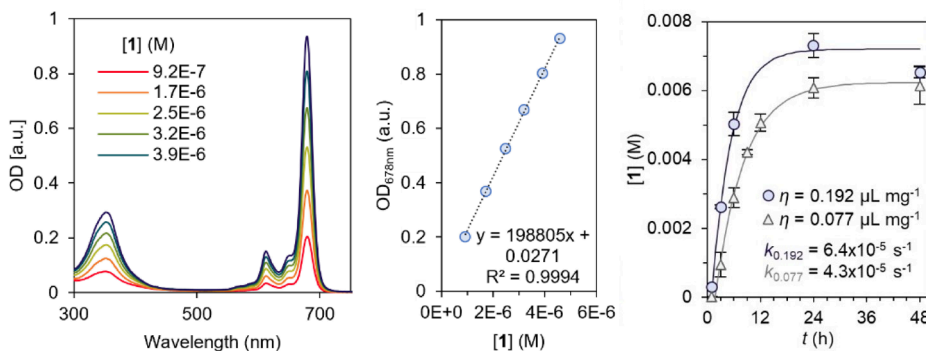
Figure 11. Phtalocyanine UV-Vis spectra and calibration graph used in the kinetic studies. Reprinted from ref. 65 with permission from John Wiley and Sons.

Solvent-free insertion of metals in porphyrin scaffold increases molecular symmetry and causes simplification of the Q-bands region in their UV-Vis absorption spectra. Such subtle changes are not sufficient to use UV-Vis spectrophotometry alone to distinguish between metallated products and free-base porphyrins,[65,75] and similar problem may arise when studying porphyrin degradation. Bruckner and co-workers attempted to use UV-Vis detection combined with HPLC to investigate porphyrin stability under grinding conditions.[66] They employed normal phase HPLC with hexane : ethylacetate mobile phase in gradient elution mode; unfortunately, the acquired data only confirmed the decrease of porphyrin concentration, and no peaks of side products were observed on the chromatograms.

Chromatography is undoubtedly an advantageous technique for analysis of complex mixtures. Derivatization of macrocycles bearing several functional groups is likely to result in a mixture of products with different degree of substitution (DS). Generally, when

a reaction proceeds via formation of multiple intermediates or by-products, separation methods are preferential for analysis as they allow reliable discrimination of the probe components. A perfect example of challenging analysis of milled mixtures was described by Djedaini-Pilard and co-workers in their work on mechanosynthesis of lipidyl-cyclodextrins (LCDs).[76] ESI-MS analysis revealed products with DS ranging from 1 to 3. Besides, methyl oleate epoxide ring opening in the presence of cyclodextrins (CDs) proceeds via formation of regio- and stereoisomers involving CD hydroxyl groups 2, 3 and 6, and epoxide carbons 9 and 10 (Figure 12), therefore the crude mixtures had a considerably more complex composition, which was elucidated with the aid of ultra-performance liquid chromatography coupled with MS. The chromatograms of mono-substituted LCDs contained 12 peaks (Figure 12) corresponding to 12 isomers that can be formed during the epoxide opening reaction. In case of di- and tri-substituted LCDs the number of possible isomers dramatically increased, resulting in multiple poorly resolved peaks.
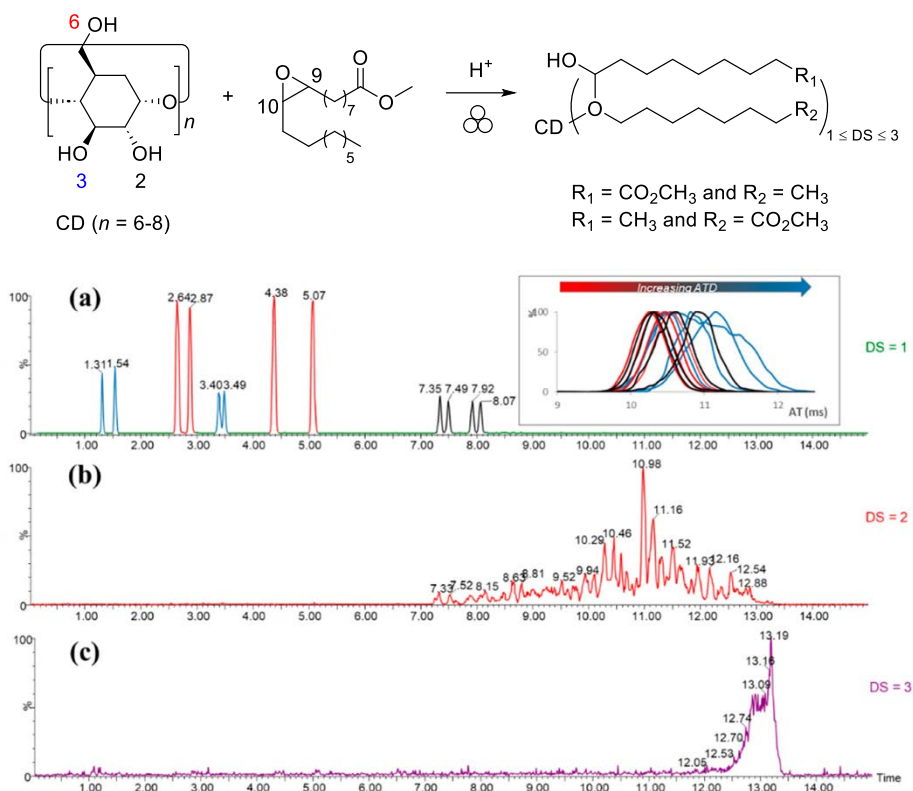
Figure 12. EICs of LCDs with DS ranging from 1 to 3 (a-c). Adapted from ref. 76 with permission from Multidisciplinary Digital Publishing Institute.

Based on the differences in the abundance of the fragments obtained during MS/MS, the 12 peaks of mono-substituted LCD were sorted into 3 groups corresponding to different regioisomers. Further structural characterization was performed using ion-mobility MS (IMMS), which enables separation of ions in the gas phase according to their size, shape and charge. The arrival time distribution (ATD) of the ions passing the mobility cell can be correlated to their collision cross section, which characterizes the

surface of interaction between the ion and the gas molecules in the mobility cell, and can be both measured experimentally and calculated for the proposed model. According to the combined results of MS/MS and IMMS analyses, the peaks of the mono-substituted LCD isomers were grouped based on the position of derivatized hydroxyl group (Figure 12).

The templated solid-state synthesis of cycHC[n] (n = 6, 8)[24] by Aav, Friscic and colleagues was studied by several methods. The conversion of monomers into cycHC[n] during aging was followed *in situ* by ^{13}C cross-polarization magic-angle spinning solid state NMR (CPMAS ssNMR) spectroscopy (Figure 13), which selectively detected the signals of the rigid macrocycles without an overlap with the dynamic linear intermediates.
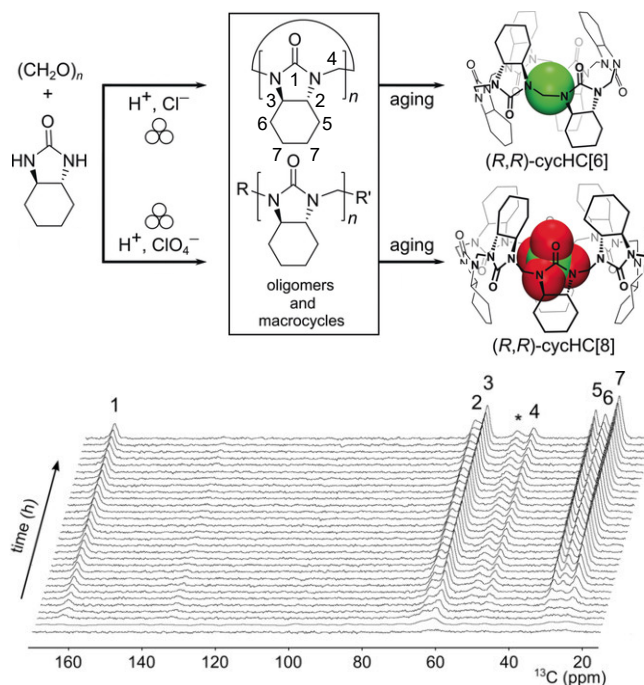
Figure 13. General scheme of cycHC[n] solid state synthesis and real-time monitoring of the reaction progress during aging by ^{13}C CPMAS ssNMR. Adapted from ref. 24 with permission from John Wiley and Sons.

A more detailed description of the crude mixture composition was attained by chromatographic analysis coupled with ESI-MS, which allowed for determination of oligomers (Figure 14). The reported HPLC-MS procedure was also recently applied by Reany, Keinan and co-workers in characterization of crude mixtures during mechanosynthesis of thio-cycHC[n].[16] The oligomers were identified based on the *m/z* values of their [M+Na]+ adducts, and varied by the chain length (2 to 15 monomeric units) and the type of terminal groups resulting from the condensation with paraformaldehyde.[22] A number of signals were assigned as protonated iminium intermediates, which could be either present in the native mixture or result from acid-induced fragmentation of longer oligomers. According to the HPLC-MS data, the crude mixtures contained macrocyclic products and various linear intermediates in different ratios, depending on the conditions used in the milling and aging steps. In addition, ball milling of a separately prepared cycHC[8] yielded a mixture of linear and macrocyclic

oligomers, confirming the reversibility of methylene bridge formation under LAG conditions. The reported analytical approach demonstrates the usefulness of HPLC-MS in uncovering the changes occurring during polycondensation and macrocyclization via DCC in the solid state.
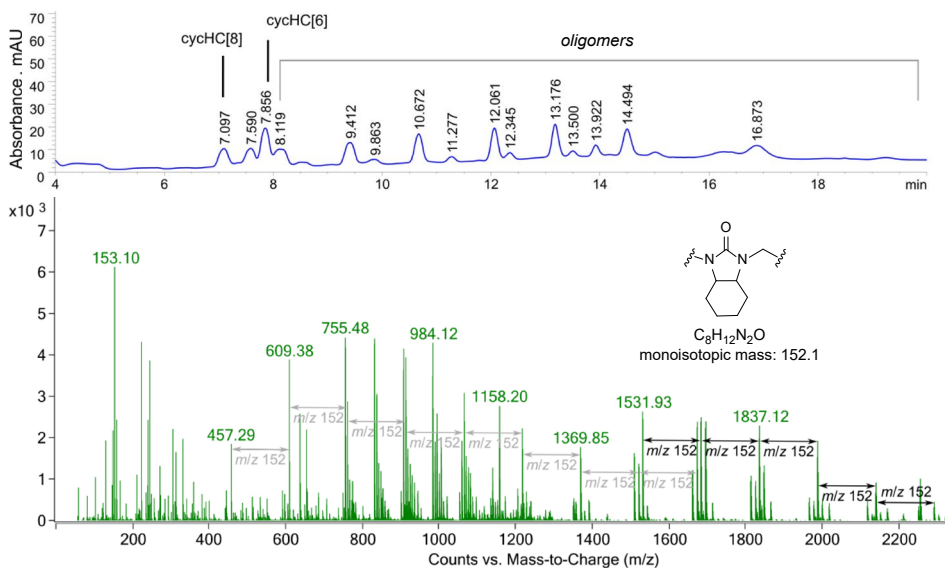

Figure 14. HPLC-UV chromatogram and (+)ESI-MS spectrum of cycHC[n] crude mixture obtained in the solid-state. Adapted from ref. 24 with permission from John Wiley and Sons.

1.3 Application of Hemicucurbiturils

Diverse HCs have gained significant attention in supramolecular chemistry due to their unique ability to form host-guest complexes. These macrocycles, characterized by well-defined hydrophobic cavities, excel in binding a wide range of anions, therefore being highly effective in anion recognition, transport, and sensing. Additionally, several receptors demonstrated their versatility by forming complexes with neutral compounds. The integration of HCs into materials and devices further showcases their potential, enabling the development of innovative solutions for analytical and biomedical applications.

1.3.1 Supramolecular Receptors for Anion Binding

All HCs possess an electron-deficient cavity, which enables encapsulation of compatibly sized anionic guests via non-covalent interactions, such as hydrogen bonds and electrostatic forces. The guest scope and affinity are largely influenced by the particular receptor structure and the solvent used as the medium. The strength of anion binding in solution is usually determined by titration techniques,[77,78] predominantly by ^{1}H NMR spectroscopy and isothermal titration calorimetry (ITC) methods, which can be used independently or complementary to each other. Additionally to association constant evaluation, NMR titration reveals specific interactions responsible for the binding event based on the changes in the signals of ^{1}H or other nuclei. ITC provides valuable information about the thermodynamic characteristics of the process. Besides, complexation of

macrocycles with anions can be explored in the gas phase by MS.[79] The application of soft ionization techniques, such as ESI, allows for detection of supramolecular complexes with outstanding selectivity and sensitivity. ESI-MS is used to investigate in-solution binding processes, and the strength of non-covalent interactions in the complex can be studied by gas phase ion dissociation methods, for instance, energy-resolved collision-induced dissociation (ER-CID).

Anion binding in water and other protic solvents is relevant to many biological processes. However, anion recognition in solution, especially aqueous media, presents two considerable challenges: receptor solubility and strong solvation of both anions and macrocycle binding site, which competes with host-guest complex formation. Considerable effort was devoted to designing HC tailored for binding anions in protic media, leading to the development of several receptors[27,28,30,80,81] with varying binding properties (Figure 15). All 6-membered HCs are known to form 1:1 complexes with halides, which are used as the templates during synthesis. The anionic guest is located in the center of the binding pocket, stabilized by the C−H···anion interactions with methine protons pointing inside the cavity. Larger anions compatible with the cavity size are bound even stronger, presumably due to their softness, as demonstrated by Bio[6] binding of halide and cyanate guests.[80] The type of substituents plays a pivotal role in the receptor properties. For instance, deprotonation of the carboxylic groups of the macrocycle leads to electrostatic repulsion effects upon binding with anions, which is especially evident in case of long flexible substituents. Replacing the latter in $(CapA)_{12}BU[6]$ and $(ButA)_{12}BU[6]$ with PEG-chains resulted in considerably stronger anion binding (Figure 15). Currently, $(PEG)_{12}BU[6]$ is recognized as the receptor with the highest recorded binding efficiency and selectivity for iodide[30] and unprecedented affinity for dicyanoaurate[81] in aqueous solutions.[82]
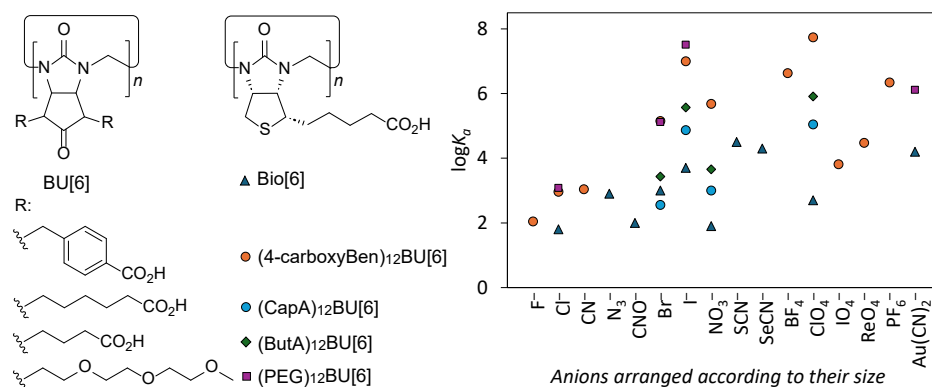
Figure 15. The binding constants acquired for Bio[6] and BU[6] complexation with anionic guests in aqueous media.

Generally, encapsulation of chaotropic anions within HC hydrophobic cavity in aqueous media is enthalpically driven and entropically disfavoured, in line with the nonclassical hydrophobic effect.[83] Šindelář and colleagues investigated the solvent influence on the thermodynamic parameters of $(PEG)_{12}BU[6]$ binding with halides.[30] Evaluation of the $X^-@(PEG)_{12}BU[6]$ complex formation in various solvents demonstrated that binding enthalpy was favorable in all cases, while the entropy was favorable or close to zero in all media, except for water and chloroform. Similar trends were observed in

anion binding by Bio[6] and Bio-L-sulfoxide[6] and corresponding esters in water and acetonitrile.[45] The entropic term is also closely linked to the solvation energy of a particular anion. Therefore, lower solvation entropy of the iodide led to less favorable entropic effects compared to other halides independently of the solvent used. Furthermore, the contribution of the enthalpy and entropy may depend on the nature of the interactions responsible for complex stabilization. For example, in contrast to halides binding in water, dicyanoaurate binding by (PEG)$_{12}$BU[6] has favorable binding entropy (TΔS = +3.4 kJ/mol) .[81]

Until recently, chiral cycHC[8] has been the only representative of 8-membered HCs, acting as a remarkably selective anion receptor in protic solvents (methanol and methanol-water mixture).[84] The enthalpy-driven formation of 1:1 inclusion complexes was shown to be dependent on the guest size, shape and charge distribution, revealing the highest affinity of the macrocycle to large chaotropic anions with symmetrically distributed electron density (Figure 16). The affinity order was established based on ESI-MS measurements in the gas phase, consistent with the results of solution and solid-state binding studies. In contrast to the 6-membered Bio[6] and BU[6], the cycHC[8] binding pocket is large enough to accommodate relatively large anions in the center, but too spacious to form stable complexes with halides. The newly reported thio-cycHC[8] encapsulates various anionic guests (I$_3^-$, PF$_6^-$, ClO$_4^-$, BF$_4^-$, TfO$^-$ and I$^-$) in chloroform exhibiting conformational adaptation.[16]
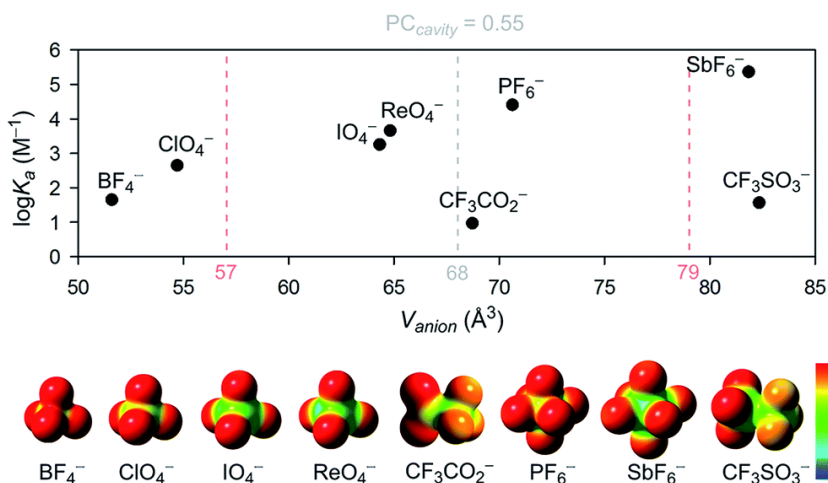
Figure 16. Dependency of cycHC[8] anion binding constants on the anion size and electrostatic surface potential. Reprinted from ref. 84 with permission from the Royal Chemical Society.

Lipophilic HCs have found application as efficient transmembrane anion transporters. Bio[6] hexaesters, hydrophobic analogs of Bio[6], selectively bind polarizable Cl$^-$ and NO$_3^-$ over harder anions (HCO$_3^-$, SO$_4^{2-}$) in acetonitrile. Once embedded into a vesicle, the hexaesters act as mobile carriers of chloride and antiporters of nitrate in aqueous media, exhibiting minimal selectivity towards HCO$_3^-$ (Figure 17). Their activity is dependent on the side chain length (butyl >> ethyl > methyl), suggesting that receptor lipophilicity enhances the rate of anionic transport.[44] Semithio-BU[6] also act as a Cl$^-$/NO$_3^-$ transmembrane transporter,[41] although with lower efficiency compared to Bio[6] derivatives.
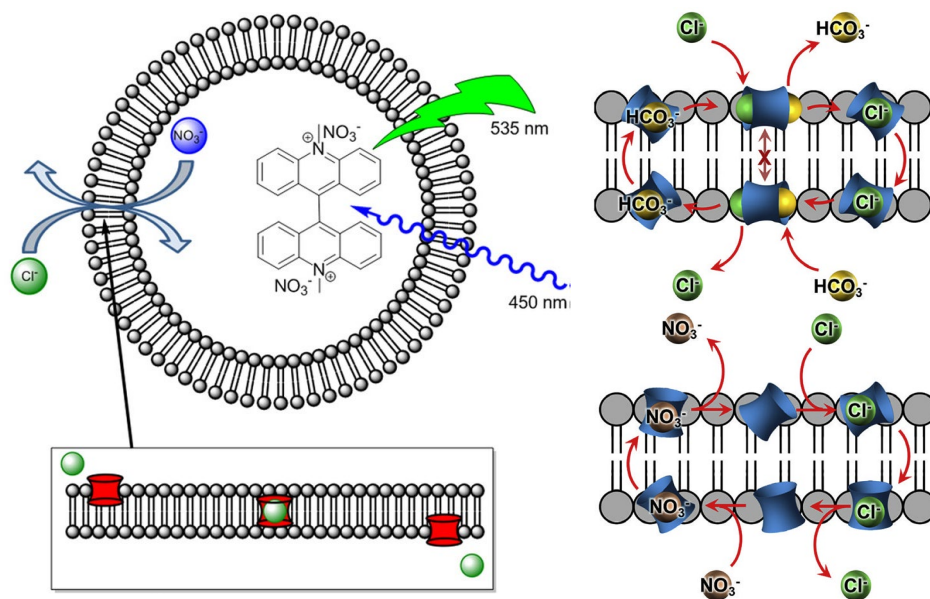
Figure 17. HC-based anion transporters (red and blue double conical shapes depict Bio[6] and BU[6] derivatives, respectively). Adapted from ref. 31, 44 with permission from Elsevier and the American Chemical Society.

Exceptionally high affinity of fluorinated BU[6]s for Cl^- and NO_3^- showcased detrimental effects of strong binding on anion transport. At the same time, (3,5-bis(trifluoromethyl)benzyl)-substituted BU[[6] able to accommodate two anions simultaneously proved to be an unprecedently potent Cl^-/HCO_3^- transporter across the lipid membrane[31] (Figure 17). Remarkably, its mono-functionalization with a crown ether and cholesterol moieties did not significantly affect the performance, implying that the binding properties contribute to the transport rate more than carrier diffusion across the membrane.[34]

1.3.2 Complexation with Neutral Guests

Examples of host-guest complexes between HCs and neutral entities are scarce, primarily due to the insufficient size of the binding pocket. Nevertheless, in addition to the hydrogen bond donors inside the cavity which are responsible for guest inclusion, the macrocycles offer multiple binding sites on the carbonyl groups of the urea monomers. The carbonyls act as hydrogen bond acceptors and facilitate complex formation with a number of neutral compounds.

Cong and colleagues demonstrated that unsubstituted HC[*n*] (n = 6, 12) interact with a hydroxyl-substituted Schiff base[85] in chloroform-methanol 1:1 (v/v) solvent mixture via a hydrogen bond between the carbonyl groups of the macrocycle and phenol hydroxyl group, resulting in the formation of a 1:1 exclusion complex with HC[6] and guest encapsulation by HC[12]. The same group reported complexation between HC[6] and ferrocene,[86] which occurred in identical medium due to hydrogen bonding between the carbonyl groups of the host and hydrogen atoms of the guest aromatic ring.

Aav's group described the formation of cycHC[*n*] (n = 6, 8) external complexes with non-dissociated inorganic and organic acids[87] using computational approaches, which was further supported by experimentally observed binding of various hydrogen bond

donors, such as phenols, carboxylic and sulphonic acids, outside the macrocycle in aprotic solvent. Notably, the stoichiometries of the host-guest complexes were difficult to evaluate and seemed to range from 1:1 to 1:3 or even higher, which is feasible due to the numerous binding sites. In addition to hydrogen bonding, the cycHC[*n*] carbonyl groups are able to coordinate with metals, which was demonstrated in 1:3 complexation with metalloporphyrins.[88]

1.3.3 Hemicucurbituril-Based Materials and Devices

Two research groups independently explored and reported the application of HCs for sensing ClO_4^- anions in water. Perchlorate occurs as environmental pollutant of both natural and anthropogenic origins and causes adverse health effects by disrupting thyroid hormone production.[89,90] The development of sensitive methods for its detection is therefore of great importance. Lubal and colleagues used $Ben_{12}BU[6]$ as an ionophore to prepare the ion-selective membrane, which was further utilized in a solid-contact ion-selective electrode[91] suitable for determination of perchlorate in water in the range from 10^{-1} to 10^{-6} M. Reany, Huskens and co-workers proposed an alternative approach to ClO_4^- sensing based on self-assembled mono-layers of semiaza-BU[6] derivatives containing lipoic amide substituents.[92] Deposition of macrocyclic anion receptors on the gold surface allowed for selective electrochemical impedance spectroscopic determination of perchlorate in the concentration range of 2–100 mM.

A very recent study by Bayley, Reany and colleagues demonstrated a peculiar application of semiaza-BU[6] derivative as a molecular adapter for stochastic chloride sensing at the single-molecule level.[93] Incorporation of the macrocycle into α-Hemolysin transformed the protein pore into a selective anion sensor, capable of detecting Cl^- in 1–30 mM concentration range.

In the context of biomedical applications, $Me_{12}BU[6]$ has been used by Bakibaev and colleagues to synthesize silver nanoparticles with antibacterial activity.[94] Furthermore, Turebayeva and co-workers reported incorporation of the $Me_{12}BU[6]$ into porous hydroxyapatite and diatomite carriers to afford biocompatible composite materials[95].

Chiral cycHC[*n*] and their ability to coordinate with metalloporphyrins were used by Paolesse's group to prepare chiral gravimetric sensors based on supramolecular complex formation.[96] These sensors were employed for the efficient discrimination between limonene and 1-phenylethylamine enantiomers, demonstrating the applicability of the macrocycles in the field of enantiorecognition, relevant for both research and industry.

2 Motivation and Aims for Work

The overview of the current state of HC chemistry demonstrates a considerable interest towards this topic. New HC-based receptors are continuously developed to result in intricate binding properties, and find remarkable applications as transmembrane anion transporters, sensors for anions and chiral compounds, and more. Currently, there have been just a few examples of host-guest complexes between HC and neutral compounds, although the latter may be important targets for binding, including various pollutants, therefore this area remains unexplored. The existing limited number of HC-based materials rely on incorporation of the macrocycles via mixing with matrix components to produce membranes or composites, as well as deposition on the metal surface. Up to my knowledge, there have been no examples of covalent immobilization of HCs on solid materials. Development of synthetic pathways to obtain new macrocyclic hosts suitable for derivatization is a challenging task. Synthetic screening and optimization are impossible without reliable analytical methods to evaluate the reaction outcome. Consequently, there is a demand for efficient tools to monitor HC synthesis and gain a better understanding of the mechanism behind it. The potency of HPLC-MS analysis has been demonstrated in separation of some HC mixtures, however, this method requires development of new conditions tailored for particular analytes.

The specific aims of the current work were:
- to develop quantitative HPLC-UV-MS procedures for analysis of crude mixtures obtained in mechanosynthesis of hemicucurbiturils;
- to investigate mono-biotinylated hemicucurbit[8]uril (mixHC[8]) solid-state assembly via quantification of the major macrocyclic products and characterization of the intermediates by HPLC-MS;
- to explore the formation of complexes between cycHC[*n*] and suitably sized neutral heterocycles, and apply cycHC[*n*] for removal of the latter from water;
- to study the anion-binding properties of the new mixHC[8] in gas phase and solution;
- to test the possibility of preparing new functional materials via covalent immobilization of mixHC[8].

3 Experimental

All experimental procedures are detailed in the supporting information of the publications I–III. Unpublished methods related to anion binding studies in the gas phase are described below.

Screening of complexation with anions by ESI-IMMS

The studies were performed on Agilent 6560 Ion Mobility Q-TOF spectrometer, equipped with a micro ESI source. The measurements were carried out in negative mode. Prior to the measurements the instrument was tuned for standard mass range. The ion source parameters were set as follows: drying gas temperature 150 °C, drying gas flow rate 3 L/min, nebulizer pressure 2 psi, capillary voltage 5500 V and fragmentor voltage 400 V. The IM-MS spectra were measured with N_2 as the drift gas. The data were acquired using MassHunter Acquisition B.09.00 and analyzed using MassHunter Qualitative Analysis B.08.00 and IM-MS Browser B.08.00.

Stock solutions of (–)-mixHC[8] (1 mM) and salts (2 or 5 mM) were prepared in methanol. Sample solutions were obtained by diluting stock solutions to 10 µM concentration and using 1:1 host : guest ratio in methanol. The samples were introduced into the ESI source via direct infusion with 5 µl flow rate.

In ER-CID studies the ions were isolated and activated by collision energy (CE) values from 0.5 to 55 V. The dissociation was monitored as a function of CE value, the resulting dissociation curves were fitted to polynomial function. The value of CE required for dissociation of half of the isolated ions (CE[50%]) was determined using MS Excel software.

Competition anion binding by ESI- MS

The ESI-MS mass spectra were acquired on Agilent 6540 Accurate-Mass Q-TOF spectrometer equipped with Agilent jet stream electrospray ionization (AJS-ESI) source. Prior to the measurements the instrument was tuned for standard mass range. The spectra were recorded in negative mode with the following source parameters: drying gas temperature 200 °C, drying gas flow rate 6 L/min, sheath gas temperature 200 °C, sheath gas flow rate 8 L/min, nebulizer pressure 60 psi, capillary voltage 2000 V and fragmentor voltage 220 V. The data were collected using MassHunter Acquisition B.09.00 and analyzed using MassHunter Qualitative Analysis B.08.00.

Stock solutions of (+)- and (–)-mixHC[8] (1 mM) and salts (1 mM) were prepared in methanol. Sample solutions were obtained by diluting stock solutions to 10 µM concentration and 1:1:1 host : guest1 : guest2 ratio in methanol. The samples were introduced into the AJS-ESI source via direct infusion with 5 µl flow rate.

Competition experiments were performed using two competing anions with same counter cation (Na^+ or TBA^+). The measurements were carried out on three different samples, and the variance was expressed as the standard deviation of the obtained results.

4 Results and Discussion

4.1 Quantification of Hemicucurbiturils in Mechanosynthesis (Publications I, III and Unpublished Results)

Isolation of a macrocycle from a crude reaction mixture by column chromatography is a tedious and time-consuming process, moreover, it is accompanied by inevitable losses of the product. Therefore, to increase time-efficiency of synthetic screening there was an urge for a convenient analytical method to quantitatively follow the reaction outcome prior to purification, in order to maximize product yield. In the current study, mechanosyntheses of Bio[6] hexa-amide and mono-functionalized hemicucurbit[8]uril represent two targets that produce complex reaction mixtures. Polyfunctionalization of a macrocycle is expected to deliver a variety of side-products with a different DS, whereas multi-component assembly via DCC proceeds through formation of numerous intermediates and products.

4.1.1 Monitoring of Biotin[6]uril Hexa-Amidation

Bio[6][43] is an appealing host molecule that carries six carboxylic groups suitable for further derivatization. To date, the post-modifications of Bio[6] conducted by Pittelkow and colleagues have included esterification of its carboxylic groups,[44] enhancing the hydrophobicity of the macrocyclic container, as well as selective sulfur oxidation,[45] which altered its binding properties. Efficient functionalization of the carboxylic groups with chiral amines offers a promising strategy to introduce additional chiral centers into the macrocycle. A mechanochemical liquid-assisted protocol of amide coupling between carboxylic acids and amines was developed in our group by Dr. Tatsiana Nikonovich (Dalidovich) and applied in the derivatization of Bio[6]. The six carboxylic groups of the macrocycle were functionalized with phenylalanine methyl ester to produce a new chiral receptor bearing 24 stereogenic centers (Figure 18).
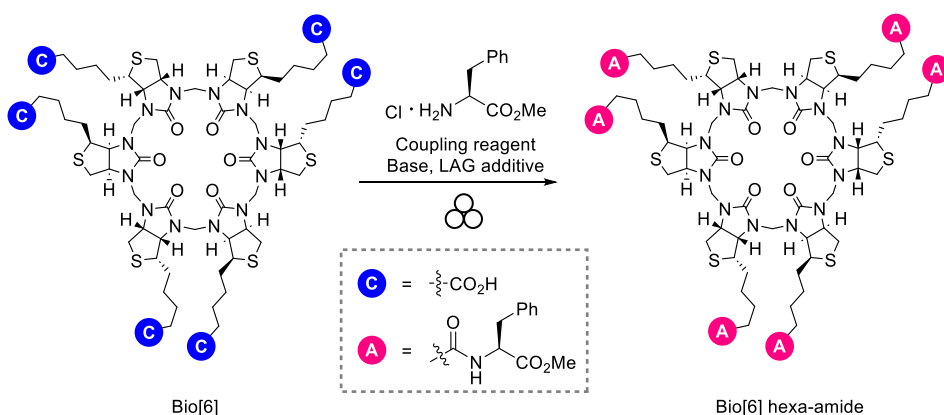

Figure 18. General scheme of Bio[6] hexa-amidation via ball milling performed by Dr. Tatsiana Nikonovich (Dalidovich).

While the amidation of Bio[6] carboxylic groups may seem straightforward, it actually poses significant synthetic and analytical challenges. The hexafunctionalization process can be seen as six consecutive steps, each demanding exceptionally high efficiency.

Failure to achieve the optimal reaction conditions results in a mixture of partially functionalized products, necessitating extensive purification and the development of highly effective analytical separation techniques.

The amide coupling between Bio[6] and phenylalanine methyl ester was selected as a convenient model for both synthetic and analytical studies. The samples collected after ball milling were dissolved in organic solvent (DMSO), leaving the salts used in the synthesis undissolved, and the supernatant was analyzed by HPLC-UV-MS. RP-HPLC was previously successfully employed for analysis of Bio[6] formation by Pittelkow.[43] Amidation of the carboxylic groups results in decreased polarity of the macrocycle, therefore allowing to expect stronger retention on C18 stationary phases. The developed HPLC conditions enabled effective separation of Bio[6], hexa-amidated Bio[6] and underfunctionalized products with DS ranging from 1 to 5 (Figure 19). The identities of the peaks were confirmed with the aid of high resolution mass spectrometry (HRMS), with the side-products and the target Bio[6] hexa-amide primarily observed as singly and doubly charged protonated species.
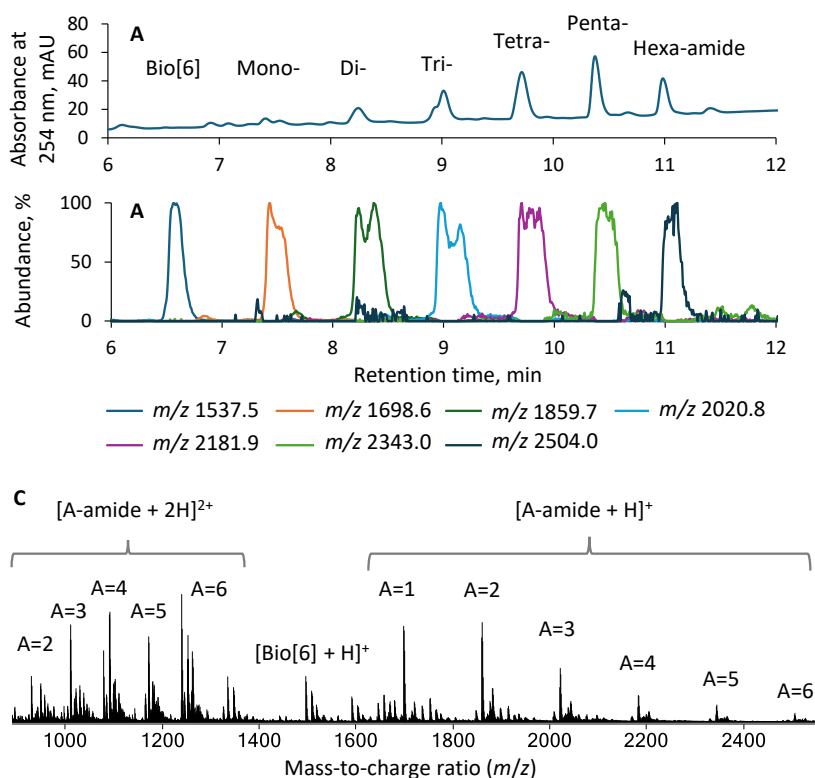
Figure 19. HPLC-UV chromatogram of the Bio[6] amidation crude mixture, containing fully- and under-functionalized products (A), EICs of the protonated macrocycles (B), and (+)ESI-HRMS spectrum of the displayed chromatogram region (C).

The HPLC-UV analysis aimed to evaluate the reaction conditions used in the hexa-amidation of Bio[6]. Although absolute quantification of the side products was not feasible as they were not isolated, the HPLC peak area percentages at 254 nm provided sufficient data for the screening purposes. The analysis was simplified by focusing only

on the peaks corresponding to Bio[6] and its amidated derivatives, with the differences in their absorption properties considered negligible. This comparative analysis of crude reaction mixtures enabled the optimization of synthetic conditions, achieving a 95% conversion to Bio[6] hexa-amide as determined by HPLC, and an 80% yield of the isolated product.

4.1.2 Determination of Yields in Mono-Biotinylated Hemicucurbit[8]uril Synthesis

Covalent assembly of mono-biotinylated mixHC[8] from different starting monomers was expected to produce diverse mixtures of products and intermediates. The ball milling stage under LAG conditions induced the acid-catalyzed multi-component condensation reaction, which generated a complex DCL. Further aging of the crude mixture at elevated temperatures enabled templated self-organization of the intermediates, resulting in two major products – chimeric mixHC[8] and homomeric cycHC[8] (Figure 20). Synthesis development and optimization were performed by Elina Suut-Tuule.
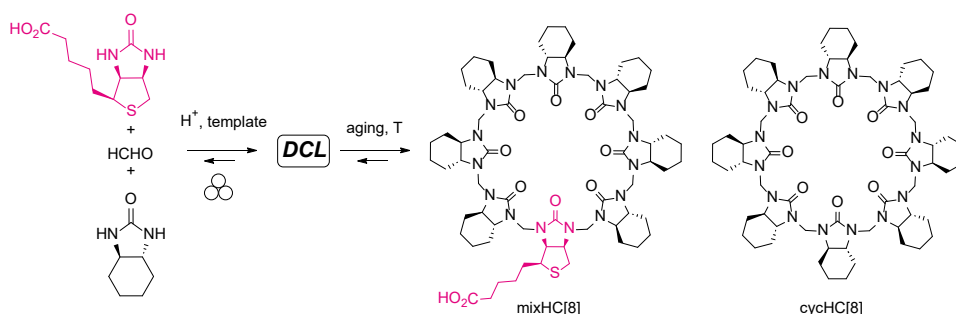

Figure 20. General scheme of mixHC[8] synthesis in the solid state.

Combinatorial analysis predicted the potential formation of approximately 50,000 compounds from the three-component mixture of starting materials, which makes the analysis of products and intermediates extremely challenging (see Chapter 4.2.1). In contrast to the solid-state synthesis of cycHC[n],[24] NMR spectroscopy was not applicable due to the complexity of the crude mixtures, which contained numerous macrocycles and intermediates with overlapping signals in the ^{1}H NMR spectra. As demonstrated previously, RP-HPLC-UV is a perfect tool to separate cycHC[n] and quantify them based on the calibration curves.[55] The reported conditions were used as the starting point for the development of chromatographic conditions.

Compared to the work on Bio[6] hexa-amidation, the mixHC[8] crude mixtures after aging did not always appear homogeneous. Besides, the milling and aging stages were likely to cause partial evaporation of water from the system, as well as absorption of moisture from the air, which influenced the concentration of the solids to an unknown extent. In order to account for these changes and increase the reliability of the results, sampling was performed in replicates, and triphenylmethane (TPM) was introduced into reaction before milling as an internal standard. The developed HPLC-UV-MS method was evaluated based on its selectivity, stability, linearity, limit of detection (LoD), limit of quantitation (LoQ), trueness and reproducibility.

Development of Chromatographic Conditions

The separation of the macrocycles formed during mixHC[8] solid-state synthesis was initially attempted on the Kinetex C18 (100 mm × 2.1 mm, 2.6 µm) column, previously employed in the analysis of cycHC[n],[21,24,55] the analytes were identified with the aid of ESI-MS. Incorporation of just one biotin unit into cycHC[8] scaffold considerably increased the macrocycle polarity, resulting in significantly different retention factors of cycHC[8] and mixHC[8]. Unfortunately, the latter eluted as a distorted broad band. Transition to a larger Kinetex XB-C18 (150 mm × 4.6 mm, 2.6 µm) column provided sharper and more symmetrical peaks of mixHC[8] and cycHC[8] (Figure 21). The selected stationary phase with di-isobutyl chains, low ligand density and inactive surface, acts as a great hydrogen bond acceptor and, therefore, improves the peak shape and selectivity of acidic compounds.[97]
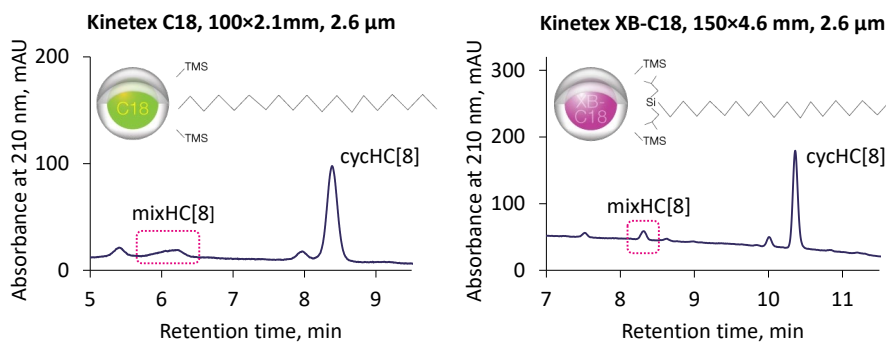

Figure 21. HPLC performance of different C18 columns in the analysis of a mixHC[8] crude reaction mixture.

4.2 Mass-Spectrometric Characterization of Mono-Biotinylated Hemicucurbit[8]uril Solid-State Assembly (Publication III)

The new mixHC[8] macrocycle was assembled in the solid state in a multi-component condensation reaction in accordance with DCC. Essentially, the synthesis included two stages. The milling step generated a complex DCL containing numerous linear and cyclic intermediates. The aging of the crude mixture shifted the DCC equilibrium towards the formation of the macrocyclic products. The detailed characterization of the DCL composition during milling and aging was determinative to the understanding of the time-dependent processes occurring in the solid state, and consequently, to the optimization of the synthetic conditions.

4.2.1 HPLC-HRMS Profiling of Dynamic Covalent Library

Selective assembly of mixHC[8] from different building blocks via DCC is extremely challenging because of the vast number of potential products and intermediates. Considering the non-C_2-symmetric biotin, various combinations of the two starting monomers result in ca 50,000 possible oligomers ($2 \leq n \leq 10$). Noteworthy, this number calculated by Dr. Marko Vendelin reflects the differences in the composition of the oligomers, as well as the order and orientation of monomeric units. In addition, the linear oligomers can have different terminal groups resulting from the acid-catalyzed condensation with paraformaldehyde, reversable formation and cleavage of the C–N covalent bond and reaction with isopropanol used in the sample preparation (Figure 29).
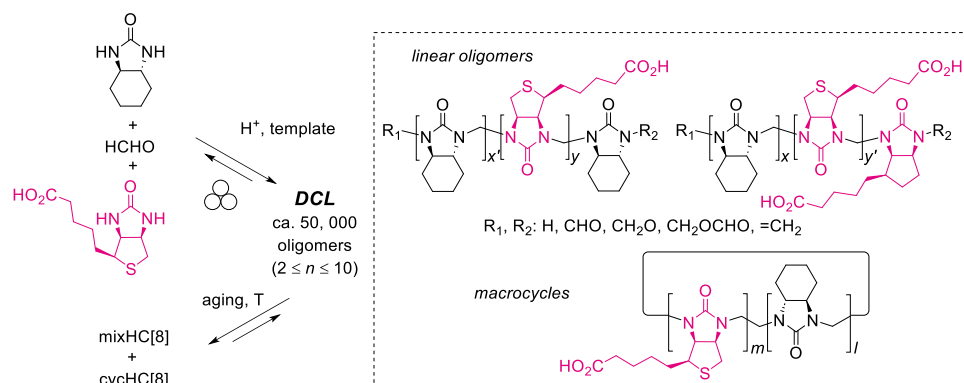
Figure 29. Complexity of DCL during mixHC[8] self-assembly.

As a result of synthetic optimization, the best reaction conditions delivered mixHC[8] and cycHC[8] in 38% and 34% HPLC yields, respectively. To gain mechanistic insight, the products and intermediates generated upon different milling duration (5, 10, 20, 30, 45 and 60 min) were identified by HPLC-HRMS analysis prior to and after aging for 24 h at 60 °C. The corresponding abundance values of 132 detected species were used to create the heat map displaying the dynamic changes during synthesis (Figure 30). HRMS identification of the crude mixture components relied on the comparison of the observed signals to the library containing 1260 linear oligomers ($2 \leq n \leq 10$) and 60 macrocycles ($3 \leq n \leq 10$). The data treatment was performed with the aid of MatchMass[99] created by Dr. Lukas Ustrnul as a free user-friendly tool to assist the analysis of complex MS data.
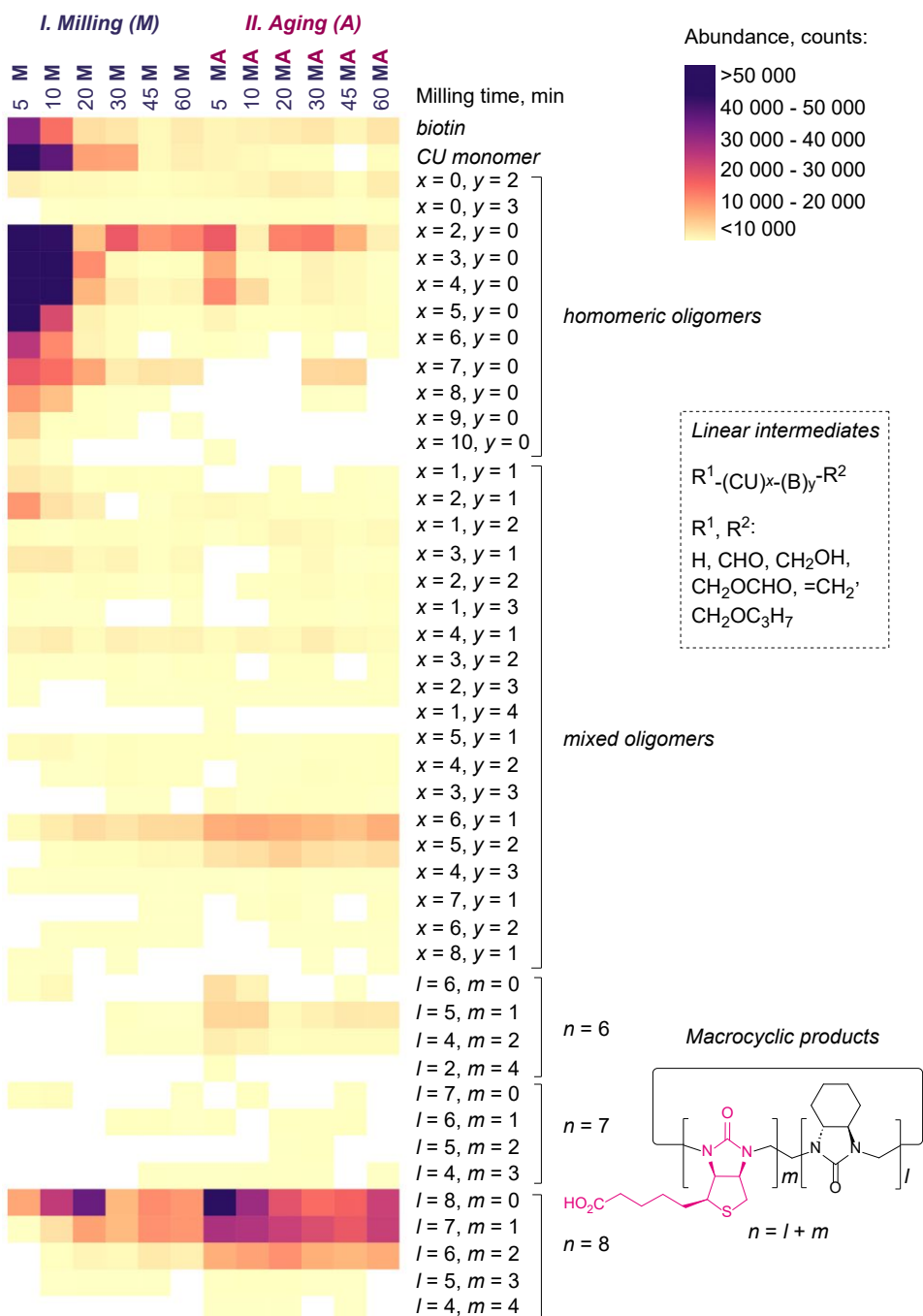
Figure 30. Heatmap visualizing the dynamic changes during mixHC[8] self-assembly.

Biotin was found to participate in the formation of various oligomers $(CU)_x(B)_y$ (CU – cycloxane urea unit, B – biotin unit, $x = 1...8$, $y = 1...4$), as well as several of mono-, di-, tri- and tetra-biotinylated mixHC[n] ($n = 6...8$). No species containing more than 4 biotin units were observed. The collected data proved the milling duration to be crucial

to the DCL composition, which in turn determined the ratio of the macrocyclic products. Homomeric oligomers prevailed at the initial phase of condensation, while generation of longer biotin-containing linear and cyclic intermediates was observed upon prolonged milling. Therefore, the ball milling duration must be sufficient to ensure the "shuffling" of the monomers and efficient distribution of biotin across the reaction mixture. The formation of cycHC[8] proceeded in a peculiar manner, as it was detected already at the milling stage with the highest abundance after 20 min, but then underwent partial disassembly. The macrocycles predominantly "ripened" during templated self-organization occurring at the aging stage. Although the data points to monomer cross-over reactions during aging, the mixtures milled for shorter period and rich in CU-homomeric oligomers delivered cycHC[8] as the dominant product, and the maximum content of the chimeric mixHC[8] was observed for the mixtures milled for 60 min. The trends revealed by HRMS analysis were consistent with the yields of macrocycles determined by HPLC-UV.

4.2.2 Tracking Changes in the Content of Selected Oligomers

Mapping the abundances of the detected oligomers and macrocycles provided a general overview of the dynamic changes occurring during milling and aging, however these values could have been misleading due to the limitations related to the linearity in MS. Therefore, a selected ion monitoring (SIM) method was developed for selective determination of short homomeric dimers and trimers in the crude mixtures. The formation of the chosen species reflected the condensation rate between different monomers. Unfortunately, the absolute quantification was not feasible in the absence of reference compounds, yet the collected data was sufficient to see the change in the content of the selected oligomers after milling and aging.

SIM approach enhances the sensitivity of the analysis towards the analytes of interest. However, it is crucial to maintain the sample concentration within the linear range of the method. The linear range for the dimers and trimers was determined based on peak areas which displayed linear dependency upon dilution of the sample solution, as the absolute concentration of the oligomers was unknown (Figure 31). During analysis, the samples containing high amounts of oligomers were additionally diluted to provide peak areas within the linear range. The obtained values were further corrected with respect to the dilution factor.
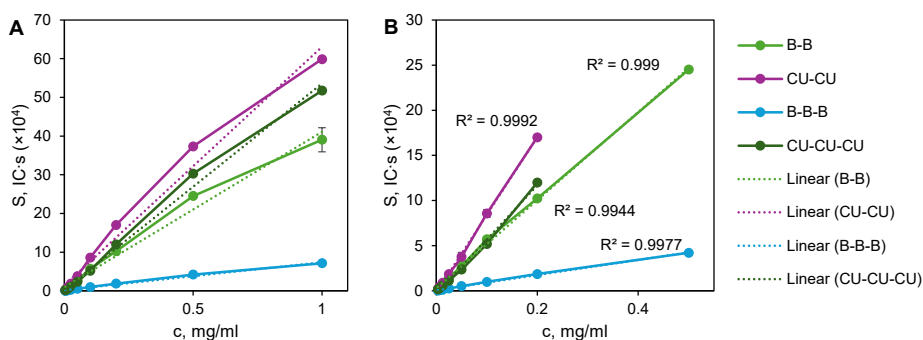

Figure 31. Linearity of the SIM method for determination of dimers and trimers (A – full studied range, B – linear range).

As we concluded in Publication III, "the changes in the content of characteristic dimers and trimers allowed to compare the rate of their condensation prior to and after the aging stage. The collected data (Figure 32) confirmed that coupling between the CU monomers is kinetically preferred and occurs at the initial phase of the polycondensation reaction. Thus, the quantity of CU-CU and CU-CU-CU drastically increased after 5 min of milling and subsequently underwent rapid decay. Such fast dynamics and decay were absent for the biotin units reflecting a major difference in condensation between biotin and CU. In contrast, the condensation of the biotin units to respective dimer and trimers reached in at the beginning of reaction its maximum and probably acts as a transient intermediate".[100]
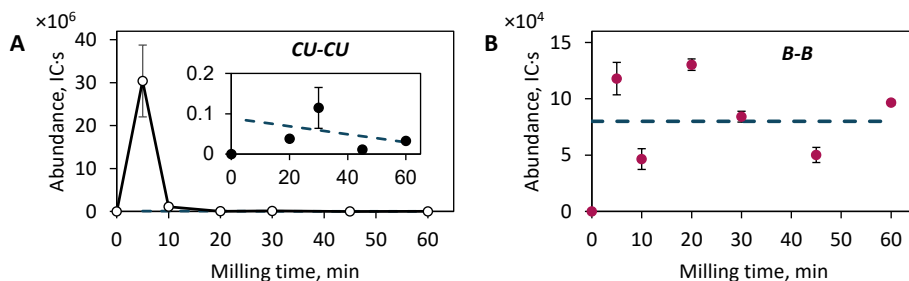
Figure 32. The changes in the content of homomeric CU-CU (A) and B-B (B) dimers depending on milling duration.

4.3 Complexation between Hemicucurbit[8]urils and Small Electron-Rich Guests (Publications II and III)

The complexation of cycHC[8] with a series of suitably sized neutral heterocycles was investigated by ^{13}C CPMAS ssNMR and ^{1}H NMR spectroscopy, which revealed the possibility of guest inclusion in the solid state and specific interactions that enable encapsulation in solution, as well as the binding strength. The cycHC[8] applicability for selective capture of neutral guests in aqueous solutions was studied in the solid-phase extraction experiments (SPE).

The new member of the cycHC[8] family, mono-biotinylated mixHC[8], was tested for its affinity towards various anions in the gas phase by ESI-MS and in solution by ITC, and compared to the cycHC[8] performance as selective anion receptor. Furthermore, we explored the possibility of utilizing the mixHC[8] carboxylic group to afford new functional materials without the loss of the macrocycle binding properties.

4.3.2 Solid-Phase Extraction of Neutral Heterocycles from Water by Cyclohexanohemicucurbit[*n*]urils

The performance of cycHC[8] as a sorbent material was compared to its homolog cycHC[6] and powdered silicarbon TH90. The six-membered heterocycle served as a control compound with a smaller cavity unable to accommodate the heterocyclic guests but with identical properties of the external surface, thus allowing to distinguish between inclusion complex formation and physiosorption. The TH90 was used to evaluate cycHC[8] sorption efficiency and selectivity compared to the common carbon-based sorbents.

Prior to extraction, the macrocycles were milled to produce fine powders with surface area of 6.03 m^2/g and 9.02 m^2/g for cycHC[6] and cycHC[8], respectively, suggesting that cycHC[*n*] would exhibit similar efficiencies. Conversely, the surface area of TH90 is substantially larger (around 1000 m²/g), which implies a higher extraction efficiency per weight unit.

SPE experiments were conducted with **1**, **3**, **6**, **9**, **10**, and **11** via stirring the dispersed solid sorbent in an aqueous solution of guest and determining the change in guest concentration upon extraction (Figure 35).

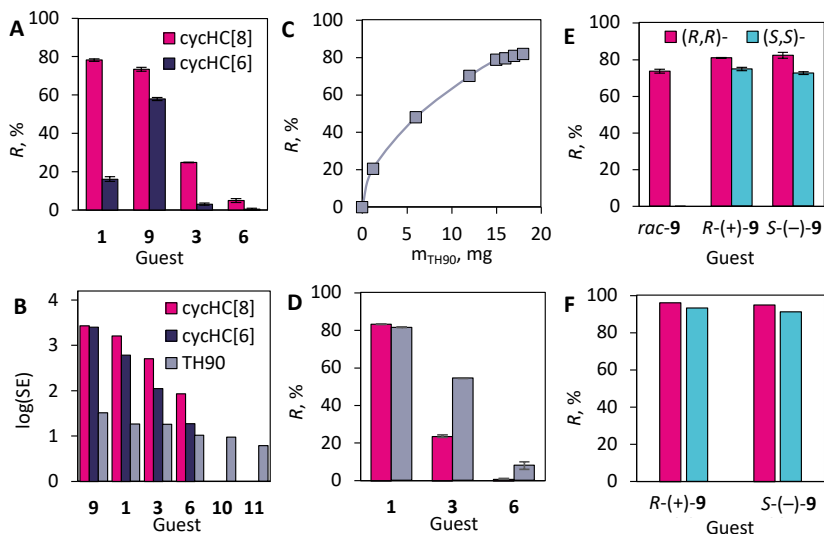*Figure 35. A – removal of heterocycles by cycHC[n], B – sorption efficiency of macrocycles and TH90, C – removal percentage dependency on the amount of TH90, D – comparison of cycHC[8] and TH90 selectivity, E – removal of racemic and enantiopure **9** by cycHC[8] used in H:G 5:1, F – removal of 9 enantiomers by cycHC[8] used in H:G 20:1. The extraction step for the guests **1, 3, 6** (A, B) was performed by Dr. Kamini Mishra.*

The macrocycles showed minimal removal of O-containing **6** and N-containing **10** and **11**. The larger cycHC[8] efficiently extracted S-containing **1** (78 %) and **9** (74%) and moderately removed **3** (25 %), while cycHC[6] was considerably less effective at removing these guests, with extraction values of 16% for **1** and only 3% for **3**. Notably, cycHC[6] removed 58% of **9**, which indicates the significant role of physiosorption (Figure 35A). As anticipated, TH90, acting as a non-selective adsorbent, removed over 50% of all studied heterocycles from water when used in the same ratio of guest to sorbent by weight. Sorption efficiency (SE) was calculated as the mass of the sorbed guest (µg) per cm^2 of the respective sorbent surface area and expressed on a logarithmic scale (Figure 35B). This demonstrated that cycHC[*n*] have a higher affinity for hydrophobic S-containing heterocycles, while TH90 performs similarly regardless of the guest's nature.

Additionally, sorption selectivity was evaluated using a mixture of guests **1**, **3**, and **6**. The adequate amount of TH90 was established by additional experiments to reveal the dependency between sorbent amount and removal percentage. The selectivity studies were planned to ensure similar removal for guest **1** (ca 80%) by cycHC[8] and TH90 (Figure 35C). The least hydrophobic compound **6** was weakly sorbed by both compounds. The selectivity of cycHC[8] was demonstrated in removal of S-heterocycles, where it showed clear preference for guest **1** in contrast to TH90 (Figure 35D).

The enantiorecognition properties of cycHC[8] were tested in the SPE of **9** as racemic mixture and enantiopure compounds. The removal experiments under standard conditions using host-guest molar ratio (H:G) 5:1 showed that (*R,R*)-cycHC[8] acts more efficiently than (*S,S*)-cycHC[8] (Figure 35E). In order to enhance possible enantiodiscrimination, the SPE was performed with H:G 20:1, however, it resulted in negligible difference in the performance of the two macrocycle (Figure 35F). Most likely, the dissimilarity in their removal potential was related to the differences between the cycHC[8] batches.

To prove that extraction of S-containing heterocycles from water by cycHC[8] occurs due to their encapsulation, the macrocycles and guests **1** and **9** were ball-milled in the presence of minute amount of water[101] and analyzed by ^{13}C CPMAS NMR (Figure 36).
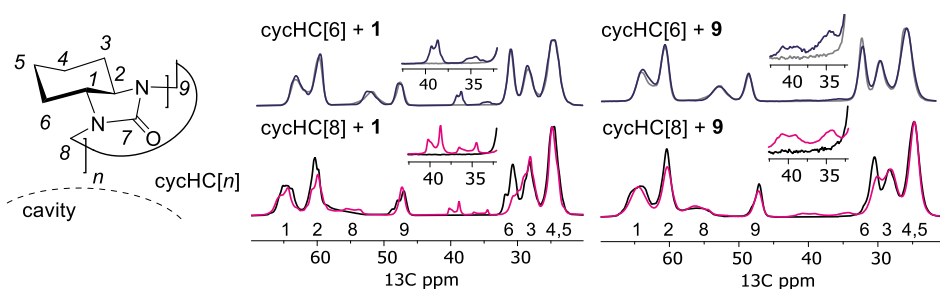
*Figure 36. ^{13}C ssNMR NMR spectra of cycHC[8] before and after LAG with the guests, recorded by Dr. Ivo Heinmaa: upper left – **1** + cycHC[6] (blue) overlayed with cycHC[6] (grey), lower left – **1** + cycHC[8] (magenta) overlayed with cycHC[8] (black), upper right – **9** + cycHC[6] (blue) overlayed with cycHC[6] grey, lower right – **9** + cycHC[8] (magenta) overlayed with cycHC[8] (black).*

The superimposed ^{13}C ssNMR spectra of the cycHC[8] milled with the guests contained characteristic changes in the signals of protons 2 and 6, indicating the formation of inclusion complexes with both compounds. These changes were absent in case of cycHC[6] macrocycle, which cannot accommodate the guests in its cavity.

In summary, the cycHC[8] was found to be a promising sorbent material for selective capture of S-containing heterocycles. However, the sorption efficiency of the macrocycle was found to be considerably limited by its surface area exposed for interactions, which prompted us to explore the possibility of immobilizing macrocycles on the surface of other materials.

4.3.3 Mono-Biotinylated Hemicucurbit[8]uril Complexes with Anions in Gas Phase (Unpublished Results)

The new mono-biotinylated mixHC[8] differed from its parent cycHC[8] in just one monomer unit, therefore it was expected to act as an efficient anion receptor. The anion recognition of the new (−)-mixHC[8] was screened in the gas phase by ESI-IMMS. Compared to the titration methods commonly used to study binding in solution (NMR, ITC), MS offers faster measurements and requires small amounts of the compounds. The drift times determined by IMMS were used to confirm encapsulation of the anionic guests. Singly charged 1:1 complexes were detected with PF_6^-, SbF_6^-, ClO_4^-, I^-, NO_3^-, Cl^-, ReO_4^-, SCN^-, $H_2PO_4^-$, Br^-, HSO_4^-, $CF_3SO_3^-$, NO_2^- and BF_4^-; no binding was observed for F^-, CO_3^{2-} and $CH_3CO_2^-$. The drift times of the deprotonated macrocycle and detected complexes with anions did not significantly differ, indicating their similar size (Table 3). The latter implied accommodation of the anion inside the cavity of the macrocycle.

Table 3. ESI-IMMS screening of anion binding to mixHC[8].

Ion	Formula	*m/z* exp	*m/z* theor	Drift time, ms
[mixHC[8]-H]⁻	$C_{67}H_{100}N_{15}O_{10}SPF_6$	1319.7469	1319.7456	45.16
[PF₆@mixHC[8]]⁻	$C_{67}H_{100}N_{16}O_{10}SPF_6$	1465.7166	1465.7176	47.65
[SbF₆@mixHC[8]]⁻	$C_{67}H_{10}ON_{16}O_{10}SSbF_6$	1555.6462	1555.6477	47.74
[ClO₄@mixHC[8]]⁻	$C_{67}H_{100}N_{16}O_{14}SCl$	1419.7021	1419.7020	47.46
[I@mixHC[8]]⁻	$C_{67}H_{100}N_{16}O_{10}SI$	1447.6591	1447.6579	47.34
[NO₃@mixHC[8]]⁻	$C_{67}H_{100}N_{17}O_{13}S$	1382.7424	1382.7413	47.17
[Cl@mixHC[8]]⁻	$C_{67}H_{100}N_{16}O_{10}SCl$	1355.7237	1355.7223	46.30
[ReO₄@mixHC[8]]⁻	$C_{67}H_{100}N_{16}O_{14}SRe$	1569.6836	1569.6861	47.69
[SCN@mixHC[8]]⁻	$C_{68}H_{100}N_{17}O_{10}S_2$	1378.7274	1378.7286	47.51
[H₂PO₄@mixHC[8]]⁻	$C_{67}H_{102}N_{16}O_{14}S\,P$	1417.7248	1417.7225	46.46
[Br@mixHC[8]]⁻	$C_{67}H_{100}N_{16}O_{10}SBr$	1399.6708	1399.6718	47.24
[HSO₄@mixHC[8]]⁻	$C_{67}H_{101}N_{16}O_{14}S_2$	1417.7188	1417.7130	46.83
[CF₃SO₃@mixHC[8]]⁻	$C_{68}H_{100}N_{16}O_{13}S_2F_3$	1469.7055	1469.7055	48.02
[NO₂@mixHC[8]]⁻	$C_{67}H_{100}N_{17}O_{12}S$	1366.7460	1366.7464	46.21
[BF₄@mixHC[8]]-	$C_{67}H_{100}N_{16}O_{10}SBF_4$	1406.7550	1406.7600	47.47

Complex kinetic stability in gas phase was studied for the selected anionic guests via MS/MS ER-CID experiments (Figure 37). All isolated complexes dissociated with elimination of an anion. The stability of the host-guest complexes was assessed based on collision energy required for dissociation of half of the species (CE[50%]). Analogous to the trends observed for cycHC[8], the low-energy dissociation of inclusion complexes with mixHC[8] was observed for the larger anions, whereas the complexes with smaller anions were more stable.
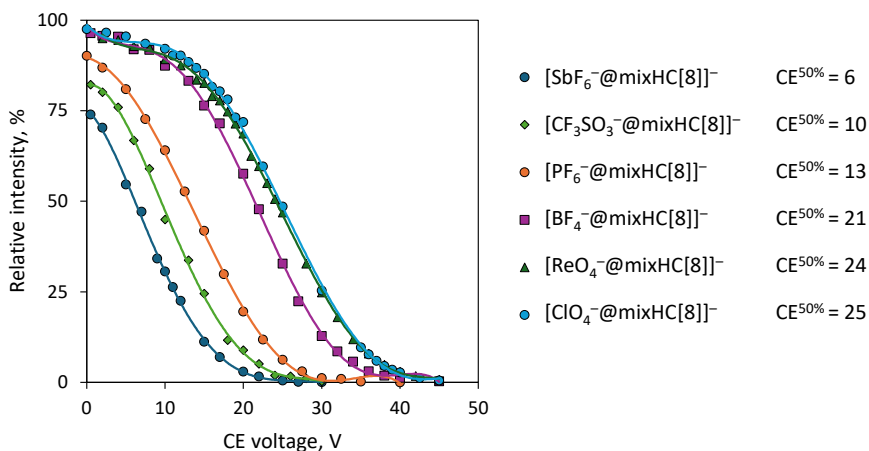
Figure 37. Dissociation curves obtained for the isolated ions in ER-CID experiments and their CE$^{50\%}$ values.

The order of mixHC[8] affinity for selected anions was determined via competition experiments. The MS spectra were recorded for tri-component mixtures containing the host and two competing guests taken in 1:1:1 molar ratio. The relative abundance of the two complexes was expressed as follows:

$$I_{HG1\,rel}, \% = \frac{I_{HG1}}{I_{HG1} + I_{HG2}} \cdot 100$$

where I_{HG1} and I_{HG2} are absolute abundances of the detected complexes.

The collected data suggested the following ranking of affinity for both mixHC[8] diastereomers: $SbF_6^- > PF_6^-$ $ReO_4^- > ClO_4^- > SCN^- \geq I^- > BF_4^- > NO_3^- > Cl^-$ (Figure 38).
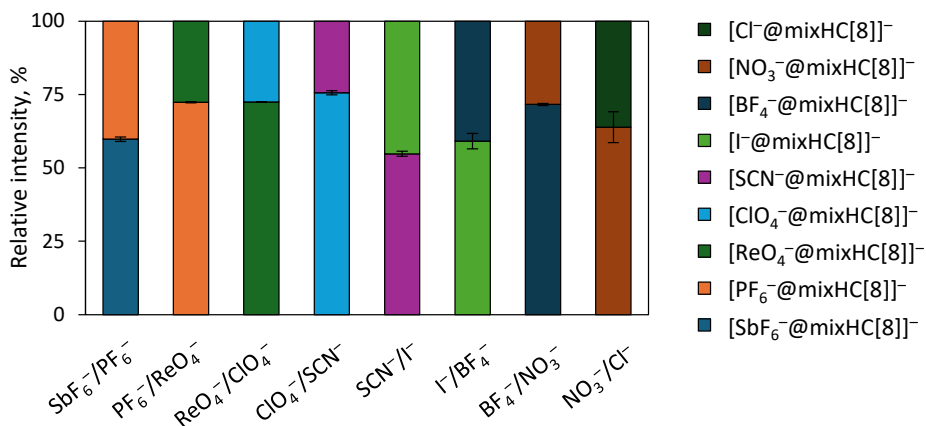
Figure S38. Results of competition experiments carried out with (–)-mixHC[8]. The error bars represent standard deviation between replicates (n = 3).

The strongest binding was observed for large chaotropic SbF_6^-, PF_6^-, ReO_4^- and ClO_4^- anions. The chosen pairs of competing guests featured anions of different geometry: octahedral (SbF_6^-, PF_6^-), tetrahedral (ReO_4^-, ClO_4^-, BF_4^-), trigonal planar NO_3^-, linear SCN^-

51

and monoatomic halides with spherical symmetry. The collected experimental data is currently being used in validation of new computational approaches which aim to predict the binding energies of the macrocycles.

4.3.4 Anion Binding by Mono-Biotinylated Hemicucurbit[8]uril in Solution

Complexation between the mixHC[8] and selected chaotropic anions (ClO_4^-, PF_6^- and SbF_6^-) in methanol and a methanol : water mixture (1:1) was studied by ITC using one set of sites model. The results obtained for the two mixHC[8] diastereomers were compared to the data on cycHC[8] binding.

Encapsulation of the anionic guests proceeded as an exothermic enthalpy-driven event. The association constants correlated with the affinity order ascertained through ESI-MS competition experiments, confirming stronger complexation with an increase in anion size (Table 4). More efficient binding of PF_6^- compared to ClO_4^- explained the advantageous properties of PF_6^- templates during solid-state synthesis of mixHC[8]. In contrast to cycHC[8] receptor,[84] the binding studies in methanol-water mixtures provided lower association constants for mixHC[8], which was especially evident in case of ClO_4^- binding. The observed decrease in the binding efficiency may be related to the stronger solvation of anions in aqueous meda, as well as electrostatic repulsion between the anionic guest and deprotonated carboxylic group of the biotin unit.

Table 4. Association constants of anion binding in solution determined by ITC.

Guest	V_{anion}, Å³	K_a, M⁻¹		
		(−)-mixHC[8]	(+)-mixHC[8]	(R,R)-cycHC[8][84]
(TBA)ClO₄	54.7	$(4.60\pm0.05)\cdot10^{2\,a}$	$(9.7\pm0.2)\cdot10^{2\,a}$	$(4.7\pm0.2)\cdot10^{2\,a}$
		$(1.90\pm0.03)\cdot10^{2\,b}$	$(4.56\pm0.02)\cdot10^{2\,b}$	–
(TBA)PF₆	70.6	$(1.05\pm0.07)\cdot10^{4\,a}$	$(1.59\pm0.04)\cdot10^{4\,a}$	$(2.8\pm0.4)\cdot10^{4\,b}$
		$(0.63\pm0.02)\cdot10^{4\,b}$	$(1.4\pm0.3)\cdot10^{4\,b}$	$(2.6\pm0.2)\cdot10^{4\,b}$
NaSbF₆	81.8	$(2.7\pm0.2)\cdot10^{4\,a}$	$(3.7\pm0.4)\cdot10^{4\,a}$	$(2.5\pm0.7)\cdot10^{5\,a}$

Association constant values were determined in [a] methanol and [b] methanol:water 1:1 using one set of sites binding model.

Noticeably, the binding studies in solution revealed peculiar dissimilarities between mixHC[8] diastereomers and cycHC[8]. In general, (+)-mixHC[8] exhibited higher association constants than (−)-diastereomer for all anions, and was binding perchlorate twice more efficiently than both (−)-mixHC[8] and cycHC[8]. The smallest differences between the affinities of the three HC[8]s were observed for PF_6^- anion. Finally, the cycHC[8] affinity for SbF_6^- was an order of magnitude higher than that of mixHC[8]s. The observed differences imply steric differences of these receptor molecules, which can be utilized in future recognition-based applications.

4.3.5 Functional Material for Selective Capture of Perchlorate

Incorporation of the biotin unit into cycHC[8] granted the new mixHC[8] a carboxylic group, suitable for derivatization and covalent binding of the macrocycle to other materials. To demonstrate it, the mixHC[8] was covalently immobilized on 3-aminopropyl silica gel (APS) via amide coupling (Figure 39), adapting the procedure for calix[6]arene reported by Tabakci.[102] The resulting solid product was repeatedly washed with DCM to remove unreacted macrocycle and tested for leaching in methanol.
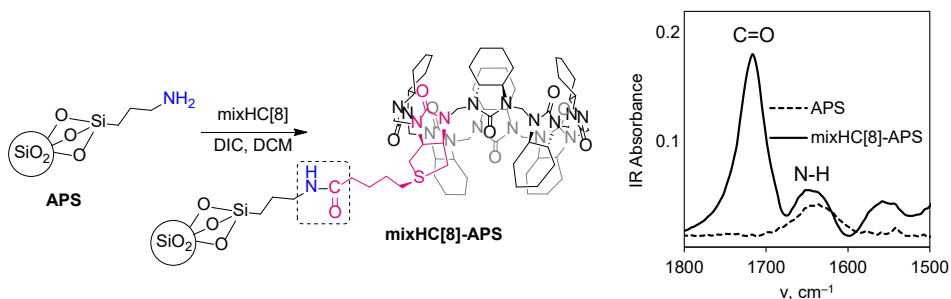
Figure 39. Covalent immobilization of mixHC[8] on APS, characterized by IR spectroscopy.

The obtained material (mixHC[8]-APS) was characterized by IR spectroscopy. The content of immobilized mixHC[8] was ca. 12% (w/w), determined based on the IR absorbance of the carbonyl groups present in the sample compared to a reference mixture of APS and mixHC[8]. The pure macrocycle is soluble in methanol, but once covalently bonded to silica it remains solid and is therefore suitable for SPE. In contrast to the cycHC[8] applied for removal of S-heterocycles from water, the mixHC[8] covered the surface of APS particles, facilitating the efficient use of the binding properties of each molecule exposed for interactions.

The new functional material was tested for selective capture of perchlorate. In the absence of interferents, all ClO_4^- was efficiently removed from its methanol solution via SPE with mixHC[8]-APS (Figure 40). Furthermore, to showcase the removal selectivity, the extraction of perchlorate was performed in the presence of a mineral matrix. A regolith simulant[103] was spiked with (TBA)ClO_4, imitating contamination with perchlorate (1% w/w). The resulting model mixture contained different cations (Ca^{2+}, Mg^{2+}, Fe^{2+}, Fe^{3+}), oxides and kosmotropic anions (SO_4^{2-}, CO_3^{2-}), but was essentially free of the organic matter. The methanolic extract of the contaminated matrix contained primarily perchlorate and sulfate anions, the latter arising from the $MgSO_4$ component. Compared to ca 15% removal of ClO_4^- in the control experiment using non-modified APS, SPE with mixHC[8]-APS provided its complete removal (Figure 39). Both APS and mixHC[8] non-selectively adsorbed sulfate (ca. 85–97%), the absence of mixHC[8] contribution to this process was proven ITC, which showed no SO_4^{2-} binding to the macrocycle in methanol.
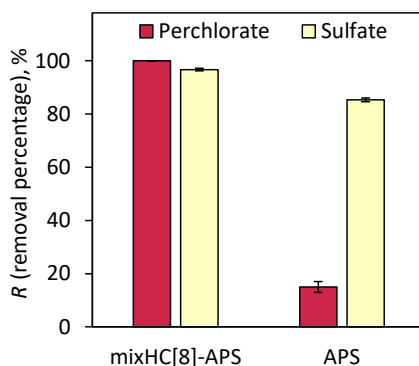
Figure 40. Perchlorate removal studies. The concentration of anions before and after SPE was determined by Dr. Priit Tikker, using ion chromatography.

The extracted perchlorate was easily released by washing mixHC[8]-APS material with water, taking advantage of the weaker binding in the aqueous medium. Such reversibility of complex formation-dissociation allows controlled capture and release of the pollutant, which can be beneficial for its further remediation.

Conclusions

The primary objectives of this thesis were to develop efficient chromatographic methods for monitoring the mechanosynthesis of hemicucurbiturils and investigate the properties of eight-membered macrocycles as functional supramolecular hosts. The key outcomes of this research are summarized as follows:

- An HPLC-UV-MS method was developed and successfully applied to screen synthetic conditions for the mechanochemical hexa-amidation of the biotin[6]uril macrocycle. This procedure enabled the separation and identification of the hexa-amide and mono-, di-, tri-, tetra- and penta-substituted side products. The acquired quantitative data based on relative peak areas was critical for optimizing reaction conditions, enabling isolation of target functionalized macrocycle in 80% yield and 99% purity.

- An HPLC-UV-MS method was developed, validated and applied in screening the solid-state synthesis of mono-biotinylated hemicucurbit[8]uril (mixHC[8]). The procedure allowed efficient separation and quantification of macrocycles, facilitating convenient yield determination prior to product isolation. The method's reliability was confirmed through selectivity, linearity, detection and quantitation limits, trueness, and reproducibility studies. Additionally, the collected data supported the validation of triphenylmethane as an internal standard. It enabled to follow changes in reaction content during entire synthetic procedure as it was added before start of the reaction in the ball mill. It was found that internal standard approach was reliable for analyzing homogenous mixtures, whereas its applicability was limited under conditions yielding inhomogeneous mixtures.

- HPLC-MS analysis was applied in profiling of the dynamic covalent library during mixHC[8] mechanochemically driven self-assembly, as well as monitoring the content of selected short homomeric oligomers. Identification and mapping of the macrocycles and linear intermediates provided valuable mechanistic insights into the dynamic changes occurring during ball-milling and aging of the reaction mixtures, crucial for synthetic optimization. The optimized conditions converged from over 100 identified intermediates into two major products, in particular new mixHC[8] was formed in 38% HPLC yield.

- Solution- and solid-state binding studies revealed that cyclohexanohemicucurbit[8]uril (cycHC[8]) forms inclusion complexes with small neutral S- and O-containing heterocycles. The macrocycle demonstrated notable potential per its surface area as a solid sorbent for the selective capture of S-containing guests from water.

- Gas-phase and solution-state host-guest studies confirmed that new mixHC[8] behaves as a selective anion receptors for chaotropic anions. The carboxylic group of the biotin unit enabled facile immobilization of mixHC[8] on the aminated silica, resulting in a functional material suitable for selective capture of perchlorate from methanolic extracts in the presence of mineral matrix.

The conducted study presents a rare example of comprehensive analysis of macrocycle assembly in the solid state, making a significant contribution to the development of new host molecules. Additionally, the discovery of hemicucurbituril inclusion complexes with neutral compounds, along with the covalent immobilization of these macrocycles on solid materials, advances the field by demonstrating the potential of 8-membered HCs as sorbents for the selective capture of environmental pollutants. The results presented in this thesis can be used in further mechanochemical studies and supramolecular applications.

References

1 E. Fischer, *Ber. Dtsch. Chem. Ges.*, 1894, **27**, 2985–2993.

2 C. J. Pedersen, *J. Am. Chem. Soc.*, 1967, **89**, 2495–2496.

3 The Nobel Prize in Chemistry 1987. NobelPrize.org. Nobel Prize Outreach AB 2024. Web <https://www.nobelprize.org/prizes/chemistry/1987/summary/> (accessed 01.09.2024)

4 The Nobel Prize in Chemistry 2016. NobelPrize.org. Nobel Prize Outreach AB 2024. Web <https://www.nobelprize.org/prizes/chemistry/2016/summary/> (accessed 01.09.2024)

5 R. Pinalli, A. Pedrini and E. Dalcanale, *Chemical Society Reviews*, 2018, **47**, 7006–7026.

6 Y. Pan, X. Hu and D. Guo, *Angew Chem Int Ed*, 2021, **60**, 2768–2794.

7 M. J. Webber and R. Langer, *Chem. Soc. Rev.*, 2017, **46**, 6600–6620.

8 D. Das, K. I. Assaf and W. M. Nau, *Frontiers in Chemistry*, 2019, **7**, 1–23.

9 J. Wankar, N. G. Kotla, S. Gera, S. Rasala, A. Pandit and Y. A. Rochev, *Adv Funct Materials*, 2020, **30**, 1909049.

10 C.-L. Deng, S. L. Murkli and L. D. Isaacs, *Chemical Society Reviews*, 2020, **49**, 7516–7532.

11 Q. Liu, Y. Zhou, J. Lu and Y. Zhou, *Chemosphere*, 2020, **241**, 125043.

12 J. Yu, D. Qi and J. Li, *Communications Chemistry*, 2020, **3**, 1–14.

13 N. N. Andersen, M. Lisbjerg, K. Eriksen and M. Pittelkow, *Isr. J. Chem.*, 2018, **58**, 435–448.

14 E. Masson, X. Ling, R. Joseph, L. Kyeremeh-Mensah and X. Lu, *RSC Advances*, 2012, **2**, 1213–1247.

15 Y. Miyahara, K. Goto, M. Oka and T. Inazu, *Angewandte Chemie International Edition*, 2004, **43**, 5019–5022.

16 R. Gujjarappa, R. Khurana, N. Fridman, E. Keinan and O. Reany, *Cell Reports Physical Science*, 2024, 102011.

17 Y. Li, N. Li, Y. Zhu, X. Meng and A. Wu, *Cryst. Growth Des.*, 2009, **9**, 4255–4257.

18 R. Aav, E. Shmatova, I. Reile, M. Borissova and F. Topić, *Org. Lett.*, 2013, **15**, 3786–3789.

19 T. Fiala and V. Sindelar, *Synlett*, 2013, **24**, 2443–2445.

20 E. Prigorchenko, S. Kaabel, T. Narva, A. Baškir, M. Fomitšenko, J. Adamson, I. Järving, K. Rissanen, T. Tamm and R. Aav, *Chem. Commun.*, 2019, **55**, 9307–9310.

21 M. Fomitšenko, E. Shmatova, M. Öeren, I. Järving and R. Aav, *Supramolecular Chemistry*, 2014, **26**, 698–703.

22 E. Prigorchenko, M. Öeren, S. Kaabel, M. Fomitšenko, I. Reile, I. Järving, T. Tamm, F. Topić, K. Rissanen and R. Aav, *Chem. Commun.*, 2015, **51**, 10921–10924.

23 K. A. Mishra, J. Adamson, M. Öeren, S. Kaabel, M. Fomitšenko and R. Aav, *Chem. Commun.*, 2020, **56**, 14645–14648.

24 S. Kaabel, R. S. Stein, M. Fomitšenko, I. Järving, T. Friščić and R. Aav, *Angew. Chem. Int. Ed.*, 2019, **58**, 6230–6234.

25 J. Svec, M. Necas and V. Sindelar, *Angew. Chem. Int. Ed.*, 2010, **49**, 2378–2381.

26 V. Havel, J. Svec, M. Wimmerova, M. Dusek, M. Pojarova and V. Sindelar, *Organic Letters*, 2011, **13**, 4000–4003.

27 M. A. Yawer, V. Havel and V. Sindelar, *Angew Chem Int Ed*, 2015, **54**, 276–279.

28 V. Havel, M. Babiak and V. Sindelar, *Chem. Eur. J.*, 2017, **23**, 8963–8968.

29   M. A. Yawer, K. Sleziakova, L. Pavlovec and V. Sindelar, *Eur. J. Org. Chem.*, 2018, **2018**, 41–47.

30   T. Fiala, K. Sleziakova, K. Marsalek, K. Salvadori and V. Sindelar, *J. Org. Chem.*, 2018, **83**, 1903–1912.

31   H. Valkenier, O. Akrawi, P. Jurček, K. Sleziaková, T. Lízal, K. Bartik and V. Šindelář, *Chem*, 2019, **5**, 429–444.

32   M. Chvojka, D. Madea, H. Valkenier and V. Šindelář, *Angew Chem Int Ed*, 2024, **63**, e202318261.

33   K. Maršálek and V. Šindelář, *Org. Lett.*, 2020, **22**, 1633–1637.

34   N. A. De Simone, M. Chvojka, J. Lapešová, L. Martínez-Crespo, P. Slávik, J. Sokolov, S. J. Butler, H. Valkenier and V. Šindelář, *J. Org. Chem.*, 2022, **87**, 9829–9838.

35   J. Sokolov and V. Šindelář, *Chemistry A European J*, 2018, **24**, 15482–15485.

36   J. Sokolov, A. Štefek and V. Šindelář, *ChemPlusChem*, 2020, **85**, 1307–1314.

37   P. Slávik, J. Torrisi, P. Jurček, J. Sokolov and V. Šindelář, *J. Org. Chem.*, 2023, **88**, 11514–11522.

38   A. Del Mauro, J. Lapešová, C. Rando and V. Šindelář, *Org. Lett.*, 2024, **26**, 106–109.

39   M. Singh, E. Solel, E. Keinan and O. Reany, *Chem. Eur. J.*, 2015, **21**, 536–540.

40   M. Singh, E. Solel, E. Keinan and O. Reany, *Chemistry A European J*, 2016, **22**, 8848–8854.

41   C. Lang, A. Mohite, X. Deng, F. Yang, Z. Dong, J. Xu, J. Liu, E. Keinan and O. Reany, *Chem. Commun.*, 2017, **53**, 7557–7560.

42   R. Khurana, F. Yang, R. Khurana, J. Liu, E. Keinan and O. Reany, *Chem. Commun.*, 2022, **58**, 3150–3153.

43   M. Lisbjerg, B. M. Jessen, B. Rasmussen, B. E. Nielsen, A. Ø. Madsen and M. Pittelkow, *Chem. Sci.*, 2014, **5**, 2647–2650.

44   M. Lisbjerg, H. Valkenier, B. M. Jessen, H. Al-Kerdi, A. P. Davis and M. Pittelkow, *J. Am. Chem. Soc.*, 2015, **137**, 4948–4951.

45   N. N. Andersen, K. Eriksen, M. Lisbjerg, M. E. Ottesen, B. O. Milhøj, S. P. A. Sauer and M. Pittelkow, *J. Org. Chem.*, 2019, **84**, 2577–2584.

46   G. Parvari, S. Annamalai, I. Borovoi, H. Chechik, M. Botoshansky, D. Pappo and E. Keinan, *Chem. Commun.*, 2014, **50**, 2494.

47   T. Lízal and V. Šindelář, *Beilstein J. Org. Chem.*, 2019, **15**, 1268–1274.

48   Q. Zeng, Q. Long, J. Lu, L. Wang, Y. You, X. Yuan, Q. Zhang, Q. Ge, H. Cong and M. Liu, *Beilstein J. Org. Chem.*, 2021, **17**, 2840–2847.

49   Y. You, A. Wang and M. Liu, *Russ J Gen Chem*, 2023, **93**, 1920–1930.

50   X. Yuan, Q. Zeng, L. Wang, Y. You, X. Cen, Q. Zhang, Q. Ge, H. Cong and M. Liu, *J Incl Phenom Macrocycl Chem*, 2023, **103**, 57–61.

51   L. Wang, J. Han, R. Pan, X. Yuan, Y. You, X. Cen, Q. Zhang, Q. Ge, H. Cong and M. Liu, *Tetrahedron Letters*, 2022, **101**, 153918.

52   S. Kaabel and R. Aav, *Isr. J. Chem.*, 2018, **58**, 296–313.

53   T. Lizal and V. Sindelar, *Isr. J. Chem.*, 2018, **58**, 326–333.

54   O. Reany, A. Mohite and E. Keinan, *Isr. J. Chem.*, 2018, **58**, 449–460.

55   M. Fomitšenko, A. Peterson, I. Reile, H. Cong, S. Kaabel, E. Prigorchenko, I. Järving and R. Aav, *New J. Chem.*, 2017, **41**, 2490–2497.

56   J. L. Howard, Q. Cao and D. L. Browne, *Chem. Sci.*, 2018, **9**, 3080–3094.

57   T. Friščić, C. Mottillo and H. M. Titi, *Angewandte Chemie*, 2020, **132**, 1030–1041.

58   L. Takacs, *J Therm Anal Calorim*, 2007, **90**, 81–84.

59   T. Friščić, S. L. Childs, S. A. A. Rizvi and W. Jones, *CrystEngComm*, 2009, **11**, 418–426.

60   M. Pascu, A. Ruggi, R. Scopelliti and K. Severin, *Chem. Commun.*, 2013, **49**, 45–47.

61   H. Shy, P. Mackin, A. S. Orvieto, D. Gharbharan, G. R. Peterson, N. Bampos and T. D. Hamilton, *Faraday Discuss.*, 2014, **170**, 59–69.

62   Q. Su and T. D. Hamilton, *Beilstein J. Org. Chem.*, 2019, **15**, 1149–1153.

63   Y. Yang, F. Bu, J. Liu, I. Shakir and Y. Xu, *Chem. Commun.*, 2017, **53**, 7481–7484.

64   D. Langerreiter, M. A. Kostiainen, S. Kaabel and E. Anaya-Plaza, *Angewandte Chemie International Edition*, 2022, **n/a**, e202209033.

65   K. Ralphs, C. Zhang and S. L. James, *Green Chem.*, 2017, **19**, 102–105.

66   A. O. Atoyebi and C. Brückner, *Inorg. Chem.*, 2019, **58**, 9631–9642.

67   L. Jicsinszky and G. Cravotto, *Molecules*, 2021, **26**, 5193.

68   D. Tan and F. García, *Chem. Soc. Rev.*, 2019, **48**, 2274–2292.

69   A. A. L. Michalchuk and F. Emmerling, *Angew Chem Int Ed*, 2022, **61**, e202117270.

70   I. Halasz, S. A. J. Kimber, P. J. Beldon, A. M. Belenguer, F. Adams, V. Honkimäki, R. C. Nightingale, R. E. Dinnebier and T. Friščić, *Nat Protoc*, 2013, **8**, 1718–1729.

71   D. Gracin, V. Štrukil, T. Friščić, I. Halasz and K. Užarević, *Angew. Chem. Int. Ed.*, 2014, **53**, 6193–6197.

72   P. F. M. de Oliveira, A. A. L. Michalchuk, A. G. Buzanich, R. Bienert, R. M. Torresi, P. H. C. Camargo and F. Emmerling, *Chem. Commun.*, 2020, **56**, 10329–10332.

73   J. G. Schiffmann, F. Emmerling, I. C. B. Martins and L. Van Wüllen, *Solid State Nuclear Magnetic Resonance*, 2020, **109**, 101687.

74   A. A. L. Michalchuk, I. A. Tumanov, S. Konar, S. A. J. Kimber, C. R. Pulham and E. V. Boldyreva, *Advanced Science*, 2017, **4**, 1700132.

75   C. Gomes, M. Peixoto and M. Pineiro, *Molecules*, 2021, **26**, 6652.

76   E. Oliva, D. Mathiron, S. Rigaud, E. Monflier, E. Sevin, H. Bricout, S. Tilloy, F. Gosselet, L. Fenart, V. Bonnet, S. Pilard and F. Djedaini-Pilard, *Biomolecules*, 2020, **10**, 339.

77   P. Thordarson, *Chem. Soc. Rev.*, 2011, **40**, 1305–1323.

78   F. P. Schmidtchen, in *Analytical Methods in Supramolecular Chemistry*, John Wiley & Sons, Ltd, 2006, pp. 55–78.

79   J. L. Casas-Hinestroza, M. Bueno, E. Ibáñez and A. Cifuentes, *Analytica Chimica Acta*, 2019, **1081**, 32–50.

80   M. Lisbjerg, B. E. Nielsen, B. O. Milhøj, S. P. A. Sauer and M. Pittelkow, *Org. Biomol. Chem.*, 2015, **13**, 369–373.

81   C. Rando, J. Vázquez, J. Sokolov, Z. Kokan, M. Nečas and V. Šindelář, *Angew Chem Int Ed*, , DOI:10.1002/anie.202210184.

82   K. I. Assaf and W. M. Nau, *Org. Biomol. Chem.*, 2023, **21**, 6636–6651.

83   F. Biedermann, W. M. Nau and H.-J. Schneider, *Angew. Chem., Int. Ed.*, 2014, **53**, 11158–11158.

84   S. Kaabel, J. Adamson, F. Topić, A. Kiesilä, E. Kalenius, M. Öeren, M. Reimund, E. Prigorchenko, A. Lõokene, H. J. Reich, K. Rissanen and R. Aav, *Chem. Sci. J.*, 2017, **8**, 2184–2190.

85   X.-Y. Jin, F. Wang, H. Cong and Z. Tao, *J. Incl. Phenom. Macrocycl. Chem.*, 2016, **86**, 249–254.

86   X.-Y. Jin, J.-L. Zhao, F. Wang, H. Cong and Z. Tao, *J. Organomet. Chem.*, 2017, **846**, 1–5.

87   M. Öeren, E. Shmatova, T. Tamm and R. Aav, *Phys. Chem. Chem. Phys.*, 2014, **16**, 19198–19205.

88   L. Ustrnul, S. Kaabel, T. Burankova, J. Martõnova, J. Adamson, N. Konrad, P. Burk, V. Borovkov and R. Aav, *Chem. Commun.*, 2019, **55**, 14434–14437.

89   E. T. Urbansky, *Environ Sci & Potlut Res*, 2002, **9**, 187–192.

90   P. Kumarathilaka, C. Oze, S. P. Indraratne and M. Vithanage, *Chemosphere*, 2016, **150**, 667–677.

91   P. Itterheimová, J. Bobacka, V. Šindelář and P. Lubal, *Chemosensors*, 2022, **10**, 115.

92   R. Khurana, F. Alami, C. A. Nijhuis, E. Keinan, J. Huskens and O. Reany, *Chemistry A European J*, 2024, **30**, e202302968.

93   O. Reany, M. Romero-Ruiz, R. Khurana, P. Mondal, E. Keinan and H. Bayley, *Angew Chem Int Ed*, 2024, e202406719.

94   P. Turebayeva, V. Luchsheva, D. Fedorishin, R. Yerkassov, A. Bakibaev, S. Bolysbekova, T. Tugambayeva, S. Sergazina and N. Nurmukhanbetova, *IJMS*, 2023, **24**, 16126.

95   G. Zhumabayeva, P. Turebayeva, A. Ukhov, D. Fedorishin, A. Gubankov, V. Luchsheva, I. Kurzina, A. Bakibaev, R. Ryskaliyeva, G. Abdullina, S. Bolysbekova and R. Yerkassov, *Materials*, 2023, **16**, 7257.

96   G. Magna, M. Šakarašvili, M. Stefanelli, G. Giancane, S. Bettini, L. Valli, L. Ustrnul, V. Borovkov, R. Aav, D. Monti, C. Di Natale and R. Paolesse, *ACS Appl. Mater. Interfaces*, 2023, **15**, 30674–30683.

97   Kinetex XB-C18 stationary phase description by Phenomenex. Web <https://www.phenomenex.com/products/kinetex-hplc-column/kinetex-xb-c18> (accessed 01.09.2024)

98   F. Cuccu, L. De Luca, F. Delogu, E. Colacino, N. Solin, R. Mocci and A. Porcheddu, *ChemSusChem*, 2022, **15**, e202200362.

99   L. Ustrnul, T. Jarg, M. Jantson, I. Osadchuk, L. Anton and R. Aav, 2024.

100   E. Suut-Tuule, T. Jarg, P. Tikker, K.-M. Lootus, J. Martõnova, R. Reitalu, L. Ustrnul, J. S. Ward, V. Rjabovs, K. Shubin, J. V. Nallaparaju, M. Vendelin, S. Preis, M. Öeren, K. Rissanen, D. Kananovich and R. Aav, *Cell Reports Physical Science*, 2024, 102161.

101   M. Dračínský, C. S. Hurtado, E. Masson and J. Kaleta, *Chem. Commun.*, 2021, **57**, 2132–2135.

102   M. Tabakci, *J Incl Phenom Macrocycl Chem*, 2008, **61**, 53–60.

103   K. M. Cannon, D. T. Britt, T. M. Smith, R. F. Fritsche and D. Batcheldor, *Icarus*, 2019, **317**, 470–478.

Acknowledgements

I am forever grateful to my supervisor Prof. Riina Aav for providing the opportunity to carry out research in her group and introducing me to the fascinating world of science. Thank you for your unwavering support, insightful discussions, and for the trust and freedom you have given me in organizing my work. Your constant encouragement has been truly inspiring. I would also like to express my deepest appreciation to Adj. Prof. Elina Kalenius for hosting and supervising me at the University of Jyvaskyla.

Doctoral studies are not just about the research, but also the amazing people you meet on the way. Therefore, I would like to extend my gratitude to all the colleagues, collaborators and co-authors with whom we interacted during these years.

We started this PhD journey together with Tanya, whom I dearly thank for the work and fun shared together, our conference trips and long evenings at the department, exchanging knowledge and just always being there for each other.

My research and progress would have not been possible without the input from the members of TalTech supramolecular chemistry group. I wish to acknowledge Dr. Dzmitry Kananovich for his passion for science, bright ideas and contagious enthusiasm. Elina, Tanya and Jaga, it has been a great pleasure working on the common projects, I believe we always made a nice synthesis-analysis team! Thank you for including me into your topics and being wonderful colleagues. I am extremely grateful to Dr. Lukas Ustrnul for his help and fruitful discussions on host-guest chemistry and data treatment. Nele, Marko, Mari-Liis, Ngan, Kristjan, Kamini, Karin, Aivar, Marina, Mario, Elena, Riin and Rauno, thank you for the inspirational group seminars, aid with the lab and department matters, delicious lunches seasoned with conversations, and memorable trips.

A very special thanks goes to the ladies from 331 office – Ženja, Elina, Ketren and Eve. No words can truly capture how much I cherish your friendship. Thank you for accepting me, brainstorming over confusing data together and being a huge support at all times.

Adapting to life in Estonia would not have been easy without the warm welcome and assistance of all the colleagues from the 3rd and 4th floors, which I deeply appreciate. I am especially thankful to Dr. Ivar Järving for sharing his technical wisdom and Assoc. Prof. Maria Kuhtinskaja for her kind help, reviewing this thesis and providing valuable feedback. Nastya, Margo and Assist. Prof. Maksim Ošeka, thank you for the good times.

I would like to thank my former co-workers from Minsk, to who I owe most of my lab skills. Thank you for encouraging me to strive for more, but most importantly for staying in touch and keeping our friendship alive. I am immensely grateful to my family and friends for their love and support despite the miles between us. Julia, thank you for repeatedly proving that time and distance do not matter when it is a bond for life.

Last but not least, my heartfelt thanks goes to my husband Sten-Fred. Thank you for sharing all the ups and downs, introducing me to Dunning-Kruger effect, attempting to teach me the basics of stoicism and always finding a way to make me smile. I would not have made it without you. But hey, house Järg will now have a doctor of their own!

Abstract

Mechanosynthesis of Hemicucurbiturils and Their Complexation: an Analytical Study

The present dissertation focuses on the development of chromatographic and mass spectrometric methods for monitoring the mechanosynthesis of hemicucurbiturils (HCs), and investigating the complexation of eight-membered macrocycles with anions and neutral electron-rich guest molecules.

Two fundamentally different mechanochemical reactions were analyzed in this thesis. The first reaction performed in a ball mill involved the hexafunctionalization of biotin[6]uril via amide coupling with phenylalanine methyl ester producing a mixture of fully and partially amidated macrocycles. An HPLC-UV-MS method developed to monitor the process and evaluate the synthetic conditions lead to optimization of the target compound's yield to 80% and purity to 99%. The second study focused on the solid-state multi-component condensation reaction of mono-biotinylated hemicucurbit[8]uril (mixHC[8]). The assembly of this macrocycle proceeds through dynamic covalent chemistry, resulting in the formation of numerous intermediates and side products, with over 100 compounds identified in this work. An HPLC-UV-MS method was developed and validated to determine the yields of the main products. To assess the representativeness of samples taken from the crude mixtures, a solid internal standard, triphenylmethane, was added to the reaction mixtures before milling. Rigorous HPLC-MS analysis of mixHC[8] crude mixtures enabled mapping of the dynamic covalent library, tracking the composition changes throughout the reaction, and gaining insights into the solid-state chemical transformations and reaction mechanism.

The host-guest studies of cycHC[8] revealed that the eight-membered hemicucurbituril is capable of forming inclusion complexes with neutral S- and O-heterocycles. Complexation of these guests was examined in both solid and solution phases using various techniques, including single-crystal X-ray diffraction, nuclear magnetic resonance spectroscopy, and isothermal titration calorimetry (ITC). Additionally, the macrocycles were tested as sorbents for removing neutral heterocycles from water through solid-phase extraction, with cycHC[8] proving particularly effective and selective for the extraction of 1,3-dithiolane from aqueous solution. The properties of the newly synthesized mixHC[8] diastereomers were investigated in the gas phase using MS and in solution by ITC. It was found that the overall anion-binding profile was similar to that of unsubstituted cycHC[8], with (+)-mixHC[8] showing stronger binding to perchlorate than its analogs. Subsequently, mono-biotinylated hemicucurbit[8]uril was covalently immobilized on aminopropyl silica gel, creating a functional material. Solid-phase extraction demonstrated that the new material is suitable for perchlorate binding from a simulated Martian soil matrix.

This research makes a significant contribution to the advancement of new supramolecular receptors through mechanochemistry. Furthermore, it was demonstrated that hemicucurbiturils are suitable host molecules for binding both anionic and neutral compounds. Moreover, the covalent immobilization of these macrocycles on solid materials opens up possibilities for their use as sorbents, such as in the selective removal of pollutants from the environment. This work is important for the development of new synthetic and analytical applications and could find use in the chemical industry and environmental monitoring sectors.

Lühikokkuvõte

Hemikukurbituriilide mehhanosünteesi ja nende komplekseerimise analüüs

Käesolevas väitekirjas keskendutakse kromatograafiliste ja massispektromeetriliste meetodite väljatöötamisele hemikukurbituriilide (HC-de) mehhanokeemilise sünteesi jälgimiseks ning kaheksaliikmeliste makrotsüklite komplekseerimise uurimisele anioonide ja neutraalsete elektronirikaste külalismolekulidega.

Selles uuringus analüüsiti kahte põhimõtteliselt erinevat mehhanokeemilist reaktsiooni. Esiteks vaadeldi kuulveskis läbiviidud biotiin[6]uriili funktsionaliseerimist kuue fenüülalaniini metüülestriga, mis andis täielikult ja osaliselt amideeritud makrotsüklite segu. Reaktsiooni jälgimiseks ja sünteesitingimuste hindamiseks töötati välja HPLC-UV-MS meetod, mis võimaldas optimeerida eesmärkühendi saagist 80%-ni ja eesmärkühendi puhtuseks saadi 99%. Teiseks uuriti mono-biotinüleeritud hemikukurbit[8]uriili (mixHC[8]) sünteesi tahkes faasis mitmekomponentses kondensatsioonireaktsioonis. Viimase makrotsükli teke toimus dünaamilise kovalentse keemia vahendusel, mille käigus moodustub arvukalt vahe- ja kõrvalprodukte. Töö käigus indentifitseeriti neist üle 100 ühendi. Põhisaaduste saagiste määramiseks töötati välja ja valideeriti HPLC-UV-MS meetod. Reaktsioonide toorsegudest võetud proovide esinduslikkuse hindamiseks lisati reaktsioonisegudele, enne nende kuulveskis jahvatamist, tahket sisestandardit trifenüülmetaani. MixHC[8] toorsegude põhjalik HPLC-MS analüüs võimaldas kaardistada tekkinud dünaamilise kovalentse raamatukogu, jälgida reaktsiooni jooksul selle muutuvat koostist, luua arusaam tahkes faasis toimuvatest keemilistest muutustest ning reaktsioonimehhanismist.

Tsükloheksanohemikukurbit[8]uriili (cycHC[8]) komplekside uuringud näitasid, et 8-ühikuline hemikukurbituriil võib moodustada laenguta S- ja O-heterotsüklitega iseorganiseeruvaid peremees-külaline süsteeme. Heterotsüklite komplekseerumist uuriti tahkes ja lahuse faasis, monokristall-röntgendifraktsiooni, tuumamagnetresonantsspektroskoopia ja isotermilise tiitrimis-kalorimeetriaga (ITC). Lisaks testiti makrotsükleid sorbentidena, et eraldada veest neutraalseid heterotsükleid tahkefaasilise ekstraktsiooni abil. Leiti, et cycHC[8] on eriti efektiivne ja selektiivne 1,3-ditiolaani sidumiseks vesilahusest. Käesoleva töö käigus esmakordselt sünteesitud mixHC[8] diastereomeeride omadusi uuriti gaasifaasis MS-i ja lahuses ITC abil. Leiti, et üldine anioonide sidumise iseloom sarnanes asendamata cycHC[8]-ga, ning lisaks näidati, et HC[8]-de sidumises on erisusi ning (+)-mixHC[8] seob perkloraati tugevamini võrreldes enda analoogidega. Seejärel immobiliseeriti mono-biotinüleeritud hemikukurbit[8]uriil kovalentselt aminopropüülsilikageelile, millega loodi funktsionaalne materjal. Tahke-faasi ekstraktsiooni abil näidati, et uus materjal sobib perkloraadi sidumiseks Marsi pinnase simuleeritud maatriksist.

Käesolev uurimistöö annab märkimisväärse panuse mehhanokeemia abil uue supramolekulaarsete retseptorite väljatöötamisse. Demonstreeriti, et hemikukurbituriilid on sobivad võõrustaja-molekulid nii anioonsete kui ka neutraalsete ühendite sidumiseks, veelgi enam nende makrotsüklite kovalentne immobiliseerimine tahkele materjalile loob võimaluse nende kasutamiseks sorbenditena, näiteks keskkonnast saasteainete selektiivseks eraldamiseks. Töö on oluline nii uue sünteesi kui analüütiliste lahenduste loomisel ja võib leida kasutust keemiatööstuse ja keskkonnaseire valdkondades.

Appendix 1

Mechanochemical Synthesis of Amides with Uronium-Based Coupling Reagents: A Method for Hexa-amidation of Biotin[6]uril

Tatsiana Dalidovich, Kamini A. Mishra, Tatsiana Shalima, Marina Kudrjašova, Dzmitry G. Kananovich,* and Riina Aav*

Read Online

ACCESS | Metrics & More | Article Recommendations | Supporting Information

ABSTRACT: Solvent-free, atom-efficient, and mechanochemically activated reactions have emerged as synthetic strategy for sustainable chemistry. Herein we report a new mechanochemical approach for the amide coupling of carboxylic acids and amines, mediated by combination of (1-cyano-2-ethoxy-2-oxoethylidenaminooxy)-dimethylaminomorpholinocarbenium hexafluorophosphate (COMU) or N,N,N',N'-tetramethylchloroformamidinium hexa-fluorophosphate (TCFH) and K_2HPO_4. The method delivers a range of amides in high yields (70−96%) and fast reaction rates. The reaction protocol is mild, keeps stereochemical integrity of the adjacent to carbonyl stereocenters, and streamlines isolation procedure for solid amide products. Minimal waste is generated due to the absence of bulk solvent. We show that K_2HPO_4 plays a dual role, acting as a base and a precursor of reactive acyl phosphate species. Amide bonds from hindered carboxylic acids and low-nucleophilic amines can be assembled within 90 minutes by using TCFH in combination with K_2HPO_4 or N-methylimidazole. The developed mechanochemical liquid-assisted amidation protocols were successfully applied to the challenging couplings of all six carboxylate functions of biotin[6]uril macrocycle with phenylalanine methyl ester, resulting in 80% yield of highly pure hexa-amide-biotin[6]uril. In addition, fast and high-yielding synthesis of peptides and versatile amide compounds can be performed in a safe and environmentally benign manner, as verified by green metrics.

KEYWORDS: mechanochemistry, solvent-free chemistry, amides, peptides, amide coupling reagents, macrocycle, hemicucurbituril, green metrics
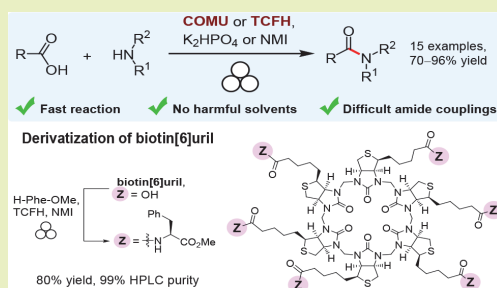
■ INTRODUCTION

The amide bond is widespread in both natural compounds and artificial materials. It occurs in molecules fundamental to life, such as peptides and proteins, as well as in synthetic polymers and in a massive array of pharmaceuticals. In fact, amide preparation from carboxylic acids and amines represents the most frequently applied chemical transformation in drug production and comprises about 25% of the current medicinal chemistry synthetic toolbox.[1] As a consequence of its wide usage, the development of sustainable amidation methods was listed among the top green chemistry research priorities by the American Chemical Society Green Chemistry Pharmaceutical Roundtable (ACS GCIPR) in 2007[2] and has been retained in the recent revision.[3] Although direct condensation of carboxylic acids and amines with water as a single byproduct can be considered a "green" landmark in the field, it remains impractical because of the process's harsh reaction conditions ($T > 100$ °C) and limited substrate scope.[4−6] A robust method of amide synthesis commonly requires prior activation of a carboxylic function to replace OH with a better leaving group.[7−9] Notably, this is also the case in biosynthetic

pathways, including the translation process and nonribosomal enzymatic transformations.[10−13] For laboratory and industrial use, vast numbers of amide coupling reagents, performing in situ activation of carboxylic acid, have been developed in the quest for faster, milder, and high-yielding amidation protocols.[14,15] The low atom economy of these reagents and accompanying safety issues are their major drawbacks, which has incited the development of alternative approaches.[16−19] Important advancements have thus far followed traditional solution-based approaches; however, solvent is actually responsible for 80−90% of mass consumption in a typical chemical process and also plays a major role in overall toxicity.[20] In this way, solvent greatly outperforms the contributions of reagents themselves. Hazardous solvents like
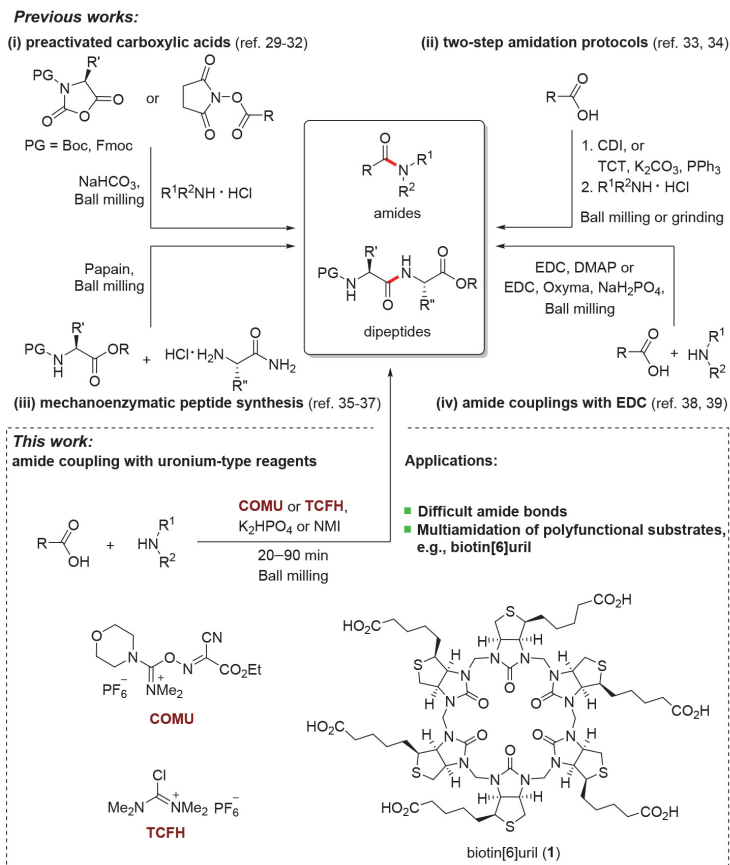
Scheme 1. Overview of the State-of-Art Mechanochemical Amidation Approaches and Outline of the Current Work[29−39]

DMF and DCM are preferred in industrial amide synthesis, reinforcing both environmental and safety concerns.[17,21] Therefore, the application of solvent-free techniques represents an efficient way to improve the overall process mass intensity and to prevent generation of hazardous waste. Recent advances in mechanochemistry and its related fields have established solvent-free reactions as environmentally friendly tools to perform chemical transformations that are no less efficient than the conventional solution-based chemistry.[22−25]

In the area of amide synthesis, the benefits of solvent-free techniques have not remained unnoticed and have been previously demonstrated in numerous studies (Scheme 1).[26−28] For example, mechanosynthesis of various amides and peptides has been performed from a series of activated carboxylic acid derivatives, such as N-carboxyanhydrides,[29,30] N-hydroxysuccinimide esters,[31] and N-acyl benzotriazoles.[32] N-Acyl imidazoles[33] and acyloxytriazine esters[34] have been produced mechanochemically from carboxylic acids prior to reacting with amines. Notably, even papain enzyme can catalyze the formation of peptides from the corresponding amino acid building blocks under solvent-free conditions.[35−37] In addition, direct coupling of amines with carboxylic acid has

been demonstrated by using 1-ethyl-3-(3-(dimethylamino)-propyl)carbodiimide (EDC) as a coupling reagent.[38,39] In general, EDC-mediated transformations have shown remarkably short reaction times (typically within 10−30 min), high yields, and simple workup protocols.

Following these prominent earlier contributions,[26−39] we aimed to further expand the scope and synthetic utility of the mechanochemical amidation methods. The current research was impelled by three objectives: First, most of the amide coupling reagents are simply not efficient enough for a range of substrates,[8] which require expansion of the established one-step mechanochemical amidation protocols beyond the previously applied EDC; for that purpose, in this work we mapped the coupling efficiency of uronium-type reagents (COMU and TCFH, Scheme 1) on several carboxylic acid/amine pairs. Second, the scope of previously published mechanochemical approaches was evaluated based mainly on peptide synthesis, while the challenging couplings of sterically hindered carboxylic acids and low nucleophilicity amines remained virtually unproven. Here we demonstrate that such difficult amide bonds can also be assembled under solvent-free conditions. Implementation of the two objectives mentioned

Scheme 2. Optimization Experiments[a]
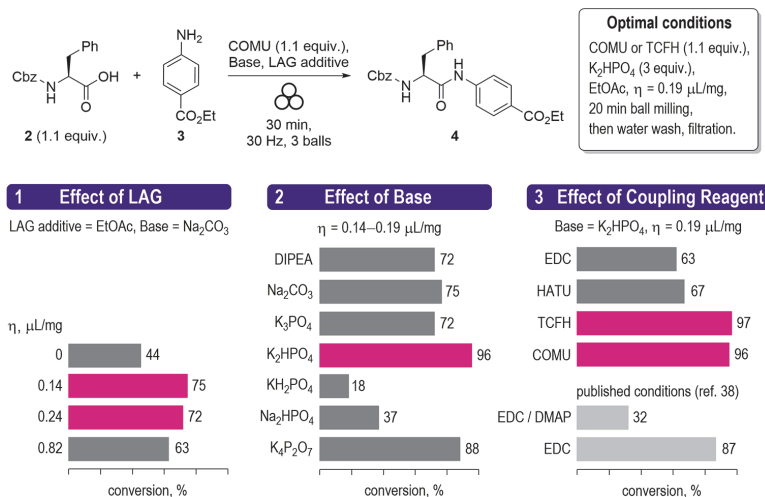
[a]Conversion of **3** into **4** according to ^{1}H NMR analysis of the crude reaction mixtures.

above was required as a prerequisite for the third objective as our ultimate goal. Chiral hemicucurbiturils[40−45] are oligomeric macrocycles and are made efficiently from uniformly functionalized monomers. Nevertheless, in spite of their relatively step-efficient synthesis, their postmodifications might be challenging. Therefore, we chose carboxyl-group bearing hemicucurbituril, the biotin[6]uril[46−48] for demonstrating applicability of mechanochemistry for uniform derivatization of oligomeric macrocycles. Despite the apparent ease of such a transformation, it also presented a substantial challenge: The 6-fold stepwise amidation of carboxylate groups in **1** is inevitably accompanied by accumulation of the "failed" under-functionalized products if incomplete coupling occurs at each step. Limited solubility of **1** in the common organic solvents dictates additional practical inconvenience of the traditional solution chemistry; in fact, only dipolar aprotic solvents like DMF can be used. Here we showed that application of solvent-free techniques, additionally reinforced with the reactive uronium-type amide coupling reagents, allows the desired functionalization of **1** in a high-yielding, scalable, and sustainable manner, avoiding harmful solvents or significant reagent excess.

■ RESULTS AND DISCUSSION

Development of Mechanochemical Amidations with Uronium-Type Reagents. At the outset, amide coupling of Cbz-protected L-phenylalanine (**2**) and ethyl 4-aminobenzoate (benzocaine, **3**), mediated by COMU as a representative "green" uronium-type amide coupling reagent,[49−51] was selected as a model process (Scheme 2). We aimed to screen and compare the results of various reaction conditions, including the evaluation of coupling efficiency for different coupling reagents beyond the COMU itself, to reveal the most promising hits in terms of product yield and green chemistry requirements. The choice of aromatic amine **3** was dictated by its reduced nucleophilicity in comparison with aliphatic amines, additionally attenuated by an electron-withdrawing ethoxycarbonyl group. We expected that suppressed reactivity

of **3** in the carbonyl addition reactions would facilitate more reliable differentiation of various coupling conditions. Use of phenylalanine derivative **2** as coupling counterpart provided an additional opportunity to examine the resistance α-stereocenter toward its possible epimerization, as commonly encountered in peptide synthesis.[9,15]

The test reactions were run in a Form-Tech Scientific FTS1000 shaker mill operating at 30 Hz by using 14 mL zirconia-coated milling jars, 3 × 7 mm zirconia milling balls and typical solid reactants loading around 0.3−0.4 g (including 0.2 mmol of amine **3** as a limiting substrate). After 30 min of milling time, a sample of the crude reaction mixture was treated with CDCl$_3$, followed by separation of insoluble inorganic materials. The conversion of amine **3** into amide **4** was determined by ^{1}H NMR analysis (see the Supporting Information for the details). The amide coupling reagent, base, and amount of liquid additive needed to assist the grinding process (Scheme 2) were identified as the three most crucial parameters affecting the yield of amide **4**, as described below.

The addition of a small volume of liquid constitutes an efficient method to enhance the performance of solvent-free mechanochemical reactions, known as liquid-assisted grinding (LAG).[22,24] The ratio of the volume of liquid (μL) added to the amount of solid present (mg) is denoted as η (μL/mg).[52] A value of $\eta = 0$ generally corresponds to dry grinding, but in a typical LAG process, η is usually between 0 and 1.[24] Although LAG cannot be described as a totally solvent-free technique, it requires a minimal amount of liquid, which is especially advantageous if a green solvent is used. Among the latter,[20,53,54] ethyl acetate appears to be the most promising and chemically compatible candidate to act as a LAG additive in COMU-mediated amide coupling. In our experiments (Scheme 2, Chart 1), the addition of ethyl acetate indeed showed a pronounced effect on the yield of amide **4**, generated in the mixture of solid reactants **2** and **3**, with COMU reagent and sodium carbonate (ca. 10 equiv) as a base. Although dry grinding provided a rather modest outcome (44% conversion),

LAG resulted in a markedly improved reaction performance, with the optimal η value in a range of 0.14−0.24 μL/mg, while the further increase of η led to slightly diminished conversion values.

The choice of base is also important in amide coupling. State-of-the-art solution approaches commonly apply non-nucleophilic tertiary amines, e.g., N,N-diisopropylethylamine (DIPEA).[15] However, the use of cheap and nontoxic inorganic salts, e.g., $NaHCO_3$, K_2CO_3, and NaH_2PO_4,[29,31,34,39] insoluble in common organic solvents, can be considered as an additional advantage of mechanochemical reactions. In our hands (Scheme 2, Chart 2), replacement of DIPEA with Na_2CO_3 gave similar conversion values (72 vs 75%). For further process optimization, a range of readily available phosphate salts, with notably distinct pK_a values, were screened. Among them, potassium pyrophosphate $K_4P_2O_7$ and dipotassium phosphate K_2HPO_4 provided the best outcomes, especially the latter (96% conversion). Generally, the performance of phosphate salts does not correlate with Brønsted basicity of the respective anions. Although the poor outcome with KH_2PO_4 (only 18% conversion) in comparison with K_2HPO_4 (96%) could be probably connected with the significantly reduced base strength of the former (respective pK_a values 2.12 vs 7.21; the pK_a of RCO_2H is typically about 4−5 in aqueous media),[55] much more basic K_3PO_4 (pK_a 12.32) also afforded amide 4 with reduced efficiency (72%). Surprisingly, the countercation effect (Na^+ vs K^+) also had a prominent impact on reaction outcome (37 vs 96%, for Na_2HPO_4 and K_2HPO_4, respectively). These results clearly indicate that the effect of an inorganic base on a solid-state reaction is more intricate than trivial proton transfer.

Finally, amide coupling reagents are essential for attaining high yields. The selection of coupling reagent was governed by considering chemical (substrate scope, reactivity), safety, and environmental issues. Uronium salts are advantageous because of their prominent reactivity and efficient reaction rates,[8,14] but the most commonly applied triazole-based reagents, such as HBTU and HATU, possess dangerous explosive properties[56] and pose significant health risks.[57] COMU was introduced as a safe and "greener" replacement.[49,50,58] To our delight, COMU also noticeably exceeded the coupling efficiencies of HATU and EDC in our experiments (Scheme 2, Chart 3), delivering a high 96% conversion. TCFH can be considered as an even more reactive alternative with better atom economy, affording a high 97% yield of amide 4 within only 10 min.

The mechanochemical amidation with COMU/K_2HPO_4 was also rapid, reaching the maximal conversion within 20 min (Figure 1; see the Supporting Information for further detail), far surpassing the rate of the solution-based process (in DMF-d_7, Figure 1). The latter reached the maximal 70% conversion after approximately 20 h (see the Supporting Information). Concurrently, about 30% of COMU reagent degraded due its well-known hydrolytic instability in DMF solutions, which is often referred as the main disadvantage of COMU.[59,60] Evidently, this drawback can be fully eliminated under solvent-free conditions.

After achieving these results in the optimization experiments, we formulated the optimal experimental procedure as follows: COMU or TCFH (1.1 equiv) as coupling reagents, K_2HPO_4 (3 equiv) as base, ethyl acetate as LAG additive, and 20 min milling time. The amount of solid base (3 equiv) was adjusted to keep η within the optimal range (∼0.2 μL/mg), but not less than 2 equiv was required according to the
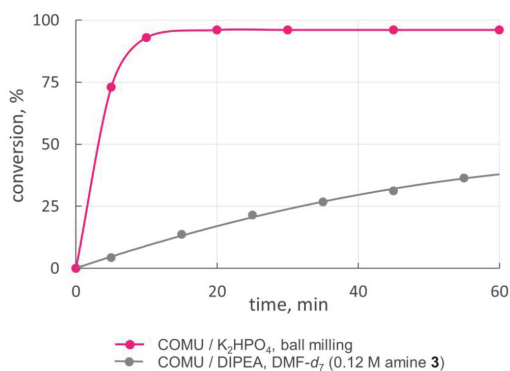
Figure 1. Accumulation of amide 4 over time in mechanochemical (purple) and solvent-based (gray) reactions.

reaction stoichiometry. Furthermore, an additional equivalent of K_2HPO_4 was required to release free amine when the ammonium salt was used as the starting material. Isolation of pure amide 4 was achieved with a high 96% yield by simple water wash and filtration since all byproducts are water-soluble. No detectable racemization of the chiral center in 4 occurred during the synthesis, as was established by the chiral-phase HPLC chromatography (see the Supporting Information).

Green Chemistry Metrics Comparison. The advantages and drawbacks of the developed mechanochemical amidation methods were further revealed and compared with the solution-based reaction by analyzing the respective green metrics (Table 1). The metrics were calculated and assessed by marking them with red, orange, or green flags by following the Clark's unified metrics toolkit (see the Supporting Information).[61] Atom economy (AE), reaction mass efficiency (RME), and process mass intensity (PMI) are defined as follows:[61]

$$AE = \frac{\text{molecular weight of product}}{\text{total molecular weight of reactants}} \times 100 \tag{1}$$

$$RME = \frac{\text{mass of isolated product}}{\text{total mass of reactants}} \times 100 \tag{2}$$

$$PMI = \frac{\text{total mass in a process}}{\text{mass of product}} \tag{3}$$

First, isolated yields and product purity were much better in mechanochemical reactions, due to the higher conversion and more facile isolation procedure discussed above. Atom economy was a bit higher for the TCFH-mediated reaction because of the lower molecular weight of TCFH. RME reflects both product yield and atom economy issues and was lower for the solution-based reaction. Comparison of PMI values clearly shows that mechanochemical reactions produce far less waste. Excluding mass-extensive workup procedures, solvent occupied 84% of PMI for the solution-based reaction and only about 15% (LAG additive) for the mechanochemical conditions. Furthermore, sustainable solvents like water and ethyl acetate were used in the latter, in contrast with toxic DMF.

To determine the safety risks, a combination of physical, health, and environmental threats must be assessed, which can be done with the help of MSDS[62] and further available safety data.[56] DMF, for instance, is a flammable (H226), acute toxic

Table 1. Comparison of Green Metrics for Mechanochemical and Solution-Based Amidation Reactions

Metrics	Mechanochemistry		Solution[a]
	COMU / K$_2$HPO$_4$	TCFH / K$_2$HPO$_4$	COMU / DIPEA in DMF
Yield (%)[b]	96 🟢	92 🟢	70 🟡
Atom economy (%)[c]	50	60	50
RME (%)	46	53	35
PMI (total), including:	196.3	203.7	1464.7
PMI (reactants)	3.4	3.1	3.7
PMI (solvent)	0.6	0.6	18.9
PMI (work-up)	192.3	200	1442.2[d]
Solvent choice	EtOAc, water 🟢	EtOAc, water 🟢	DMF 🔴
Work-up, isolation	filtration 🟢	filtration 🟢	chromatography 🔴
Health and safety	🟡	🔴	🔴
Main hazard statements[e]	H302, H312	H360	H226, 312, 332, 360

[a]Following the published protocol, see ref 51. [b]Yield of isolated product. [c]Including coupling reagent. [d]Excluding column chromatography. [e]See the Supporting Information for additional safety data.

(H312, 332), as well as a reproductive toxin (H360) and can thus be cited as the main hazard contributor for the solution-based process, which therefore received a red flag. For the mechanochemical reactions, the TCFH-mediated process was given a red flag due to the production of tetramethylurea byproduct (reproductive toxin, H360). In contrast, exothermic decomposition with a thermal onset of 127 °C can be considered as the main hazard of COMU, according to a recent study.[56] However, this property enables an orange flag since the temperature increase inside of the milling jar has not been examined. On the basis of the literature reports on temperature monitoring during the milling,[63,64] we could expect that the temperature increase during the milling stays lower than the thermal onset of COMU. To conclude, although the developed mechanochemical amidation conditions cannot be considered totally safe, the risks are minimal because of its room-temperature operation and relatively low amount of produced waste, as opposed to the solution-based reaction (see the Supporting Information for additional safety considerations).

Substrate Scope for Mapping Reactivity with COMU and TCFH. Having established the optimal conditions, substrate scope, and limitations was briefly examined on a range of amine and acid coupling partners (Scheme 3).

The substrate scope included, besides others, N- and C-protected amino acids and pharmaceutically relevant starting materials, e.g., (S)-naproxen, (S)-ibuprofen, benzocaine 3, and N-Boc-protected piperazine. In addition to the foremost example of Cbz-masked amide (S)-4 comprehensively described above, its Fmoc-protected analogue (R)-5 was obtained in a high 95% yield by using the COMU-mediated reaction. Following the same protocol, dipeptides 6 and 7 with sterically hindered amino acid residues (phenylalanine and valine) were flawlessly prepared in high yields. No detectable epimerization of the stereocenters was noted in these cases. Coupling of (S)-(+)-6-methoxy-α-methyl-2-naphthaleneacetic acid [(S)-naproxen] with amine 3 provided a more demanding

test for stereochemical integrity, since 2-arylpropionic acids are prone to easy epimerization.[65−68] Amide product (S)-8 was obtained from (S)-naproxen with a high 86% yield and excellent stereochemical purity (>99% ee). This was also the case in the TCFH-mediated reaction, which showed high reactivity and a subtle amount of epimerization for (S)-9. However, amidation of (S)-ibuprofen (98% ee) produced (S)-10 with slightly degraded optical purity (93−94% ee). Crude amides 10, 12, and 15 appeared as oils immediately following the milling, which eventually enabled a chromatographic isolation for these cases (see the Supporting Information).

One advantage of TCFH- over COMU-mediated amide coupling is the higher reactivity of the former reagent, which makes it more suitable for less reactive substrates. This property was explicitly revealed during the amidation of sterically hindered *ortho*-substituted benzoic acids. Thus, coupling of benzoic acid with benzocaine 3 proceeded well under the COMU-mediated protocol, furnishing amide 11 in a 93% yield after 20 min of milling time. Conversely, 2,4,6-trimethylbenzoic acid under the same conditions produced only 22% of target amide 14, without any further improvement, even when a longer milling time (up to 60 min) was applied. After the brief optimization studies (see the Supporting Information), we found that a slight excess (1.3 equiv) of more reactive TCFH and at least 60 min of milling time are required to attain a high 89% yield of 14. Moreover, chromatographic purification of 14 was necessary to separate mesitoic anhydride impurity. Diminished reactivity was also observed for 2,6-difluorobenzoic acid, furnishing amides 15 and 16 in reactions with N-Boc piperazine and low nucleophilicity amine 3 in acceptable yields after milling times of 40 and 60 min, respectively. However, coupling of the same amines with benzoic and 3,5-bis(trifluoromethyl)benzoic acids proceeded flawlessly, producing amides 12 and 13 with excellent yields and brief reaction times.

Activating Effect of Phosphate Salts. During the optimization studies, the enhancement of yields with

Scheme 3. Substrate Scope for Mechanochemical Amidation with COMU/K₂HPO₄ and TCFH/K₂HPO₄ Systems
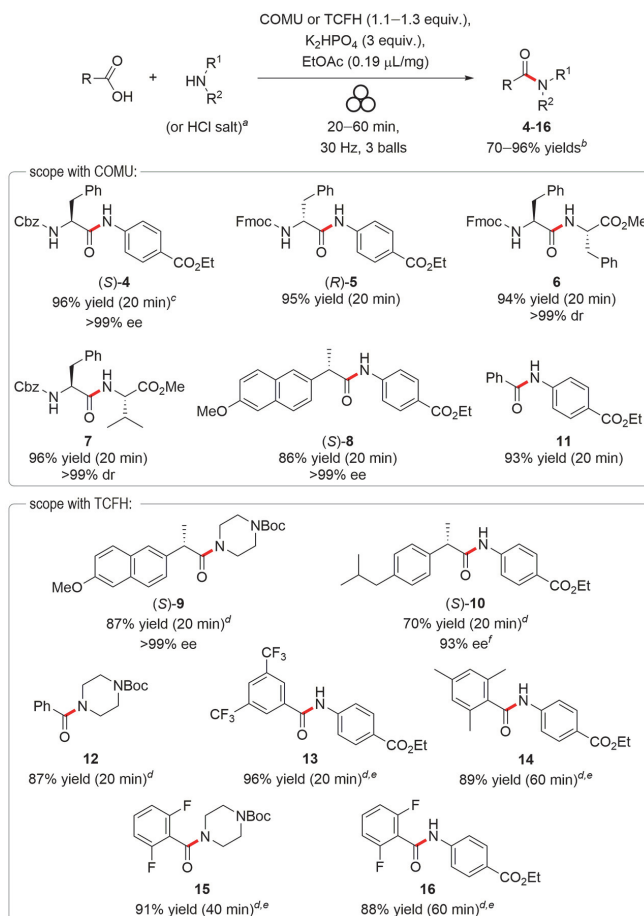
dipotassium phosphate and potassium pyrophosphate was especially notable (Scheme 2, Chart 2). We speculated that phosphate salts could additionally contribute to the activation of the carboxyl substrate 2 via the formation of acyl phosphate intermediates containing a "high-energy" phosphoester bond, prone to easy nucleophilic amine attack.[69,70] Interestingly, the same pathway is also involved in the ATP-dependent biosynthesis of amide bond-containing biomolecules.[11] The plausibility of our assumption is further supported by existing literature showing that acyl phosphates can be indeed generated in solution by the dicyclohexylcarbodiimide (DCC)-mediated coupling of carboxylic acids with phosphate salts.[71−73] To confirm the credibility of our hypothesis, mechanochemical synthesis of acyl phosphates from carboxylic acids and phosphate salts, mediated by COMU and TCFH, was attempted.

As expected, 20 min of ball milling of COMU (1.1 equiv) with acetic acid (1 equiv) and K₂HPO₄ (3 equiv) yielded 60%

of acetyl phosphate 17, which was confirmed by NMR analysis of the freshly obtained reaction mixture in D₂O solution (Figure 2). Acetyl phosphate 17 displayed a singlet signal at δ = −2.1 ppm in ³¹P NMR, which rapidly disappeared after the addition of morpholine, both in D₂O solution and in the solid state (see the Supporting Information). In the ¹³C NMR spectrum, carbonyl group 17 showed a doublet signal at δ = 168.1 ppm (J_{CP} = 8.8 Hz), due to its coupling with the neighboring phosphorus.[69] Significantly lower yields of 17 were attained with K₃PO₄ or with TCFH as coupling reagent (Figure 2). The reaction of acetic acid with K₄P₂O₇ produced acetyl pyrophosphate 18 in a 50% yield, according to ³¹P NMR analysis. As a result of the nonequivalence of phosphorus atoms in 18, a pair of doublet signals appeared in ³¹P NMR, at δ = −5.0 and −17.9 ppm (d, J_{PP} = 21.7 Hz), thus confirming its structure.[71] As an extra example, the generation of acyl phosphate 19 (50% yield, δ = −7.6 ppm in ³¹P NMR) was also
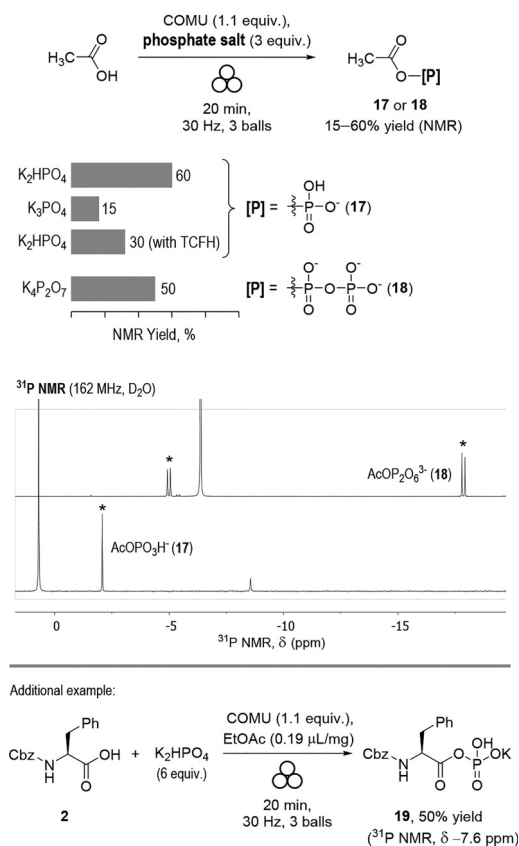
Figure 2. Mechanochemical generation of acyl phosphates **17**, **19**, and acetyl pyrophosphate **18**. Signals of **17** and **18** in the traces of ^{31}P NMR spectra are marked with asterisks. Other signals belong to inorganic phosphates (see the Supporting Information).

successful from Cbz-masked phenylalanine **2**, which was similar to the acetic acid outcome.

These results clearly indicate that generation of acyl phosphates can indeed take place in these newly developed mechanochemical amidation approaches and could account for the observed enhanced efficiency of K_2HPO_4 and $K_4P_2O_7$ additives. To evaluate the contribution of the acyl phosphate pathway (Scheme 4), via intermediate **C**) against the manifested activated ester pathway (via intermediates **A** and **B**),[50,74] the following experiment was undertaken. Amide coupling reaction of potassium salt of **2** with amine **3** without the phosphate salt additive afforded amide **4** in 80% yield, 16% lower than that obtained with K_2HPO_4. It was concluded from these results that in the amidation reaction leading to **4**, K_2HPO_4 acts primarily as a base performing the deprotonation of **2**, but it also contributes at least 16% to the formation of amide **4** via acyl phosphate **19**. This estimation correlates well with the results of other optimization experiments (Scheme 2, Chart 2). For example, K_3PO_4 produced a rather low 15% yield of acetyl phosphate **17** (Figure 2), which also agrees with the lower conversion to amide **4** in the comparison with K_2HPO_4.

Scheme 4. Plausible Mechanistic Pathways Leading to Amide Product
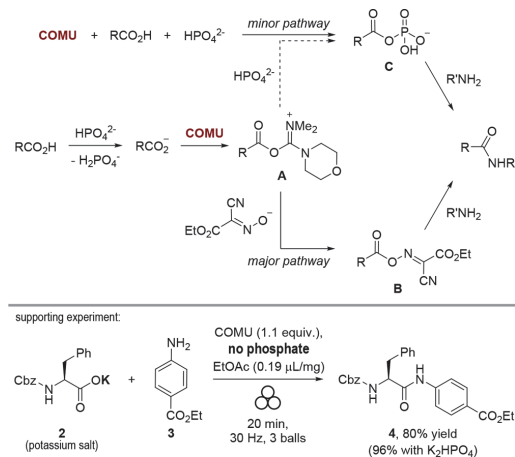
The acyl phosphate pathway probably contributes less in the case of the more reactive TCFH reagent, which also produced a rather low 30% yield of **17** (Figure 2). The exact mechanistic sequence leading to acyl phosphates **C** from COMU, RCO_2H, and K_2HPO_4 remains unclear but may include the reaction of acyl uronium intermediate **A** with HPO_4^{2-} anion (Scheme 4) or, alternatively, the initial formation of uronium phosphate[75] by the reaction of COMU with K_2HPO_4.

Challenging Amide Bond Formation. As shown above, the coupling of low nucleophilic amine **3** with sterically hindered mesitoic acid could be efficiently mediated by the TCFH/K_2HPO_4 reagent system (Scheme 3). In accordance with existing literature,[65,76] we selected the coupling of electron-deficient 4-aminobenzonitrile **20** with 2-methyl-2-phenylpropanoic acid **21** (Scheme 5), an even more arduous way to test the performance of mechanochemical amidation protocols. A brief screening of various coupling conditions was undertaken, and conversion to amide product **22** was determined by ^{1}H NMR analysis after 60 min of milling time (Scheme 5).

The use of EDC alone,[38] or the COMU/K_2HPO_4 system, yielded only a low ~10% conversion. Combination of TCFH and K_2HPO_4 delivered a noticeably better outcome but still failed to raise the conversion above 22%. According to the recent study of Beutner et al.,[65] a combination of N-methylimidazole (NMI) and TCFH reagent provided a high yield of **22** in solution, due to in situ generation of reactive N-acyl imidazolium ions. To our gratification, the same combination of reagents also worked well under the solvent-free conditions, affording respectable 84% conversion after a 60−min reaction time. Finally, a slight excess (1.3 equiv) of TCFH reagent, along with a bit longer milling time (90 min), allowed us to obtain pure amide **22** in 92% isolated yield after an aqueous workup (see the Supporting Information). Following the same reaction protocol, the coupling of **21** with sterically hindered 2,4,6-trimethylaniline was performed and furnished corresponding amide **23** with a 92% yield. Notably, high yields of amides **22** and **23** were attained in a rather efficient reaction time of 1.5 h, in significant contrast with the solution-based reaction (21 h for amide **22**).[65]

Scheme 5. Mechanochemical Coupling of Hindered Carboxylic Acids and Poor Nucleophilic Amines
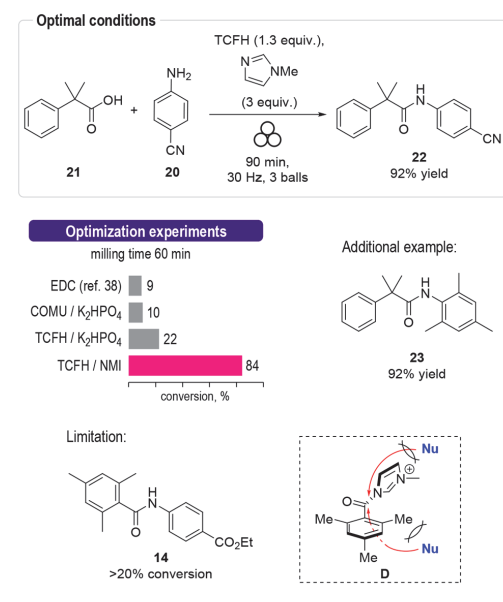

Surprisingly, the same highly reactive combination of reagents failed to render amide **14** from mesitoic acid with yields exceeding 20%. This was also the case in the CD$_3$CN solution (see the Supporting Information). We found that the reaction was stopped due to the formation of sterically bulky and therefore nonplanar *N*-acyl imidazolium **D**, which in contrast to the analogous species produced from benzoic acid was totally inert toward the subsequent reaction with amine **3** (see the Supporting Information for further details). The inertness of **D** could be explained by the efficient steric shielding of the carbonyl group with both neighboring mesityl and imidazolyl moieties, preventing attack of a nucleophile

along the Bürgi–Dunitz trajectory (Scheme 5). This stands in sharp contrast to the successful TCFH/K$_2$HPO$_4$-mediated transformation, where the less sterically crowded intermediate species are expected to form (e.g. mesitoyl chloride, uronium, or phosphate).

Amide Coupling of Biotin[6]uril. As a part of our ongoing efforts toward the development of new chiral supramolecular receptors,[42,77−81] we needed an expedient synthetic procedure for derivatization of biotin[6]uril (**1**),[46] easily available in multigram quantities by HCl-catalyzed condensation of formaldehyde with D-biotin. The starting macrocyclic molecule, notable for its anion binding properties, common for the cucurbituril family,[41,82−85] satisfies six carboxylic functions, which could be conveniently coupled with various amines, thus providing facile access to a library of diversely functionalized chiral macrocyclic receptors. Although amide coupling of carboxylates in **1** might appear simple, unencumbered by any steric or electronic influence, full amidation of **1** is challenging because it proceeds via six consecutive steps. For example, if a high 97% yield were produced during each step, then the fully functionalized product would eventually generate only a $(0.97)^6 \cdot 100\% = 83\%$ yield, while the rest of the produced material would contain a set of "failed" under-functionalized molecules, thus necessitating time-consuming, laborious, and mass-inefficient chromatographic purification. The situation resembles the synthesis of oligopeptides and oligonucleotides, in which an extremely high coupling efficiency (>99% per coupling step) is required to attain reasonable yields and high purity of long-chain oligomers, and it is customarily achieved by using an excess of highly reactive coupling reagents.[58] The low solubility of **1** in the environmentally benign and volatile organic solvents, compatible with the conventional amidation protocols (e.g., ethyl acetate), constitutes an additional restriction of the solution-based chemistry. We believed that the high coupling efficiency observed under the solvent-free conditions would allow us to perform the desired functionalization in a high-yielding, and scalable manner without using an excess of reagents, toxic solvents, or laborious purification.

As a convenient model reaction for this study, we selected the amide coupling of **1** with methyl ester of phenylalanine **24**

Scheme 6. Derivatization of Biotin[6]uril (1)[a]
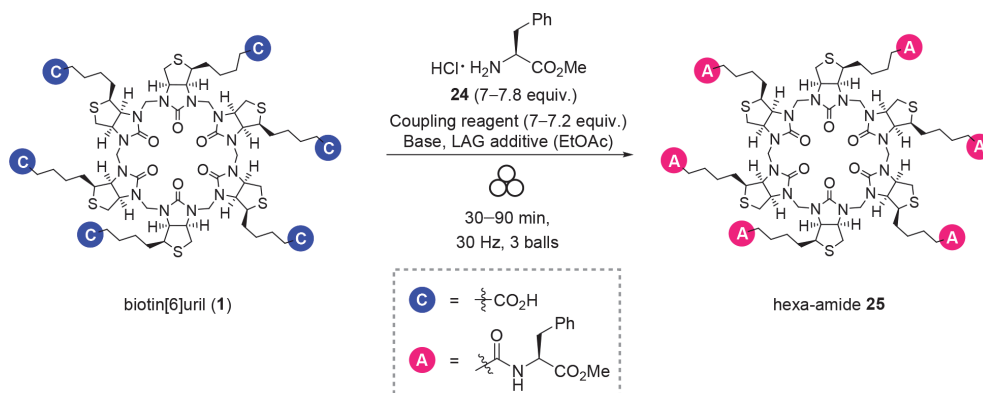
[a]Via six-fold amidation with L-phenylalanine methyl ester (**24**).
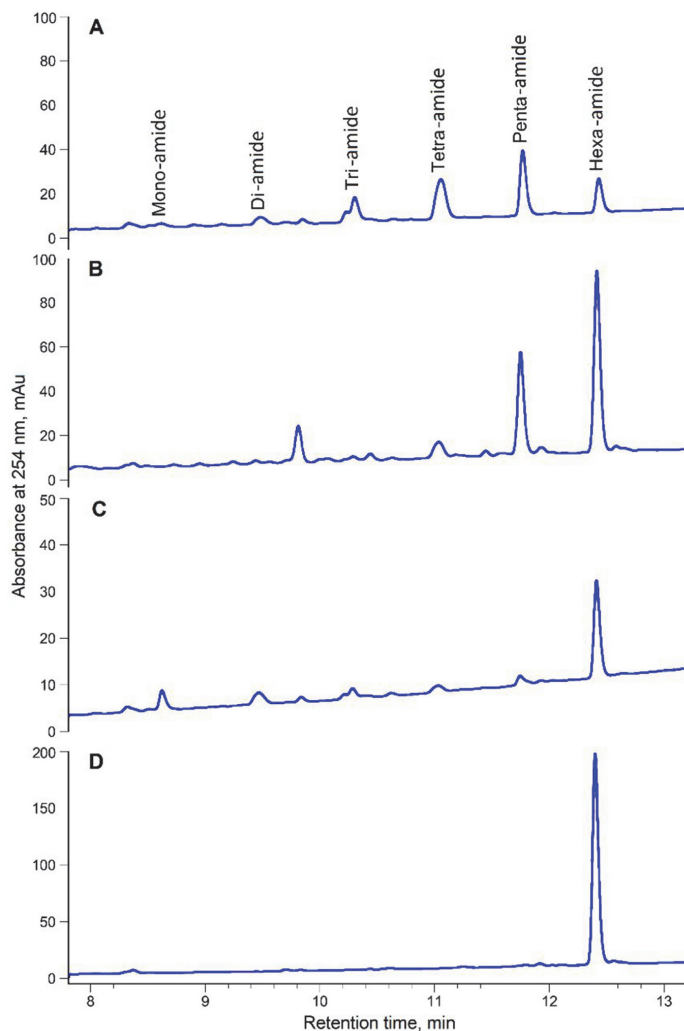
Figure 3. Derivatization of biotin[6]uril **1** via amide coupling with phenylalanine methyl ester **24**. Traces of HPLC chromatograms for the selected reaction mixtures: (A) COMU/K$_2$HPO$_4$; (B) EDC/DMAP; (C) TCFH/NMI; (D) TCFH/NMI with EtOAc as LAG additive.

(used as HCl salt, see Scheme 6). At its outset, this task required us to explore the performance of different amide coupling conditions. Only a slight excess of amine **24** and a coupling reagent (7−7.8 equiv, which is 1.16−1.3 equiv per CO$_2$H group of **1**) were applied in the optimization experiments. It was expected that more reactive combinations of reagents would deliver higher yields of hexa-amide product **25**. On the basis of our previous findings, the order of coupling efficiency for the different reagent systems can be roughly plotted as follows: EDC ∼ COMU/K$_2$HPO$_4$ < TCFH/K$_2$HPO$_4$ ≪ TCFH/NMI. Although such generalizations must be made with care since the coupling performance is substrate-dependent[8,86] and exceptions are possible, e.g., case of amide

14 above, this preliminary reactivity plot provided a helpful guide.

Outcomes of the test reactions were analyzed by HPLC (Figure 3, see the Supporting Information for further detail) and quantified by calculating HPLC area percentage for the hexa-amide product **25** (S_{rel}, Table 2), relative to under-functionalized compounds.

These initial experiments (Table 2, entries 1−4) clearly indicated that complete hexafunctionalization of **1** is difficult to perform. Thus, both the COMU and TCFH/K$_2$HPO$_4$ systems produced a mixture of phenylalanine-derivatized biotin[6]urils, containing all possible products from mono- to hexa-amide **25**, with the latter displaying a rather low 16% contribution (entries 1 and 2; Figure 3A). The use of EDC/DMAP

Table 2. Amide Coupling of Biotin[6]uril 1 with Phenylalanine Methyl Ester 24

Entry	Reaction conditions[a]	Liquid chemicals (additives, solvents)	η, μL/mg	Time, min	S_{rel}, %[b]
1	COMU/K_2HPO_4	EtOAc	0.19	90	16
2	TCFH/K_2HPO_4	EtOAc	0.19	90	16
3	EDC/DMAP[c]	CH_3NO_2	0.25	90	55
4	TCFH/NMI	NMI	0.29	90	52
5	ball milling TCFH/NMI[d]	NMI	0.32	60	86
6	TCFH/NMI[d]/NaCl[e]	NMI	0.16	60	73
7	TCFH/NMI[d]	NMI, DMF	0.53	60	97
8	TCFH/NMI[d]	NMI, heptane	0.64	60	84
9	**TCFH/NMI[d]**	**NMI, EtOAc**	**0.64**	**60**	**98**
10	slurry stirring TCFH/NMI[d]	NMI, EtOAc	0.64	60	95
11	solution (DMF) HATU, DIPEA	DIPEA, DMF	2.1	60	68
12	TCFH, NMI[d]	NMI, DMF	2.4	60	98

[a]Reaction conditions: biotin[6]uril (50–70 mg, 0.03–0.05 mmol), **24** (7 equiv), coupling reagent (7 equiv), and base (18 equiv), unless other specified. [b]HPLC area percentage of hexa-amide **25**, relative to other amide products. [c]12 equiv of DMAP was used, following the published procedure; see ref 38. [d]With 7.2 equiv of TCFH, 7.8 equiv of **24**, and 21 equiv of NMI. [e]NaCl was used as grinding additive.

combination (entry 3),[38] was more successful in this case, primarily producing a mixture of penta- and hexa-amides (Figure 3B). The highly reactive TCFH/NMI combination (entry 4) generated hexa-amide **25** as its main reaction product, but it was noticeably contaminated with under-functionalized compounds (52% HPLC area, Figure 3C).

Notably, at least 90 min of milling had to be applied, since samples taken after 30 and 60 min still showed incomplete conversion (see the Supporting Information). Although the FTS1000 shaker mill could hypothetically achieve a long milling time, we considered any time longer than 1.5 h as impractical; therefore, our next goal was to adjust the reaction parameters accordingly, in order to reach at least 90% conversion within a 1.5 h reaction time.

Applying a slightly greater excess of TFCH (1.2 equiv per carboxylate) and NMI (3.5 equiv per carboxylate) noticeably improved the yield of target product **25** (86% HPLC area, entry 5) and also shortened the reaction time. For further improvement, a screening of optimal η and LAG additive was performed. Since NMI is a liquid and liquid tetramethylurea is produced, the addition of solid NaCl was attempted to reduce the initial η to 0.16 μL/mg. However, this distinctly reduced the yield of the product (73% HPLC area, entry 6). In contrast, the addition of a few drops (ca. 35–50 μL) of solvent noticeably improved the outcome (entries 7–9) and was best when polar solvents like DMF or EtOAc were added (entries 7 and 9). These results clearly indicate that the nature of LAG additive plays an important role[39] and can substantially increase reaction rate, a probable result of the favorable interactions of the polar reactants with the mobile surface layers of LAG additive and improved mass transfer.[24] The outcome with EtOAc was especially remarkable, providing **25** with the best purity (98% HPLC area, Figure 3D). Since the reaction mixture visibly liquefied as the reaction progressed (due to the generation of tetramethylurea), slurry stirring was also tried instead of ball milling (entry 10) and resulted in a slightly reduced coupling efficiency.

Solution-based amide couplings were performed in DMF (entries 11 and 12) for the comparison with mechanosynthesis. Homogeneous solutions were obtained with an amount of solvent (ca. 0.5 mL) comparable to the weight of solid reactants (ca. 0.24 g), which kept η at around 2 μL/mg. In the DMF solution, HATU was another frequently used and highly reactive uronium-based amide coupling reagent that produced

a rather modest outcome (entry 11). Conversely, the coupling efficiency of the TCFH/NMI combination in DMF solution (entry 12) was virtually the same as that in DMF-free transformation to a solid state (entry 9). Importantly, a bulk amount of harmful solvent was fully avoided in the latter.

Under the optimal reaction conditions (entry 9), desired hexa-amide product **25** was isolated in a nearly quantitative yield and 95% HPLC purity (relative to all other peaks) after a simple water wash and filtration. The purity of product was further increased (99% according to HPLC) by following a simple purification protocol (filtration of chloroform solution via Celite, and then precipitation with hexane from EtOAc solution [see the Supporting Information]). The same amide coupling reaction was also successful at loadings that were 3 times higher (150 mg of **1** per milling jar, 300 mg total), creating **25** in 80% isolated yield and 99% HPLC purity, albeit with a longer milling time (90 min).

■ CONCLUSIONS

In conclusion, we have developed an efficient mechanochemical protocol for the direct synthesis of amides from carboxylic acids and amines by employing uronium-type amide coupling reagents (COMU and TCFH) and K_2HPO_4 as a base. The reaction protocols demonstrated fast reaction rates (typically within 20 min), generally high yields, an absence of noticeable epimerization for stereogenic centers adjacent to carbonyl group, and a simple isolation procedure for solid amide products. In addition to faster rates of solvent-free amide couplings in contrast to the solution-based protocols, the absence of solvent eliminated reagent compatibility issues, e.g., COMU and DMF, greatly reduced the amount of waste generated and significantly attenuated safety risks. The dual role of K_2HPO_4 as both base and activating reagent for a carboxylic acid substrate was also manifested. The rapid formation (within 60–90 min) of amide products was observed for even challenging coupling partners, such as sterically hindered carboxylic acids and poor nucleophilic amines, within the TCFH/K_2HPO_4 and TCFH/NMI reagent systems. However, the full amidation of polyfunctionalized substrates, e.g., biotin[6]uril, was found to be especially challenging, even though the single amide bond itself is not difficult to form. Highly reactive coupling conditions (TCFH/NMI), prolonged reaction times (60–90 min), and suitable LAG additives (EtOAc) are essential for producing hexa-amide

25 in high yield and purity. This efficient and environmentally benign synthetic methodology is useful for the preparation of analogues of a new supramolecular host, **25**, as well as for the synthesis of peptides and amides, which could be used in various fields of applied chemistry.

■ ASSOCIATED CONTENT

Ⓢ Supporting Information

The Supporting Information is available free of charge at https://pubs.acs.org/doi/10.1021/acssuschemeng.0c05558.

Detailed information about experimental methods, additional data for characterizations of products, kinetics and mechanistic studies, ^{1}H and ^{13}C NMR spectra, HPLC chromatograms, and green chemistry metrics (PDF)

■ AUTHOR INFORMATION

Corresponding Authors

Dzmitry G. Kananovich − Tallinn University of Technology, School of Science, Department of Chemistry and Biotechnology, 12618 Tallinn, Estonia; Email: dzmitry.kananovich@taltech.ee

Riina Aav − Tallinn University of Technology, School of Science, Department of Chemistry and Biotechnology, 12618 Tallinn, Estonia; ⦿ orcid.org/0000-0001-6571-7596; Email: riina.aav@taltech.ee

Authors

Tatsiana Dalidovich − Tallinn University of Technology, School of Science, Department of Chemistry and Biotechnology, 12618 Tallinn, Estonia

Kamini A. Mishra − Tallinn University of Technology, School of Science, Department of Chemistry and Biotechnology, 12618 Tallinn, Estonia; ⦿ orcid.org/0000-0001-5512-2767

Tatsiana Shalima − Tallinn University of Technology, School of Science, Department of Chemistry and Biotechnology, 12618 Tallinn, Estonia

Marina Kudrjašova − Tallinn University of Technology, School of Science, Department of Chemistry and Biotechnology, 12618 Tallinn, Estonia

Complete contact information is available at:
https://pubs.acs.org/10.1021/acssuschemeng.0c05558

■ ACKNOWLEDGMENTS

■ ABBREVIATIONS

AE, atom economy; CDI, N,N′-carbonyldiimidazole; COMU, (1-cyano-2-ethoxy-2-oxoethylidenaminooxy)dimethylamino-morpholinocarbenium hexafluorophosphate; DCC, dicyclohexylcarbodiimide; DCM, dichloromethane; DIPEA, N,N-diisopropylethylamine; DMAP, 4-dimethylaminopyridine; DMF, N,N-dimethylformamide; EDC, 1-ethyl-3-(3-(dimethylamino)-propyl) carbodiimide; HATU, hexafluorophosphate azabenzotriazole tetramethyl uronium; HBTU, hexafluorophosphate benzotriazole tetramethyl uronium; HPLC, high-performance liquid chromatography; LAG, liquid-assisted grinding; MSDS, material safety data sheet; NMI, N-methylimidazole; Oxyma, ethyl cyanohydroxyiminoacetate; PMI, process mass intensity; RME, reaction mass efficiency; TCFH, N,N,N′,N′-tetramethylchloroformamidinium hexafluorophosphate; TCT, 2,4,6-trichloro-1,3,5-triazine

■ REFERENCES

(1) Boström, J.; Brown, D. G.; Young, R. J.; Keserü, G. M. Expanding the Medicinal Chemistry Synthetic Toolbox. *Nat. Rev. Drug Discovery* **2018**, 17, 709−727.

(2) Constable, D. J. C.; Dunn, P. J.; Hayler, J. D.; Humphrey, G. R.; Leazer, J. L., Jr.; Linderman, R. J.; Lorenz, K.; Manley, J.; Pearlman, B. A.; Wells, A.; et al. Key Green Chemistry Research Areas − a Perspective from Pharmaceutical Manufacturers. *Green Chem.* **2007**, 9, 411−420.

(3) Bryan, M. C.; Dunn, P. J.; Entwistle, D.; Gallou, F.; Koenig, S. G.; Hayler, J. D.; Hickey, M. R.; Hughes, S.; Kopach, M. E.; Moine, G.; Richardson, P.; Roschangar, F.; Steven, A.; Weiberth, F. J. Key Green Chemistry Research Areas from a Pharmaceutical Manufacturers' Perspective Revisited. *Green Chem.* **2018**, 20, 5082−5103.

(4) Dalu, F.; Scorciapino, M. A.; Cara, C.; Luridiana, A.; Musinu, A.; Casu, M.; Secci, F.; Cannas, C. A Catalyst-Free, Waste-Less Ethanol-Based Solvothermal Synthesis of Amides. *Green Chem.* **2018**, 20, 375−381.

(5) Charville, H.; Jackson, D. A.; Hodges, G.; Whiting, A.; Wilson, M. R. The Uncatalyzed Direct Amide Formation Reaction − Mechanism Studies and the Key Role of Carboxylic Acid H-Bonding. *Eur. J. Org. Chem.* **2011**, 2011, 5981−5990.

(6) Gelens, E.; Smeets, L.; Sliedregt, L. A. J. M.; van Steen, B. J.; Kruse, C. G.; Leurs, R.; Orru, R. V. A. An Atom Efficient and Solvent-Free Synthesis of Structurally Diverse Amides Using Microwaves. *Tetrahedron Lett.* **2005**, 46, 3751−3754.

(7) Dunetz, J. R.; Magano, J.; Weisenburger, G. A. Large-Scale Applications of Amide Coupling Reagents for the Synthesis of Pharmaceuticals. *Org. Process Res. Dev.* **2016**, 20, 140−177.

(8) Valeur, E.; Bradley, M. Amide Bond Formation: Beyond the Myth of Coupling Reagents. *Chem. Soc. Rev.* **2009**, 38, 606−631.

(9) Montalbetti, C. A. G. N.; Falque, V. Amide Bond Formation and Peptide Coupling. *Tetrahedron* **2005**, 61, 10827−10852.

(10) Trobro, S.; Åqvist, J. Mechanism of Peptide Bond Synthesis on the Ribosome. *Proc. Natl. Acad. Sci. U. S. A.* **2005**, 102, 12395−12400.

(11) Goswami, A.; Van Lanen, S. G. Enzymatic Strategies and Biocatalysts for Amide Bond Formation: Tricks of the Trade Outside of the Ribosome. *Mol. BioSyst.* **2015**, 11, 338−353.

(12) Philpott, H. K.; Thomas, P. J.; Tew, D.; Fuerst, D. E.; Lovelock, S. L. A Versatile Biosynthetic Approach to Amide Bond Formation. *Green Chem.* **2018**, 20, 3426−3431.

(13) Petchey, M. R.; Grogan, G. Enzyme-Catalysed Synthesis of Secondary and Tertiary Amides. *Adv. Synth. Catal.* **2019**, 361, 3895−3914.

(14) El-Faham, A.; Albericio, F. Peptide Coupling Reagents, More than a Letter Soup. *Chem. Rev.* **2011**, 111, 6557−6602.

(15) Han, S.-Y.; Kim, Y.-A. Recent Development of Peptide Coupling Reagents in Organic Synthesis. *Tetrahedron* **2004**, 60, 2447−2467.

(16) de Figueiredo, R. M.; Suppo, J.-S.; Campagne, J.-M. Nonclassical Routes for Amide Bond Formation. *Chem. Rev.* **2016**, *116*, 12029−12122.

(17) Sabatini, M. T.; Boulton, L. T.; Sneddon, H. F.; Sheppard, T. D. A Green Chemistry Perspective on Catalytic Amide Bond Formation. *Nat. Catal.* **2019**, *2*, 10−17.

(18) Pattabiraman, V. R.; Bode, J. W. Rethinking Amide Bond Synthesis. *Nature* **2011**, *480*, 471−479.

(19) Massolo, E.; Pirola, M.; Benaglia, M. Amide Bond Formation Strategies: Latest Advances on a Dateless Transformation. *Eur. J. Org. Chem.* **2020**, *2020*, 4641.

(20) Constable, D. J. C.; Jimenez-Gonzalez, C.; Henderson, R. K. Perspective on Solvent Use in the Pharmaceutical Industry. *Org. Process Res. Dev.* **2007**, *11*, 133−137.

(21) MacMillan, D. S.; Murray, J.; Sneddon, H. F.; Jamieson, C.; Watson, A. J. B. Evaluation of Alternative Solvents in Common Amide Coupling Reactions: Replacement of Dichloromethane and *N,N*-Dimethylformamide. *Green Chem.* **2013**, *15*, 596−600.

(22) Do, J.-L.; Friščić, T. Chemistry 2.0: Developing a New, Solvent-Free System of Chemical Synthesis Based on Mechanochemistry. *Synlett* **2017**, *28*, 2066−2092.

(23) James, S. L.; Adams, C. J.; Bolm, C.; Braga, D.; Collier, P.; Friščić, T.; Grepioni, F.; Harris, K. D. M.; Hyett, G.; Jones, W.; Krebs, A.; Mack, J.; Maini, L.; Orpen, A. G.; Parkin, I. P.; Shearouse, W. C.; Steed, J. W.; Waddell, D. C. Mechanochemistry: Opportunities for New and Cleaner Synthesis. *Chem. Soc. Rev.* **2012**, *41*, 413−447.

(24) Do, J.-L.; Friščić, T. Mechanochemistry: A Force of Synthesis. *ACS Cent. Sci.* **2017**, *3*, 13−19.

(25) Hernández, J. G.; Bolm, C. Altering Product Selectivity by Mechanochemistry. *J. Org. Chem.* **2017**, *82*, 4007−4019.

(26) Margetić, D.; Štrukil, V. Carbon−Nitrogen Bond-Formation Reactions. *Mechanochemical Organic Synthesis* **2016**, 141−233.

(27) Kaupp, G.; Schmeyers, J.; Boy, J. Quantitative Solid-State Reactions of Amines with Carbonyl Compounds and Isothiocyanates. *Tetrahedron* **2000**, *56*, 6899−6911.

(28) Cao, Q.; Crawford, D. E.; Shi, C.; James, S. L. Greener Dye Synthesis: Continuous, Solvent-Free Synthesis of Commodity Perylene Diimides by Twin-Screw Extrusion. *Angew. Chem., Int. Ed.* **2020**, *59*, 4478−4483.

(29) Declerck, V.; Nun, P.; Martinez, J.; Lamaty, F. Solvent-Free Synthesis of Peptides. *Angew. Chem., Int. Ed.* **2009**, *48*, 9318−9321.

(30) Hernández, J. G.; Juaristi, E. Green Synthesis of α,β- and β,β-Dipeptides under Solvent-Free Conditions. *J. Org. Chem.* **2010**, *75*, 7107−7111.

(31) Bonnamour, J.; Métro, T.-X.; Martinez, J.; Lamaty, F. Environmentally Benign Peptide Synthesis Using Liquid-Assisted Ball-Milling: Application to the Synthesis of Leu-Enkephalin. *Green Chem.* **2013**, *15*, 1116−1120.

(32) Gonnet, L.; Tintillier, T.; Venturini, N.; Konnert, L.; Hernandez, J.-F.; Lamaty, F.; Laconde, G.; Martinez, J.; Colacino, E. *N*-Acyl Benzotriazole Derivatives for the Synthesis of Dipeptides and Tripeptides and Peptide Biotinylation by Mechanochemistry. *ACS Sustainable Chem. Eng.* **2017**, *5*, 2936−2941.

(33) Métro, T.-X.; Bonnamour, J.; Reidon, T.; Sarpoulet, J.; Martinez, J.; Lamaty, F. Mechanosynthesis of Amides in the Total Absence of Organic Solvent from Reaction to Product Recovery. *Chem. Commun.* **2012**, *48*, 11781−11783.

(34) Duangkamol, C.; Jaita, S.; Wangngae, S.; Phakhodee, W.; Pattarawarapan, M. An Efficient Mechanochemical Synthesis of Amides and Dipeptides Using 2,4,6-Trichloro-1,3,5-Triazine and PPh₃. *RSC Adv.* **2015**, *5*, 52624−52628.

(35) Hernández, J. G.; Ardila-Fierro, K. J.; Crawford, D.; James, S. L.; Bolm, C. Mechanoenzymatic Peptide and Amide Bond Formation. *Green Chem.* **2017**, *19*, 2620−2625.

(36) Ardila-Fierro, K. J.; Crawford, D. E.; Körner, A.; James, S. L.; Bolm, C.; Hernández, J. G. Papain-Catalysed Mechanochemical Synthesis of Oligopeptides by Milling and Twin-Screw Extrusion: Application in the Juliá−Colonna Enantioselective Epoxidation. *Green Chem.* **2018**, *20*, 1262−1269.

(37) Bolm, C.; Hernández, J. G. From Synthesis of Amino Acids and Peptides to Enzymatic Catalysis: A Bottom-Up Approach in Mechanochemistry. *ChemSusChem* **2018**, *11*, 1410−1420.

(38) Štrukil, V.; Bartolec, B.; Portada, T.; Đilović, I.; Halasz, I.; Margetić, D. One-Pot Mechanosynthesis of Aromatic Amides and Dipeptides from Carboxylic Acids and Amines. *Chem. Commun.* **2012**, *48*, 12100−12102.

(39) Porte, V.; Thioloy, M.; Pigoux, T.; Métro, T.-X.; Martinez, J.; Lamaty, F. Peptide Mechanosynthesis by Direct Coupling of *N*-Protected α-Amino Acids with Amino Esters. *Eur. J. Org. Chem.* **2016**, *2016*, 3505−3508.

(40) Kaabel, S.; Aav, R. Templating Effects in the Dynamic Chemistry of Cucurbiturils and Hemicucurbiturils. *Isr. J. Chem.* **2018**, *58*, 296−313.

(41) Andersen, N. N.; Lisbjerg, M.; Eriksen, K.; Pittelkow, M. Hemicucurbit[n]Urils and Their Derivatives − Synthesis and Applications. *Isr. J. Chem.* **2018**, *58*, 435−448.

(42) Kaabel, S.; Stein, R. S.; Fomitšenko, M.; Järving, I.; Friščić, T.; Aav, R. Size-Control by Anion Templating in Mechanochemical Synthesis of Hemicucurbiturils in the Solid State. *Angew. Chem., Int. Ed.* **2019**, *58*, 6230−6234.

(43) Mohite, A. R.; Reany, O. Inherently Chiral Bambus[4]Urils. *J. Org. Chem.* **2020**, *85*, 9190−9200.

(44) Sokolov, J.; Šindelář, V. Chiral Bambusurils for Enantioselective Recognition of Carboxylate Anion Guests. *Chem. - Eur. J.* **2018**, *24*, 15482−15485.

(45) Sokolov, J.; Štefek, A.; Šindelář, V. Functionalized Chiral Bambusurils: Synthesis and Host-Guest Interactions with Chiral Carboxylates. *ChemPlusChem* **2020**, *85*, 1307−1314.

(46) Lisbjerg, M.; Jessen, B. M.; Rasmussen, B.; Nielsen, B. E.; Madsen, A. Ø.; Pittelkow, M. Discovery of a Cyclic 6 + 6 Hexamer of D-Biotin and Formaldehyde. *Chem. Sci.* **2014**, *5*, 2647−2650.

(47) Lisbjerg, M.; Nielsen, B. E.; Milhøj, B. O.; Sauer, S. P. A.; Pittelkow, M. Anion Binding by Biotin[6]Uril in Water. *Org. Biomol. Chem.* **2015**, *13*, 369−373.

(48) Lisbjerg, M.; Valkenier, H.; Jessen, B. M.; Al-Kerdi, H.; Davis, A. P.; Pittelkow, M. Biotin[6]Uril Esters: Chloride-Selective Trans-membrane Anion Carriers Employing C—H···Anion Interactions. *J. Am. Chem. Soc.* **2015**, *137*, 4948−4951.

(49) El-Faham, A.; Funosas, R. S.; Prohens, R.; Albericio, F. COMU: A Safer and More Effective Replacement for Benzotriazole-Based Uronium Coupling Reagents. *Chem. - Eur. J.* **2009**, *15*, 9404−9416.

(50) El-Faham, A.; Subirós-Funosas, R.; Albericio, F. A Novel Family of Onium Salts Based Upon Isonitroso Meldrum's Acid Proves Useful as Peptide Coupling Reagents. *Eur. J. Org. Chem.* **2010**, *2010*, 3641−3649.

(51) El-Faham, A.; Albericio, F. COMU: A Third Generation of Uronium-Type Coupling Reagents. *J. Pept. Sci.* **2010**, *16*, 6−9.

(52) Friščić, T.; Childs, S. L.; Rizvi, S. A. A.; Jones, W. The Role of Solvent in Mechanochemical and Sonochemical Cocrystal Formation: A Solubility-Based Approach for Predicting Cocrystallisation Outcome. *CrystEngComm* **2009**, *11*, 418−426.

(53) Prat, D.; Hayler, J.; Wells, A. A Survey of Solvent Selection Guides. *Green Chem.* **2014**, *16*, 4546−4551.

(54) Prat, D.; Wells, A.; Hayler, J.; Sneddon, H.; McElroy, C. R.; Abou-Shehada, S.; Dunn, P. J. CHEM21 Selection Guide of Classical-and Less Classical-Solvents. *Green Chem.* **2016**, *18*, 288−296.

(55) Lundblad, R. L., Macdonald, F., Eds. *Handbook of Biochemistry and Molecular Biology*; CRC Press: Boca Raton, FL, 2010.

(56) Sperry, J. B.; Minteer, C. J.; Tao, J.; Johnson, R.; Duzguner, R.; Hawksworth, M.; Oke, S.; Richardson, P. F.; Barnhart, R.; Bill, D. R.; Giusto, R. A.; Weaver, J. D. Thermal Stability Assessment of Peptide Coupling Reagents Commonly Used in Pharmaceutical Manufacturing. *Org. Process Res. Dev.* **2018**, *22*, 1262−1275.

(57) McKnelly, K. J.; Sokol, W.; Nowick, J. S. Anaphylaxis Induced by Peptide Coupling Agents: Lessons Learned from Repeated Exposure to HATU, HBTU, and HCTU. *J. Org. Chem.* **2020**, *85*, 1764−1768.

(58) Isidro-Llobet, A.; Kenworthy, M. N.; Mukherjee, S.; Kopach, M. E.; Wegner, K.; Gallou, F.; Smith, A. G.; Roschangar, F. Sustainability Challenges in Peptide Synthesis and Purification: From R&D to Production. *J. Org. Chem.* **2019**, *84*, 4615−4628.

(59) Subirós-Funosas, R.; Nieto-Rodriguez, L.; Jensen, K. J.; Albericio, F. COMU: Scope and Limitations of the Latest Innovation in Peptide Acyl Transfer Reagents. *J. Pept. Sci.* **2013**, *19*, 408−414.

(60) Kumar, A.; Jad, Y. E.; de la Torre, B. G.; El-Faham, A.; Albericio, F. Re-Evaluating the Stability of COMU in Different Solvents. *J. Pept. Sci.* **2017**, *23*, 763−768.

(61) McElroy, C. R.; Constantinou, A.; Jones, L. C.; Summerton, L.; Clark, J. H. Towards a Holistic Approach to Metrics for the 21st Century Pharmaceutical Industry. *Green Chem.* **2015**, *17*, 3111−3121.

(62) SDS Search and Product Safety Center. https://www.sigmaaldrich.com/safety-center.html (accessed on 15 July 2020).

(63) Cindro, N.; Tireli, M.; Karadeniz, B.; Mrla, T.; Užarević, K. Investigations of Thermally Controlled Mechanochemical Milling Reactions. *ACS Sustainable Chem. Eng.* **2019**, *7*, 16301−16309.

(64) Schmidt, R.; Martin Scholze, H.; Stolle, A. Temperature Progression in a Mixer Ball Mill. *Int. J. Ind. Chem.* **2016**, *7*, 181−186.

(65) Beutner, G. L.; Young, I. S.; Davies, M. L.; Hickey, M. R.; Park, H.; Stevens, J. M.; Ye, Q. TCFH−NMI: Direct Access to *N*-Acyl Imidazoliums for Challenging Amide Bond Formations. *Org. Lett.* **2018**, *20*, 4218−4222.

(66) Lopez, F. J.; Ferriño, S. A.; Reyes, M. S.; Román, R. Asymmetric Transformation of the Second Kind of Racemic Naproxen. *Tetrahedron: Asymmetry* **1997**, *8*, 2497−2500.

(67) Blasco, M. A.; Gröger, H. Organocatalytic Racemization of *α*-Aryl Propionates in the Presence of Water. *Synth. Commun.* **2013**, *43*, 9−15.

(68) Chen, C.-S.; Chen, T.; Shieh, W.-R. Metabolic Stereoisomeric Inversion of 2-Arylpropionic Acids. On the Mechanism of Ibuprofen Epimerization in Rats. *Biochim. Biophys. Acta, Gen. Subj.* **1990**, *1033*, 1−6.

(69) Gao, X.; Deng, H.; Tang, G.; Liu, Y.; Xu, P.; Zhao, Y. Intermolecular Phosphoryl Transfer of *N*-Phosphoryl Amino Acids. *Eur. J. Org. Chem.* **2011**, *2011*, 3220−3228.

(70) Di Sabato, G.; Jencks, W. P. Mechanism and Catalysis of Reactions of Acyl Phosphates. I. Nucleophilic Reactions. *J. Am. Chem. Soc.* **1961**, *83*, 4393−4400.

(71) Kluger, R.; Huang, Z. Acyl Pyrophosphates: Activated Analogs of Pyrophosphate Monoesters Permitting New Designs for Inactivation of Targeted Enzymes. *J. Am. Chem. Soc.* **1991**, *113*, 5124−5125.

(72) Biron, J.-P.; Pascal, R. Amino Acid N-Carboxyanhydrides: Activated Peptide Monomers Behaving as Phosphate-Activating Agents in Aqueous Solution. *J. Am. Chem. Soc.* **2004**, *126*, 9198−9199.

(73) Leman, L. J.; Orgel, L. E.; Ghadiri, M. R. Amino Acid Dependent Formation of Phosphate Anhydrides in Water Mediated by Carbonyl Sulfide. *J. Am. Chem. Soc.* **2006**, *128*, 20−21.

(74) Twibanire, J. K.; Grindley, T. B. Efficient and Controllably Selective Preparation of Esters Using Uronium-Based Coupling Agents. *Org. Lett.* **2011**, *13*, 2988−2991.

(75) Xiong, B.; Hu, C.; Gu, J.; Yang, C.; Zhang, P.; Liu, Y.; Tang, K. Efficient and Controllable Esterification of P(O)-OH Compounds Using Uronium-Based Salts. *ChemistrySelect* **2017**, *2*, 3376−3380.

(76) Larrivée-Aboussafy, C.; Jones, B. P.; Price, K. E.; Hardink, M. A.; McLaughlin, R. W.; Lillie, B. M.; Hawkins, J. M.; Vaidyanathan, R. DBU Catalysis of *N,N'*-Carbonyldiimidazole-Mediated Amidations. *Org. Lett.* **2010**, *12*, 324−327.

(77) Aav, R.; Shmatova, E.; Reile, I.; Borissova, M.; Topić, F.; Rissanen, K. New Chiral Cyclohexylhemicucurbit[6]Uril. *Org. Lett.* **2013**, *15*, 3786−3789.

(78) Prigorchenko, E.; Öeren, M.; Kaabel, S.; Fomitšenko, M.; Reile, I.; Järving, I.; Tamm, T.; Topić, F.; Rissanen, K.; Aav, R. Template-Controlled Synthesis of Chiral Cyclohexylhemicucurbit[8]Uril. *Chem. Commun.* **2015**, *51*, 10921−10924.

(79) Kaabel, S.; Adamson, J.; Topić, F.; Kiesilä, A.; Kalenius, E.; Öeren, M.; Reimund, M.; Prigorchenko, E.; Lõokene, A.; Reich, H. J.; Rissanen, K.; Aav, R. Chiral Hemicucurbit[8]Uril as an Anion Receptor: Selectivity to Size, Shape and Charge Distribution. *Chem. Sci.* **2017**, *8*, 2184−2190.

(80) Prigorchenko, E.; Kaabel, S.; Narva, T.; Baškir, A.; Fomitšenko, M.; Adamson, J.; Järving, I.; Rissanen, K.; Tamm, T.; Aav, R. Formation and Trapping of the Thermodynamically Unfavoured Inverted-Hemicucurbit[6]Uril. *Chem. Commun.* **2019**, *55*, 9307−9310.

(81) Ustrnul, L.; Kaabel, S.; Burankova, T.; Martõnova, J.; Adamson, J.; Konrad, N.; Burk, P.; Borovkov, V.; Aav, R. Supramolecular Chirogenesis in Zinc Porphyrins by Enantiopure Hemicucurbit[n]-Urils (n= 6,8). *Chem. Commun.* **2019**, *55*, 14434−14437.

(82) Yawer, M. A.; Havel, V.; Sindelar, V. A Bambusuril Macrocycle That Binds Anions in Water with High Affinity and Selectivity. *Angew. Chem., Int. Ed.* **2015**, *54*, 276−279.

(83) Lizal, T.; Sindelar, V. Bambusuril Anion Receptors. *Isr. J. Chem.* **2018**, *58*, 326−333.

(84) Masson, E.; Ling, X.; Joseph, R.; Kyeremeh-Mensah, L.; Lu, X. Cucurbituril Chemistry: A Tale of Supramolecular Success. *RSC Adv.* **2012**, *2*, 1213−1247.

(85) Aav, R.; Kaabel, S.; Fomitšenko, M. Cucurbiturils: Synthesis, Structures, Formation Mechanisms, and Nomenclature; In *Comprehensive Supramolecular Chemistry II*; Atwood, J. L., Ed.; Elsevier: Oxford, 2017; pp 203−220. DOI: 10.1016/B978-0-12-409547-2.12514-4.

(86) Hachmann, J.; Lebl, M. Search for Optimal Coupling Reagent in Multiple Peptide Synthesizer. *Biopolymers* **2006**, *84*, 340−347.

Appendix 2

Cyclohexanohemicucurbit[8]uril Inclusion Complexes With Heterocycles and Selective Extraction of Sulfur Compounds From Water

Tatsiana Shalima[1], Kamini A. Mishra[1], Sandra Kaabel[2], Lukas Ustrnul[1], Simona Bartkova[1], Kaia Tõnsuaadu[3], Ivo Heinmaa[4] and Riina Aav[1]*

[1]Department of Chemistry and Biotechnology, School of Science, Tallinn University of Technology, Tallinn, Estonia, [2]Department of Chemistry, McGill University, Montreal, QC, Canada, [3]Laboratory of Inorganic Materials, School of Engineering, Institute of Materials and Environmental Technology, Tallinn University of Technology, Tallinn, Estonia, [4]Laboratory of Chemical Physics, National Institute of Chemical Physics and Biophysics, Tallinn, Estonia

Solid-phase extraction that utilizes selective macrocyclic receptors can serve as a useful tool for removal of chemical wastes. Hemicucurbiturils are known to form inclusion complexes with suitably sized anions; however, their use in selective binding of non-charged species is still very limited. In this study, we found that cyclohexanohemicucurbit [8]uril encapsulates five- and six-membered sulfur- and oxygen-containing unsubstituted heterocycles, which is investigated by single-crystal X-ray diffraction, NMR spectroscopy, isothermal titration calorimetry, and thermogravimetry. The macrocycle acts as a promising selective sorption material for the extraction of sulfur heterocycles, such as 1,3-dithiolane and α-lipoic acid, from water.

INTRODUCTION

Hemicucurbiturils, formed in templated single-step oligomerization reactions (Kaabel and Aav, 2018), are single-bridged cucurbituril-type macrocycles (Andersen et al., 2018; Lizal and Sindelar, 2018; Xi et al., 2018) that bear an electron-deficient hydrophobic cavity. The latter grants these macrocycles the ability to encapsulate anions (Buschmann et al., 2005; Cucolea et al., 2016; Kaabel et al., 2017; Assaf and Nau, 2018; Reany et al., 2018; Vázquez and Sindelar, 2018; Andersen et al., 2019; Kandrnálová et al., 2019; Valkenier et al., 2019; Maršálek and Šindelář, 2020); in addition, the formation of complexes with acids and some neutral species has been reported in the previous work. In particular, unsubstituted hemicucurbit[n]urils (n = 6, 12) bind phenol derivatives (Jin et al., 2016a; 2016b) and ferrocene (Jin et al., 2017), and cyclohexanohemicucurbit[n]urils cycHC [n] (n = 6, 8, 12) (Li et al., 2009; Aav et al., 2013; Prigorchenko et al., 2015, 2019; Mishra et al., 2020) form external complexes with both inorganic and organic acids (Öeren et al., 2014; Ustrnul et al., 2019, 2021). We envisioned that heterocycles 1–13 have relatively high electron densities compared to carbocycles and may therefore be able to occupy space within the eight-membered cycHC[8] (**Figure 1**).

S-heterocycles are compounds of interest as these substances are bioactive (Rezanka et al., 2006; Lamberth et al., 2015) and may contribute to the distinct aromas of food (Mottram and Mottram, 2002; Mahadevan and Farmer, 2006; Schoenauer and Schieberle, 2018), and heterocycle **2** is added as an odorant to the natural gas. Unsubstituted S-containing heterocycles, such as 1,3-dithiolane **1** and

FIGURE 1 | Structure of cycHC[n] and cycHC[8], highlighting the electron-poor cavity for guest binding and characteristic atom numbers, and the scope of studied guests.
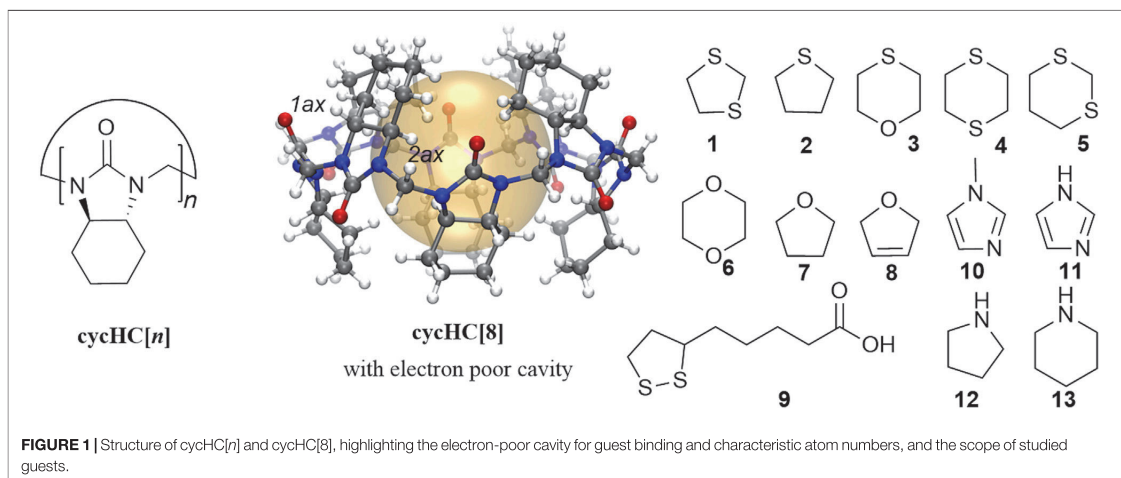
1,4-thioxane **3**, are found in meat (Garbusov et al., 1976) and around chemical warfare dumping sites where they are formed due to the degradation of mustard gas (Røen et al., 2010; Magnusson et al., 2016; Vanninen et al., 2020). Bioactive α-lipoic acid **9** exhibits antioxidant properties (Rochette et al., 2013; Salehi et al., 2019), and to date, cyclodextrins have been used to enhance its solubility and bioavailability (Lin-Hui et al., 1995; Maeda et al., 2010; Takahashi et al., 2011; Ikuta et al., 2013; Racz et al., 2013; Caira et al., 2017; Celebioglu and Uyar, 2019). Carbon-based materials are used for solid-phase extraction (SPE) of S-heterocycles from water (Lees et al., 2017; Jõul et al., 2018); however, such systems are designed to non-selectively retain all non-polar to moderately polar components.

In this study, we report that cycHC[8] encapsulates neutral electron-rich heterocycles containing sulfur and oxygen atoms and acts as a selective sorbent material for suitably sized S-heterocycles. Complexation was characterized by ^{1}H NMR titration and isothermal titration calorimetry (ITC), single-crystal X-ray diffraction (SC-XRD), ^{13}C solid-state CPMAS NMR (ssNMR), and thermogravimetric analysis (TGA) and applied in SPE.

MATERIALS AND METHODS

Materials, Reagents, and Solvents

All reagents and solvents were purchased from commercial suppliers. Ultrapure water for sample preparation in ITC and extraction studies was obtained by means of Milli-Q® IQ 7003/05/10/15. Macrocyclic host compounds (cycHC[n]) were synthesized in our laboratory according to the procedures described in the literature (Aav et al., 2013; Prigorchenko et al., 2015; Kaabel et al., 2019).

Binding of Heterocycles in Solid State

Single crystals of the host–guest complexes were obtained from saturated cycHC[8] solutions in methanol by adding 20 µL of the

respective guest compound. SC-XRD data were collected at 123 K on a Rigaku Compact HomeLab diffractometer, equipped with a Saturn 944 HG CCD detector and an Oxford Cryostream cooling system using monochromatic Cu-Kα radiation (1.54178Å) from a MicroMax™-003 sealed tube microfocus X-ray source. The crystallographic data are deposited with the Cambridge Crystallographic Data Centre (CCDC 2069875–2069879) and can be obtained free of charge via www.ccdc.cam.ac.uk/data_request/cif.

Complexation between 1,3-dithiolane and cycHC[n] upon SPE was investigated by simultaneous thermogravimetry and differential thermal analysis coupled with evolved gas mass spectrometric analysis (TG-DTA/EGA-MS). The measurements were performed in the apparatus consisting of a Setaram SetSys-Evo 1600 thermal analyzer and a Pfeiffer OmniStar quadrupole mass spectrometer. Additionally, binding of 1,3-dithiolane and α-lipoic acid by cycHC[n] was characterized with ^{13}C ssNMR spectroscopy. The solid complexes were obtained via ball milling of cycHC[8] with the respective guest in the presence of a small amount of water. The ssNMR spectra were acquired on a Bruker Avance II spectrometer at 14.1 T magnetic field (^{13}C resonance frequency 150.91 MHz) using a home-built MAS probe for 25 × 4-mm Si$_3$N$_4$ rotors.

Binding of Heterocycles in Solution

Complexation-induced shifts of cycHC[8] were studied by ^{1}H NMR spectroscopy in 3 mM CD$_3$OD solution upon addition of 60 eq. of the respective guest compound. Association constants for the complexation with 1,3-dithiolane, 1,4-thioxane, and 1,4-dioxane were determined by ^{1}H NMR titration. ^{1}H NMR (400 MHz) spectra in solution were recorded on a Bruker Avance III spectrometer. Thermodynamic measurements by ITC were performed on a MicroCal PEAQ-ITC calorimeter using a 200-µL calorimetric cell and a 40-µL syringe.

Characterization of the Sorbents

Prior to analysis and further extraction experiments, cycHC[n] were milled in an FTS-1000 shaker mill at 30 Hz frequency by using a 14-ml ZrO$_2$-coated grinding jar charged with 3 × 7-mm ZrO$_2$ milling balls for 30 min. Surface area analysis of the milled cycHC[n] was performed on a KELVIN 1040/1042 Sorptometer at 150°C with N$_2$ as an adsorptive gas and He as a carrier gas. The obtained data were processed by Kelvin 1042 V3.12 software. Microscopic investigation of cycHC[n] particle sizes and their distribution was carried out before and after milling. Solid samples were examined by using an Olympus BX61 microscope. The acquired images were further analyzed by CellProfiler (version 4.0.3) software (Carpenter et al., 2006; McQuin et al., 2018).

Extraction of Heterocycles From Aqueous Solutions

SPE was performed for 0.4–2.7 mM aqueous solutions of heterocyclic guests. A solid sorbent [5 or 20 M excess of cycHC[n] or powdered silicarbon TH90 special, Aktivkohle, taken in the equivalent amount by weight/extraction performance to that of the macrocyclic host] was dispersed in the guest solution and rotated for 30–60 min on a Vortex-Genie 2 mixer or Stuart magnetic stirrer. The heterogeneous mixture was further separated by using either a Hettich Universal 32R centrifuge or RC membrane syringe filters, and the liquid phase was analyzed for the guest content by HPLC or UV spectrophotometry. HPLC determination was performed on an Agilent 1200 Series HPLC system equipped with a multiple wavelength detector (MWD), Macherey-Nagel Nucleoshell RP18 column (150 × 3.0 mm, 2.7 μm), or Phenomenex Kinetex XB-C18 column (150 × 4.6 mm, 2.6 μm). UV absorption was measured by using a Jasco V-730 dual beam spectrophotometer and Varian Cary 50 UV-vis spectrophotometer in 10 mm quartz cuvettes. Mettler Toledo AB204-2 analytical balances (precision 0.1 mg) and Radwag MYA 11.4Y microbalances (precision 0.006 mg) were used in sample preparation.

Reusability of cycHC[8] was investigated by comparing its removal efficiency after four sorption–desorption cycles. The sorption step was performed analogously to the extraction procedure. The desorption step included rinsing the material with water, drying for 6 h at 110–120°C in the oven, followed by additional drying for 3 h under vacuum. The dried macrocycle was milled according to the general procedure and utilized in the subsequent cycle.
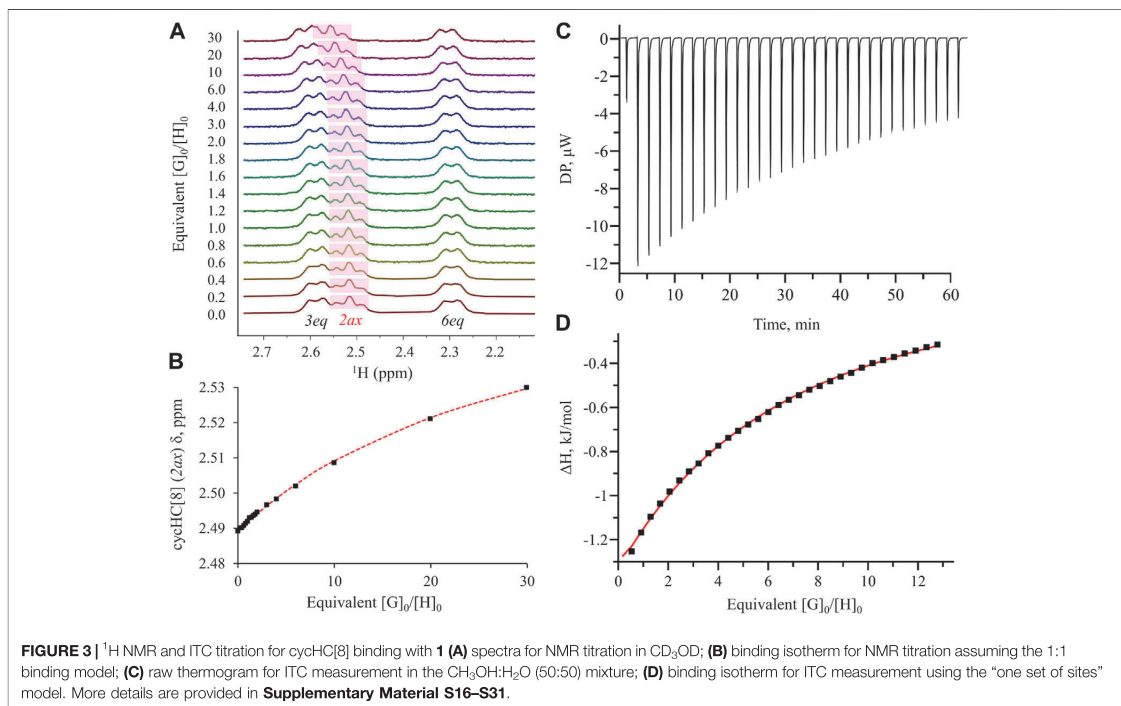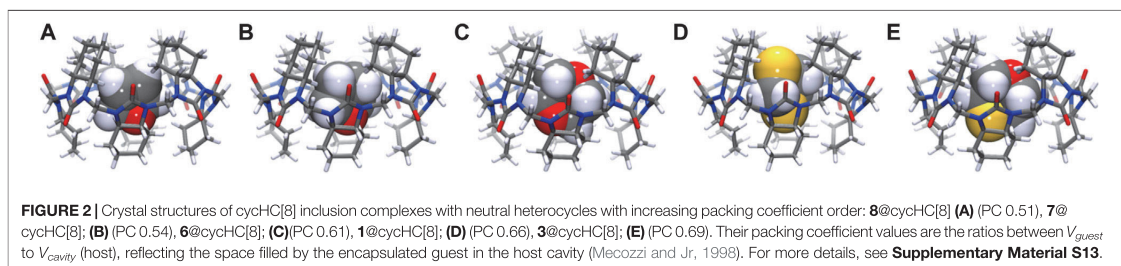
RESULTS AND DISCUSSION

SC-XRD of Inclusion Complexes

A series of compatibly sized electron-rich S-, O-, and N-heterocyclic compounds were crystallized via slow evaporation, and compounds 1, 3, 6, 7, and 8 formed inclusion complexes with cycHC[8] upon co-crystallization (**Figure 2** and **Supplementary Materials S4–S13**). The N-containing heterocycles, 12 and 13, and the largest explored guest, 4, did not yield crystals of inclusion complexes with cycHC[8]. Packing of 1 and 3 inclusion complexes with cycHC[8] gave rise to isomorphous (Z' = 4) crystal structures (**Supplementary**

Materials S10,11), in an arrangement previously unrecorded for cycHC[8] inclusion complexes. The packing of complexes involving O-containing smaller heterocycles 6, 7, and 8 appears to be mainly directed by hydrogen bonding interactions with methanol such that the resulting crystal structures are isomorphous to each other (**Supplementary Materials S6–S8**) and the previously published methanol solvate of cycHC[8] (Prigorchenko et al., 2015). The smaller guest molecules 6, 7, and 8 had a total site occupancy limited to 50–75% of the resolved disorder components. The remaining electron density map exhibited no clear features, making it impossible to resolve whether the diffuse component of the guest disorder also includes partial substitutional disorder from methanol. In contrast, the position of the larger S-containing guests, 1 and 3, is more conserved within the respective crystal structures (**Supplementary Materials S12,13**) with almost no diffuse component observed, indicating that these guests have fewer orientations available within cycHC[8]. Notably, analyzing the disorder models of all inclusion complexes reveals a similarity throughout, namely, where guests are oriented with heteroatoms close to the portals of cycHC[8] (**Figure 2** and **Supplementary Materials S6–S13**). In several structures, heterocycles are located at a suitable distance (2.7–2.8 Å) from a methanol molecule at the portal of cycHC[8] and can therefore potentially accept hydrogen bonds via the portals of the macrocycle. This process would explain the observed conservation of this type of guest orientation motif. The guest molecules are tightly enwrapped within cycHC[8], especially the largest S-containing compounds, 1 and 3, that fill close to 70% of the cavity volume (**Figure 2**, complexes D and E), indicating that guest binding and release must be accompanied by opening and closing of the host portals. Similar conformational dynamics of cycHC[8] have been previously observed and computationally described in the binding of large anionic guests (Kaabel et al., 2017).

^{1}H NMR and ITC Binding Studies in Solution

Furthermore, we evaluated host-guest complex formation in CD3OD solution. Inclusion complex formation was followed by an observed chemical shift change of cycHC[8] proton H2ax (**Figure 1** and **Supplementary Materials S14, S15**) positioned inside the cavity. Our screening study revealed that S-containing five-membered heterocycles 1 and 2 caused larger chemical shift changes of 0.064 and 0.048 ppm, respectively, compared to the six-membered heterocycles 3, 4, 5, and 6. A negligible shift was observed for 7, while no shift was observed for 8 or the N_heterocycles 10 and 11. Signals of 9 overlapped with the characteristic cycHC[8] signal, and, therefore, its encapsulation could not be evaluated by ^{1}H NMR. Nevertheless, all chemical shift changes were relatively small compared to those that occurred upon binding of anions (Kaabel et al., 2017). The binding of 1, 3, and 6 was further evaluated by ^{1}H NMR titration (**Figures 3A,B**). The guest binding in methanol followed the order of logP values (**Supplementary Materials S48**) and agreed with our screening study; the strongest binding was shown for 1, followed by 3 and 6, with values of K = 7.9 ± 0.2 M^{-1}, 2.18 ± 0.04 M^{-1}, and 1.77 ± 0.04 M^{-1}, respectively (**Supplementary Materials S16–S22**) for the 1:1 binding model.

FIGURE 2 | Crystal structures of cycHC[8] inclusion complexes with neutral heterocycles with increasing packing coefficient order: **8**@cycHC[8] **(A)** (PC 0.51), **7**@cycHC[8]; **(B)** (PC 0.54), **6**@cycHC[8]; **(C)** (PC 0.61), **1**@cycHC[8]; **(D)** (PC 0.66), **3**@cycHC[8]; **(E)** (PC 0.69). Their packing coefficient values are the ratios between V_{guest} to V_{cavity} (host), reflecting the space filled by the encapsulated guest in the host cavity (Mecozzi and Jr, 1998). For more details, see **Supplementary Material S13**.

FIGURE 3 | ^{1}H NMR and ITC titration for cycHC[8] binding with **1 (A)** spectra for NMR titration in CD$_3$OD; **(B)** binding isotherm for NMR titration assuming the 1:1 binding model; **(C)** raw thermogram for ITC measurement in the CH$_3$OH:H$_2$O (50:50) mixture; **(D)** binding isotherm for ITC measurement using the "one set of sites" model. More details are provided in **Supplementary Material S16–S31**.

TABLE 1 | Thermodynamic parameters from ITC measurements for complexation of guests **1**, **3**, and **6** with cycHC[8] for the 1:1 binding model. All energy values are given in kJ/mol.

No.	Guest	Solvent	ΔH°	−TΔS°	ΔG°	Ka, M$_{-1}$
1	**1**	CH$_3$OH	−9.8 ± 0.6	3.6	−6.2	13.1 ± 0.8
2	**1**	CH$_3$OH:H$_2$O (50:50)	−20.4 ± 0.9	10.2	−10.2	65.6 ± 2.5
3	**3**	CH$_3$OH	−13.7 ± 1.2	11.4	−2.3	2.5 ± 0.2
4	**3**	CH$_3$OH:H$_2$O (50:50)	−42.9 ± 3.9	39.6	−3.3	3.7 ± 0.3

The thermodynamic characteristics of binding were collected by ITC (**Figures 3C,D**; **Table 1** and **Supplementary Materials S23–S31**). Binding of **6** with cycHC[8] in methanol was too weak

to be determined by ITC; however, K values for S-heterocycles **1** and **3** were in agreement with NMR data, showing the strongest binding for guest **1** (**Table 1**, lines 1 and 3). The binding of both guests in

methanol was enthalpically favorable and entropically unfavorable. A similar binding character was observed upon the binding of chaotropic anions to cycHC[8] in protic media (Kaabel et al., 2017). Although chaotropicity is mainly attributed to ionic species, chaotrope-like organic molecules have been reported in studies of crystalline hydrates (Dobrzycki et al., 2019). The chaotropic character (Assaf and Nau, 2018) is most strongly exhibited in aqueous media, and higher solvent polarity can enhance binding to the hydrophobic host. We further studied the binding of **1** and **3** in mixtures of CH_3OH and H_2O (**Supplementary Materials S25–S27,S29**). In the presence of water, binding of the guests was indeed stronger, increasing the association constant of **1** from 13 M^{-1} in CH_3OH to a value of 66 M^{-1} in the 1:1 $CH_3OH:H_2O$ (50:50) mixture (**Table 1**, lines 1–2). For the bulkier and less hydrophobic guest **3**, the observed increase in the association constant was smaller (**Table 1**, lines 3–4). Binding enthalpy was strongly increased in the presence of water, accompanied by a rise in the entropy penalty for both guests (**Table 1**). Any further increase in the proportion of water proved impossible due to the limited solubility of cycHC[8].

Characterization of Solid cycHC[*n*] and SPE Experiments

The low water solubility of the hydrophobic cycHC[8] and its ability to form inclusion complexes prompted us to investigate whether cycHC[8] can be used for the sorption of heterocycles from water *via* SPE. In parallel with cycHC[8], powdered silicarbon (TH90) and cycHC[6] were used. The cycHC[6] consists of the same monomers, so the hydrophobic properties of the outer surface are very similar to those of cycHC[8], but its cavity is much smaller (35 $Å^3$) (Prigorchenko et al., 2015), and thus, it cannot accommodate the heterocycles studied. Hence, cycHC[6] served as an analog for differentiation between external physisorption and inclusion complex formation during extraction. The commonly used activated carbon-based sorbent TH90 was chosen as a reference to evaluate the efficiency and selectivity of sorption. The cycHC[*n*] compounds were milled before their use in extraction; microscopy studies and image analysis of the cycHC[*n*] showed that milling led to a relatively uniform particle size of 5 μm (**Supplementary Materials S32–35**). The Brunauer–Emmett–Teller (BET) analysis of cycHC[*n*] by N_2 adsorption–desorption (**Supplementary Materials S36,37**) found the available surface area to be relatively similar for both cycHC[6] and cycHC[8] with values of 6.03 m^2/g and 9.02 m^2/g, respectively; therefore, the cycHC[*n*] homologs are expected to have similar extraction efficiencies. In contrast, the surface area of commercially available TH90 is much larger (ca. 1000 m^2/g), which allows us to predict higher extraction efficiency per weight.
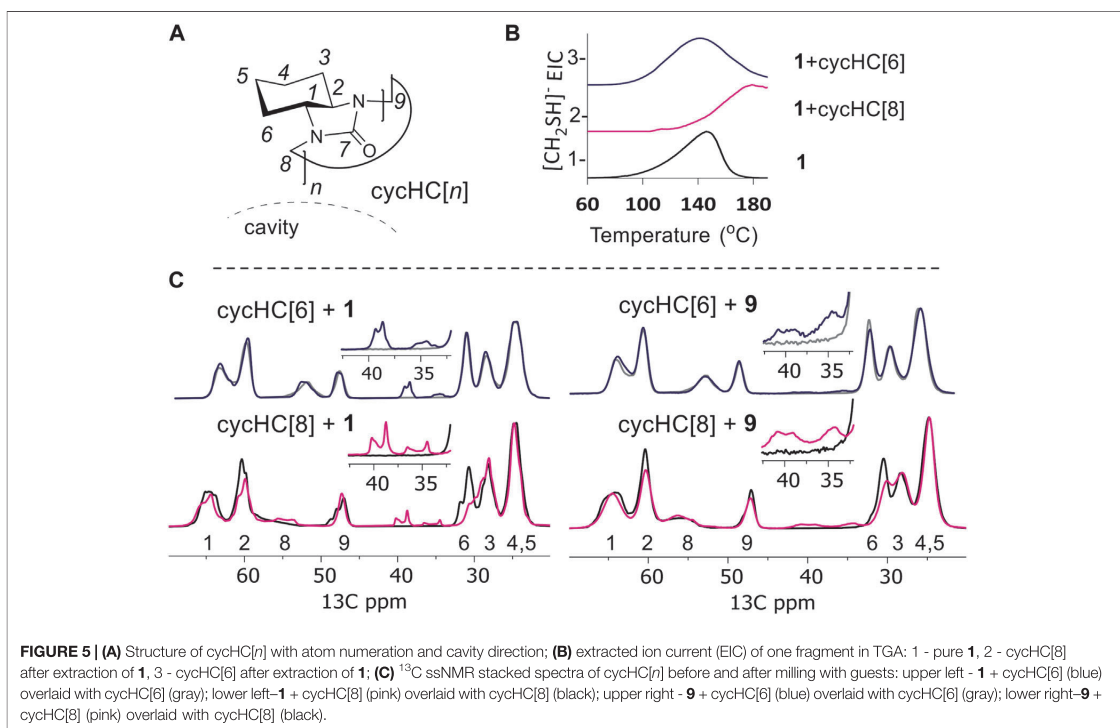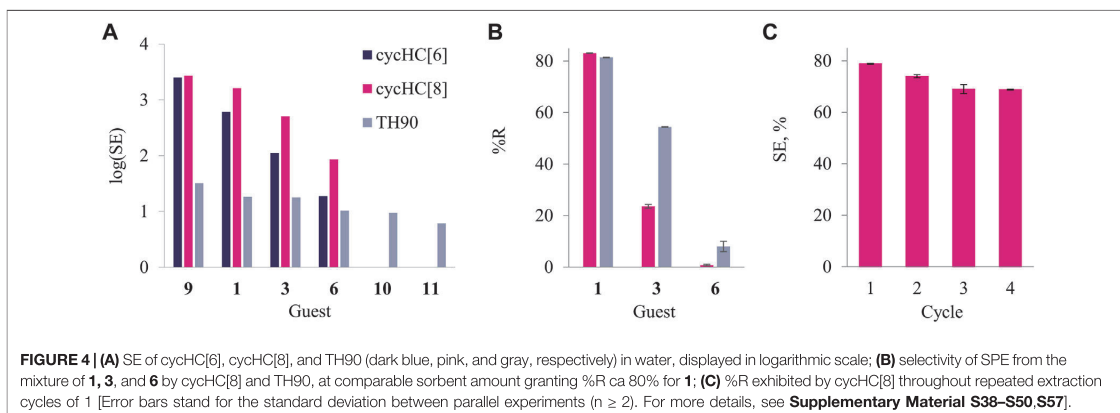
SPE was performed for heterocycles **1, 3, 6, 9, 10**, and **11** by stirring the dispersed solid sorbent in an aqueous solution of each guest; the change in the guest concentration upon extraction was then determined (**Supplementary Materials S47,48**). The cycHC[*n*] demonstrated negligible removal of O-containing **6**, as well as N-containing **10** and **11**. The larger cycHC[8] proved to efficiently extract the S-containing **1** (78%) and moderately remove **3** (25%), while cycHC[6] was considerably less efficient at removing these guests, with a 16% extraction value for **1** and only 3% value for **3**.

As expected, TH90 acts as a non-selective adsorbent, and taken in the same ratio of guest to sorbent (by weight), it removes over 50% of all of the studied heterocycles from water. Sorption efficiency (*SE*) was expressed as the mass of the sorbed guest (μg) per cm^2 of the respective sorbent surface area and converted into logarithmic scale. The latter demonstrates that cycHC[*n*] possess higher affinity toward hydrophobic S-containing heterocycles, while TH90 exhibits roughly the same performance independently of the guest nature (**Figure 4A**). Furthermore, we evaluated sorption selectivity using a mixture of guests **1, 3**, and **6**, and the amount of sorbent (cycHC[8] and TH90) providing ca. 80% removal percentage (%R) for guest **1** (**Supplementary Materials S49, S50**). Both sorbents showed low sorption of the least hydrophobic guest **6**, although TH90 proved to remove ca. 10 times more than cycHC[8]. More importantly, over two times difference was observed between the affinity of two S-heterocycles **1** and **3**; cycHC[8] is 2.3 times more selective than TH90 (**Figure 4B** and **Supplementary Material S50**); in addition, cycHC[8] sorbent is reusable after binding of **1**. A simple washing and drying procedure, followed by milling, allows the reactivation of the sorbent's surface for future use without significant loss in binding efficiency for at least four cycles (**Figure 4C** and **Supplementary Materials S57–58**).

TGA and ^{13}C ssNMR Studies

The formation of inclusion complexes in the cycHC[8] sorbent after SPE of **1** was confirmed by TGA, by identifying the formation of the characteristic fragmentation product $[CH_2SH]^-$ (*m/z* 47) of **1** when bound to cycHC[*n*] sorbents and in pure form (see **Supplementary Material S51** for details). The evolution profiles for pure **1** and its complex with cycHC[6] (**Figure 5B**) occur at similar temperatures of 148°C and 138°C, respectively, indicating that no inclusion complexes form with the smaller macrocycle. Furthermore, the complex with cycHC[8] releases the characteristic degradation product at a significantly higher temperature, 189°C, indicating additional interactions between cycHC[8] and one which impact higher thermal stability to **1** (**Figure 5B** and **Supplementary Material S51**). SPE of the largest and most hydrophobic guest in this study, **9**, leads to similar efficiency of extraction by cycHC[6] and cycHC[8], with %R values of 46 and 78%, respectively (**Supplementary Materials S47,48**), which may indicate a different binding behavior of **9** to cycHC[*n*] in comparison to **1**. To better understand the interaction of guests **1** and **9** with cycHC[8] and cycHC[6], we investigated complex formation using ^{13}C ssNMR spectroscopy (**Figure 5C** and **Supplementary Materials S52–56**). Recently, complex formation *via* mechanochemical agitation of cucurbit[7]uril was followed by ssNMR (Dračínský et al., 2021). Powders obtained by liquid-assisted grinding of cycHC[*n*] with the guest in the presence of water served as the model for binding during the extraction process at the solute–solid interphase. **Figure 5C** illustrates the changes induced upon binding of **1** with cycHC[8] and cycHC[6] (**Supplementary Materials S53,54**). The most significant change after milling is observed in the ^{13}C signal of carbons 2 and 6, pointing inside the cavity of cycHC[8] (**Figure 5C** lower left and **Supplementary Material S54**). Intensities of these signals are decreased and the chemical shift in position 6 changed from

FIGURE 4 | (A) SE of cycHC[6], cycHC[8], and TH90 (dark blue, pink, and gray, respectively) in water, displayed in logarithmic scale; **(B)** selectivity of SPE from the mixture of **1**, **3**, and **6** by cycHC[8] and TH90, at comparable sorbent amount granting %R ca 80% for **1**; **(C)** %R exhibited by cycHC[8] throughout repeated extraction cycles of 1 [Error bars stand for the standard deviation between parallel experiments (n ≥ 2). For more details, see **Supplementary Material S38–S50,S57**].

FIGURE 5 | (A) Structure of cycHC[n] with atom numeration and cavity direction; **(B)** extracted ion current (EIC) of one fragment in TGA: 1 - pure **1**, 2 - cycHC[8] after extraction of **1**, 3 - cycHC[6] after extraction of **1**; **(C)** ^{13}C ssNMR stacked spectra of cycHC[n] before and after milling with guests: upper left - **1** + cycHC[6] (blue) overlaid with cycHC[6] (gray); lower left–**1** + cycHC[8] (pink) overlaid with cycHC[8] (black); upper right - **9** + cycHC[6] (blue) overlaid with cycHC[6] (gray); lower right–**9** + cycHC[8] (pink) overlaid with cycHC[8] (black).

30.6 to 29.8 ppm, evidencing the formation of inclusion complex **1**@cycHC[8]. In contrast, the spectra of **1** milled with cycHC[6] do not evidence such changes (**Figure 5C** upper left and **Supplemetary Material S53**), confirming that physisorption on the surface of cycHC[n] does not have a significant effect on sorbent ssNMR shifts. In an analogous experiment with **9** (**Figure 5C** right and **Supplementary Materials S54–S56**)

similar trends can be observed, that is, a change in the signal intensities of carbons 2 and 6 of cycHC[8], accompanied by a slight chemical shift change at carbon 6 (**Figure 5C** lower right) and no change in the spectrum of cycHC[6] (**Figure 5C** upper right). Thus, the prominent selectivity of cycHC[8] toward binding of five-membered S-heterocycles **1** and **9** is explained by inclusion complex formation during SPE. Unfortunately, no

enantioselectivity was observed during extraction of stereoisomers of **9** (**Supplementary Material S48**).

CONCLUSION

Encapsulation of five- and six-membered electron-rich heterocyclic guests by cycHC[8] is mostly related to their size, which must be complementary with the host cavity, and the hydrophobic effect is one of the driving forces of the interaction. From the binding studies of **1** and **3** with cycHC[8] in methanol and a methanol–water mixture, complex formation was found to be even more favorable in the presence of water and the thermodynamic characteristics resembled the binding of chaotropic anions. We showed that cycHC[8] can serve as a selective solid sorbent material for SPE of sulfur heterocycles from aqueous solutions; in addition, cycHC[8] was successfully applied for selective extraction of **1** and **9**. The ssNMR, TGA, and comparative extraction by homologous cycHC[6] and commonly used TH90 revealed that prominent selectivity of cycHC[8] toward binding of five-membered S-heterocycles is driven by inclusion complex formation. Design of advanced material with increased surface area would enhance the extraction performance even further. Crucially, the solid cycHC [8] sorbent material can be reused, which makes it a candidate for applications in selective SPE systems or the removal of pollutants and other target compounds from water, based on molecular recognition properties.

DATA AVAILABILITY STATEMENT

The datasets presented in this study can be found in **Supplementary Material.**

REFERENCES

Aav, R., Shmatova, E., Reile, I., Borissova, M., Topić, F., and Rissanen, K. (2013). New Chiral Cyclohexylhemicucurbit[6]uril. *Org. Lett.* 15, 3786–3789. doi:10.1021/ol401766a

Andersen, N. N., Eriksen, K., Lisbjerg, M., Ottesen, M. E., Milhøj, B. O., Sauer, S. P. A., et al. (2019). Entropy/Enthalpy Compensation in Anion Binding: Biotin[6] uril and Biotin-L-Sulfoxide[6]uril Reveal Strong Solvent Dependency. *J. Org. Chem.* 84, 2577–2584. doi:10.1021/acs.joc.8b02797

Andersen, N. N., Lisbjerg, M., Eriksen, K., and Pittelkow, M. (2018). Hemicucurbit [n]urils and Their Derivatives - Synthesis and Applications. *Isr. J. Chem.* 58, 435–448. doi:10.1002/ijch.201700129

Assaf, K. I., and Nau, W. M. (2018). The Chaotropic Effect as an Assembly Motif in Chemistry. *Angew. Chem. Int. Ed.* 57, 13968–13981. doi:10.1002/anie.201804597

Buschmann, H.-J., Cleve, E., and Schollmeyer, E. (2005). Hemicucurbit[6]uril, a Selective Ligand for the Complexation of Anions in Aqueous Solution. *Inorg. Chem. Commun.* 8, 125–127. doi:10.1016/j.inoche.2004.11.020

Caira, M., Bourne, S., and Mzondo, B. (2017). Encapsulation of the Antioxidant R-(+)-α-Lipoic Acid in Permethylated α- and β-Cyclodextrins: Thermal and X-ray Structural Characterization of the 1:1 Inclusion Complexes. *Molecules* 22, 866. doi:10.3390/molecules22060866

Carpenter, A. E., Jones, T. R., Lamprecht, M. R., Clarke, C., Kang, I., Friman, O., et al. (2006). CellProfiler: Image Analysis Software for Identifying and

AUTHOR CONTRIBUTIONS

FUNDING

ACKNOWLEDGMENTS

SUPPLEMENTARY MATERIAL

The Supplementary Material for this article can be found online at: https://www.frontiersin.org/articles/10.3389/fchem.2021.786746/full#supplementary-material

Quantifying Cell Phenotypes. *Genome Biol.* 7, R100. doi:10.1186/gb-2006-7-10-r100

Celebioglu, A., and Uyar, T. (2019). Encapsulation and Stabilization of α-Lipoic Acid in Cyclodextrin Inclusion Complex Electrospun Nanofibers: Antioxidant and Fast-Dissolving α-Lipoic Acid/Cyclodextrin Nanofibrous Webs. *J. Agric. Food Chem.* 67, 13093–13107. doi:10.1021/acs.jafc.9b05580

Cucolea, E. I., Buschmann, H.-J., and Mutihac, L. (2016). Hemicucurbiturils as Receptors in Extraction and Transport of Some Amino Acids. *Supramolecular Chem.* 28, 727–732. doi:10.1080/10610278.2015.1121267

Dobrzycki, Ł., Socha, P., Ciesielski, A., Boese, R., and Cyrański, M. K. (2019). Formation of Crystalline Hydrates by Nonionic Chaotropes and Kosmotropes: Case of Piperidine. *Cryst. Growth Des.* 19, 1005–1020. doi:10.1021/acs.cgd.8b01548

Dračínský, M., Hurtado, C. S., Masson, E., and Kaleta, J. (2021). Stuffed Pumpkins: Mechanochemical Synthesis of Host-Guest Complexes with Cucurbit[7]uril. *Chem. Commun.* 57, 2132–2135. doi:10.1039/D1CC00240F

Garbusov, V., Rehfeld, G., Wölm, G., Golovnja, R. V., and Rothe, M. (1976). Volatile Sulfur Compounds Contributing to Meat Flavour. Part. I. Components Identified in Boiled Meat. *Nahrung* 20, 235–241. doi:10.1002/food.19760200302

Ikuta, N., Sugiyama, H., Shimosegawa, H., Nakane, R., Ishida, Y., Uekaji, Y., et al. (2013). Analysis of the Enhanced Stability of R(+)-Alpha Lipoic Acid by the Complex Formation with Cyclodextrins. *Ijms* 14, 3639–3655. doi:10.3390/ijms14023639

Jin, X.-Y., Wang, F., Cong, H., and Tao, Z. (2016a). Host-guest Interactions between Hemicucurbiturils and a Hydroxyl-Substituted Schiff Base. *J. Incl. Phenom. Macrocycl. Chem.* 86, 249–254. doi:10.1007/s10847-016-0659-3

Jin, X.-Y., Wang, F., Cong, H., and Tao, Z. (2016b). Host-guest Interactions of Hemicurcurbiturils with Aminophenols. *J. Incl. Phenom. Macrocycl. Chem.* 86, 241–248. doi:10.1007/s10847-016-0653-9

Jin, X.-Y., Zhao, J.-L., Wang, F., Cong, H., and Tao, Z. (2017). Formation of an Interaction Complex of Hemicurcurbit[6]uril and Ferrocene. *J. Organomet. Chem.* 846, 1–5. doi:10.1016/j.jorganchem.2017.05.053

Jõul, P., Vaher, M., and Kuhtinskaja, M. (2018). Evaluation of Carbon Aerogel-Based Solid-phase Extraction Sorbent for the Analysis of Sulfur Mustard Degradation Products in Environmental Water Samples. *Chemosphere* 198, 460–468. doi:10.1016/j.chemosphere.2018.01.157

Kaabel, S., and Aav, R. (2018). Templating Effects in the Dynamic Chemistry of Cucurbiturils and Hemicurcurbiturils. *Isr. J. Chem.* 58, 296–313. doi:10.1002/ijch.201700106

Kaabel, S., Adamson, J., Topić, F., Kiesilä, A., Kalenius, E., Öeren, M., et al. (2017). Chiral Hemicurcurbit[8]uril as an Anion Receptor: Selectivity to Size, Shape and Charge Distribution. *Chem. Sci.* 8, 2184–2190. doi:10.1039/c6sc05058a

Kaabel, S., Stein, R. S., Fomitšenko, M., Järving, I., Friščić, T., and Aav, R. (2019). Size-Control by Anion Templating in Mechanochemical Synthesis of Hemicurcurbiturils in the Solid State. *Angew. Chem. Int. Ed.* 58, 6230–6234. doi:10.1002/anie.201813431

Kandrnálová, M., Kokan, Z., Havel, V., Nečas, M., and Šindelář, V. (2019). Hypervalent Iodine Based Reversible Covalent Bond in Rotaxane Synthesis. *Angew. Chem. Int. Ed.* 58, 18182–18185. doi:10.1002/anie.201908953

Lamberth, C., Walter, H., Kessabi, F. M., Quaranta, L., Beaudegnies, R., Trah, S., et al. (2015). The Significance of Organosulfur Compounds in Crop Protection: Current Examples from Fungicide Research. *Phosphorus, Sulfur, Silicon Relat. Elem.* 190, 1225–1235. doi:10.1080/10426507.2014.984033

Lees, H., Vaher, M., and Kaljurand, M. (2017). Development and Comparison of HPLC and MEKC Methods for the Analysis of Cyclic Sulfur Mustard Degradation Products. *Electrophoresis* 38, 1075–1082. doi:10.1002/elps.201600418

Li, Y., Li, L., Zhu, Y., Meng, X., and Wu, A. (2009). Solvent Effect on Pseudopolymorphism of Hemicyclohexylcucurbit[6]uril. *Cryst. Growth Des.* 9, 4255–4257. doi:10.1021/cg9007262

Lin-Hui, T., Zheng-Zhi, P., and Ying, Y. (1995). Inclusion Complexes of α- Andβ-Cyclodextrin with α-lipoic Acid. *J. Incl. Phenom. Macrocycl. Chem.* 23, 119–126. doi:10.1007/BF00707889

Lizal, T., and Sindelar, V. (2018). Bambusuril Anion Receptors. *Isr. J. Chem.* 58, 326–333. doi:10.1002/ijch.201700111

Maeda, H., Onodera, T., and Nakayama, H. (2010). Inclusion Complex of α-lipoic Acid and Modified Cyclodextrins. *J. Incl. Phenom. Macrocycl. Chem.* 68, 201–206. doi:10.1007/s10847-010-9767-7

Magnusson, R., Nordlander, T., and Östin, A. (2016). Development of a Dynamic Headspace Gas Chromatography-Mass Spectrometry Method for On-Site Analysis of Sulfur Mustard Degradation Products in Sediments. *J. Chromatogr. A.* 1429, 40–52. doi:10.1016/j.chroma.2015.12.009

Mahadevan, K., and Farmer, L. (2006). Key Odor Impact Compounds in Three Yeast Extract Pastes. *J. Agric. Food Chem.* 54, 7242–7250. doi:10.1021/jf061102x

Maršálek, K., and Šindelář, V. (2020). Monofunctionalized Bambus[6]urils and Their Conjugates with Crown Ethers for Liquid-Liquid Extraction of Inorganic Salts. *Org. Lett.* 22, 1633–1637. doi:10.1021/acs.orglett.0c00216

McQuin, C., Goodman, A., Chernyshev, V., Kamentsky, L., Cimini, B. A., Karhohs, K. W., et al. (2018). CellProfiler 3.0: Next-Generation Image Processing for Biology. *Plos Biol.* 16, e2005970. doi:10.1371/journal.pbio.2005970

Mecozzi, S., and Jr, J. R. (1998). The 55 % Solution: A Formula for Molecular Recognition in the Liquid State. *Chem. Eur. J.* 4, 1016–1022. doi:10.1002/(SICI)1521-3765(19980615)4:6<1016:AID-CHEM1016>3.0.CO;2-B

Mishra, K. A., Adamson, J., Öeren, M., Kaabel, S., Fomitšenko, M., and Aav, R. (2020). Dynamic Chiral Cyclohexanohemicurcurbit[12]uril. *Chem. Commun.* 56, 14645–14648. doi:10.1039/D0CC06817A

Mottram, D. S., and Mottram, H. R. (2002). An Overview of the Contribution of Sulfur-Containing Compounds to the Aroma in Heated Foods. In*ACS Symposium Series, Heteroatomic Aroma Compound.* Editors G. A. Reineccius and T. A. Reineccius 826, 73–92. doi:10.1021/bk-2002-0826.ch004

Öeren, M., Shmatova, E., Tamm, T., and Aav, R. (2014). Computational and Ion Mobility MS Study of (All-S)-Cyclohexylhemicurcurbit[6]uril Structure and Complexes. *Phys. Chem. Chem. Phys.* 16, 19198–19205. doi:10.1039/C4CP02202E

Prigorchenko, E., Kaabel, S., Narva, T., Baškir, A., Fomitšenko, M., Adamson, J., et al. (2019). Formation and Trapping of the Thermodynamically Unfavoured

Inverted-Hemicurcurbit[6]uril. *Chem. Commun.* 55, 9307–9310. doi:10.1039/C9CC04990H

Prigorchenko, E., Öeren, M., Kaabel, S., Fomitšenko, M., Reile, I., Järving, I., et al. (2015). Template-controlled Synthesis of Chiral Cyclohexylhemicurcurbit[8]uril. *Chem. Commun.* 51, 10921–10924. doi:10.1039/c5cc04101e

Racz, C.-P., Santa, S., Tomoaia-Cotisel, M., Borodi, G., Kacso, I., Pirnau, A., et al. (2013). Inclusion of α-lipoic Acid in β-cyclodextrin. Physical-Chemical and Structural Characterization. *J. Incl. Phenom. Macrocycl. Chem.* 76, 193–199. doi:10.1007/s10847-012-0191-z

Reany, O., Mohite, A., and Keinan, E. (2018). Hetero-Bambusurils. *Isr. J. Chem.* 58, 449–460. doi:10.1002/ijch.201700138

Rezanka, T., Sobotka, M., Spizek, J., and Sigler, K. (2006). Pharmacologically Active Sulfur-Containing Compounds. *Aiamc* 5, 187–224. doi:10.2174/187152106776359002

Rochette, L., Ghibu, S., Richard, C., Zeller, M., Cottin, Y., and Vergely, C. (2013). Direct and Indirect Antioxidant Properties of α-lipoic Acid and Therapeutic Potential. *Mol. Nutr. Food Res.* 57, 114–125. doi:10.1002/mnfr.201200608

Røen, B. T., Unneberg, E., Tørnes, J. A., and Lundanes, E. (2010). Headspace-trap Gas Chromatography-Mass Spectrometry for Determination of sulphur Mustard and Related Compounds in Soil. *J. Chromatogr. A.* 1217, 2171–2178. doi:10.1016/j.chroma.2010.01.088

Salehi, B., Berkay Yılmaz, Y., Antika, G., Boyunegmez Tumer, T., Fawzi Mahomoodally, M., Lobine, D., et al. (2019). Insights on the Use of α-Lipoic Acid for Therapeutic Purposes. *Biomolecules* 9, 356. doi:10.3390/biom9080356

Schoenauer, S., and Schieberle, P. (2018). Structure-Odor Correlations in Homologous Series of Mercapto Furans and Mercapto Thiophenes Synthesized by Changing the Structural Motifs of the Key Coffee Odorant Furan-2-Ylmethanethiol. *J. Agric. Food Chem.* 66, 4189–4199. doi:10.1021/acs.jafc.8b00857

Takahashi, H., Bungo, Y., and Mikuni, K. (2011). The Aqueous Solubility and Thermal Stability of α-Lipoic Acid Are Enhanced by Cyclodextrin. *Biosci. Biotechnol. Biochem.* 75, 633–637. doi:10.1271/bbb.100596

Ustrnul, L., Burankova, T., Öeren, M., Juhhimenko, J., Ilmarinen, J., Siilak, K., et al. (2021). Binding between Cyclohexanohemicurcurbit[n]urils and Polar Organic Guests. *Front. Chem.* 9, 468. doi:10.3389/fchem.2021.701028

Ustrnul, L., Kaabel, S., Burankova, T., Martõnova, J., Adamson, J., Konrad, N., et al. (2019). Supramolecular Chirogenesis in Zinc Porphyrins by Enantiopure Hemicurcurbit[n]urils (N = 6, 8). *Chem. Commun.* 55, 14434–14437. doi:10.1039/c9cc07150d

Valkenier, H., Akrawi, O., Jurček, P., Sleziaková, K., Lízal, T., Bartik, K., et al. (2019). Fluorinated Bambusurils as Highly Effective and Selective Transmembrane Cl−/HCO3− Antiporters. *Chem* 5, 429–444. doi:10.1016/j.chempr.2018.11.008

Vanninen, P., Östin, A., Bełdowski, J., Pedersen, E. A., Söderström, M., Szubska, M., et al. (2020). Exposure Status of Sea-Dumped Chemical Warfare Agents in the Baltic Sea. *Mar. Environ. Res.* 161, 105112. doi:10.1016/j.marenvres.2020.105112

Vázquez, J., and Sindelar, V. (2018). Supramolecular Binding and Release of Sulfide and Hydrosulfide Anions in Water. *Chem. Commun.* 54, 5859–5862. doi:10.1039/C8CC00470F

Xi, Y., Man, C., Fang, W., Xian-Yi, J., Hang, C., and Zhu, T. (2018). Development of a Sub-group of the Cucurbituril Family, Hemicurcurbiturils: Synthesis and Supramolecular Chemistry. *Mini-rev. Org. Chem.* 15, 274–282.

Appendix 3

Article

Mechanochemically driven covalent self-assembly of a chiral mono-biotinylated hemicucurbit[8]uril

Covalent self-assembly of chimeric hemicucurbituril

R,R- or *S,S-*   D-

(+)- or (−)-mixHC[8]

milling   ripening   DoE

Monitoring reaction composition
Comprehensive analysis

Perchlorate removal by functionalized material

Perchlorate
Sulfate

APS-mixHC[8]   APS

Suut-Tuule and Jarg et al. demonstrate that mechanochemistry enhances reactivity and significantly improves selectivity in the solid-state synthesis of mono-biotinylated hemicucurbit[8]urils. The application of the chimeric macrocycle is showcased by its immobilization on silica and subsequent use as a selective solid-phase extraction material for perchlorate removal.

Elina Suut-Tuule, Tatsiana Jarg, Priit Tikker, ..., Kari Rissanen, Dzmitry Kananovich, Riina Aav

riina.aav@taltech.ee

Highlights

Dynamic covalent chemistry in solid state delivers chimeric hemicucurbit[8]urils

Two major products are amplified from ca. 50,000 possible compounds

Mechanochemistry and anionic templation drive covalent self-assembly

Silica modified by biotinylated macrocycle is suitable for perchlorate capture

Cell Reports
Physical Science

CellPress
OPEN ACCESS
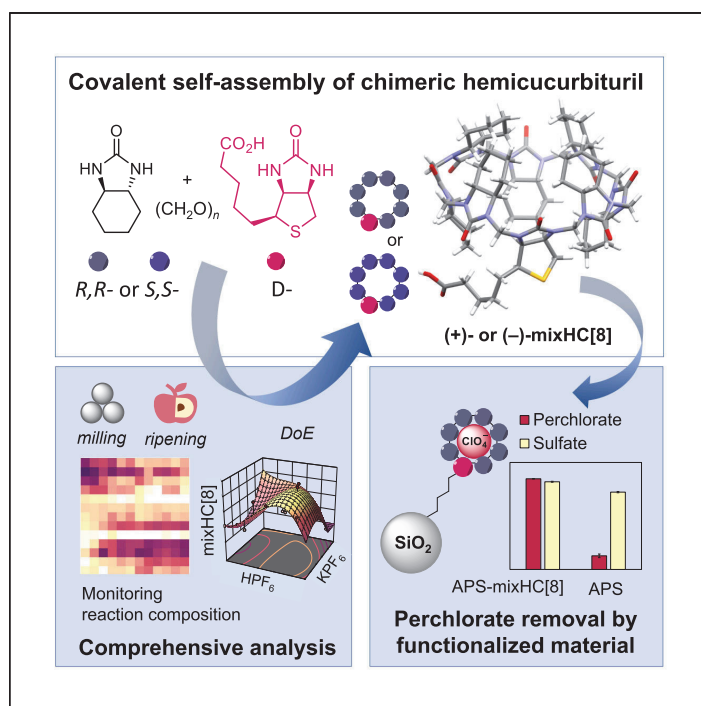
Article

Mechanochemically driven covalent self-assembly of a chiral mono-biotinylated hemicucurbit[8]uril

Elina Suut-Tuule,[1,8] Tatsiana Jarg,[1,8] Priit Tikker,[2] Ketren-Marlein Lootus,[1] Jevgenija Martõnova,[1]
Rauno Reitalu,[1] Lukas Ustrnul,[1] Jas S. Ward,[3] Vitalijs Rjabovs,[4,5] Kirill Shubin,[6]
Jagadeesh V. Nallaparaju,[1] Marko Vendelin,[7] Sergei Preis,[2] Mario Öeren,[1] Kari Rissanen,[3]
Dzmitry Kananovich,[1] and Riina Aav[1,9,10,*]

SUMMARY

Solution-based synthesis of complex molecules with high efficiency leverages supramolecular control over covalent bond formation. Herein, we present the mechanosynthesis of chiral mono-biotinylated hemicucurbit[8]urils (mixHC[8]s) via the condensation of D-biotin, (R,R)- or (S,S)-cyclohexa-1,2-diylurea, and paraformaldehyde. The selectivity of self-assembly is enhanced through mechanochemistry and by fostering non-covalent interactions, achieved by eliminating solvents and conducting the reaction in the solid state. Rigorous analysis of intermediates reveals key processes and chemical parameters influencing dynamic covalent chemistry. The library of ca. 50,000 theoretically predicted intermediates and products leads to covalent self-assembly of chiral hemicucurbiturils. Mechanochemically prepared diastereomeric (−)- and (+)-mixHC[8]s are suitable for anion binding and derivatization. Immobilization of the macrocycles on aminated silica produces a functional material capable of selective capture of anions, as demonstrated by efficient perchlorate removal from a spiked mineral matrix.

INTRODUCTION

The spontaneous organization of molecular species relies on non-covalent interactions, resulting in intricate aggregates. Such supramolecular self-assembly can facilitate the formation of covalent bonds leading to complex molecules and may be exceptionally responsive to minor changes in the reaction conditions, resulting in the amplification of particular products.[1] In the case of increased molecular crowding, the dynamics of an interaction between species is accelerated compared to a dilute environment, which has been demonstrated for strongly hydrogen-bonded base pairs of nucleic acids.[2] Furthermore, in the solid state at extreme concentrations, unobstructed by solvent, the number of non-covalent interactions between counterparts increases, enabling the formation of products that are less favored in solution.[3,4] Mechanochemical activation enhances chemical reactivity and provides a solvent-free sustainable approach in chemical syntheses.[5–7]

Single-bridged cucurbituril-type molecular containers, hemicucurbit[n]urils (HC[n]s) are renowned for their anion-binding properties and typically assembled from urea monomers in a one-pot reaction with dynamic covalent chemistry (DCC).[8–10] Although the size of the macrocycle can be controlled by anion templation,[8,11–15] HC[n]s prevalently consist of six units.[12,16,17] Up to date, 8-membered HC[n]s have been synthesized exclusively from chiral C_2-symmetric cyclohexa-1,2-diylurea (CU)

[1]Tallinn University of Technology, Department of Chemistry and Biotechnology, 12618 Tallinn, Estonia

[2]Tallinn University of Technology, Department of Materials and Environmental Technology, 19086 Tallinn, Estonia

[3]University of Jyvaskyla, Department of Chemistry, 40014 Jyväskylä, Finland

[4]National Institute of Chemical Physics and Biophysics, 12618 Tallinn, Estonia

[5]Institute of Chemistry and Chemical Technology, Riga Technical University, 1048 Riga, Latvia

[6]Latvian Institute of Organic Synthesis, 1006 Riga, Latvia

[7]Tallinn University of Technology, Department of Cybernetics, 12618 Tallinn, Estonia

[8]These authors contributed equally

[9]X (formerly Twitter): @RiinaAav

[10]Lead contact

*Correspondence: riina.aav@taltech.ee

https://doi.org/10.1016/j.xcrp.2024.102161

CellPress
OPEN ACCESS

Cell Reports
Physical Science
Article

monomers, and the corresponding (*R*,*R*)- and (*S*,*S*)-cyclohexanohemicucurbit[8]urils (cycHC[8]s) can be assembled both in solution[18] and the solid state.[17] Their larger cavity expands the range of applications, and the insertion of another functional monomer, such as D-biotin, into the cycHC[8] scaffold can further enhance receptor versatility. Biotin is a naturally occurring and commercially available compound with a carboxylic group suitable for derivatization. Furthermore, it has previously been used in the synthesis of chiral macrocycles.[13] So far, the reported chimeric HC[*n*]s assembled from non-equivalent urea monomers have been limited to 6-membered hybrid HC[*n*]s prepared in solution via multi-step approaches[19,20] and mono-functionalized bambus[6]urils obtained in a one-pot reaction.[21–23] The difficulties in the single-step formation of non-uniformly composed macrocycles arise from a plethora of possible linear and cyclic intermediates. Consequently, arranging a chaotic mixture into a well-organized molecule presents considerable challenges, and the number of combinations increases with the number of monomeric units.

Mechanochemistry has been utilized in the synthesis of several macrocycles,[17,24–30] inducing covalent assembly of uniformly structured monomers. As mechanosynthesis enables overcoming the solubility barriers and promotes reactions between compounds with drastic polarity differences, its potential can be exploited even further. To the best of our knowledge, there have been no reports describing covalent self-assembly of macrocycles from mixtures of various monomers in the solid state. The formation of chiral chimeric HC[*n*]s via DCC in the solid state could pave the way to novel synthetic approaches, unlocking access to versatile applications.

The present work describes a mechanochemically activated solid-state condensation of (*R*,*R*)- or (*S*,*S*)-CU, D-biotin ((*S*,*S*,*R*)-B), and paraformaldehyde and their selective covalent self-assembly into the enantiopure mono-biotinylated HC[8]s (−)-((*S*,*S*,*R*)(*R*,*R*)₇)-mixHC[8] or (+)-((*S*,*S*,*R*)(*S*,*S*)₇)-mixHC[8], along with homomeric cycHC[8]s. The challenges of assembling a chimeric mono-functionalized 8-membered macrocycle are related to the number of possible combinations of monomeric units and their chemical reactivity. Fine-tuning of the reaction conditions enabled amplification of the two major products, chimeric mixHC[8] and homomeric cycHC[8], among 498 potential 8-membered HC[*n*]s[31] (Figure 1; theoretical number of linear cyclic oligomers in the supplemental experimental procedures; Data S1).

The covalent assembly process is essentially solvent free and has a very low process mass intensity (PMI; the mass of all used reagents per formed product[32]). The most significant chemical and technical factors affecting macrocyclization were identified with response surface methodology (RSM) and thorough analysis of intermediates by high-performance liquid chromatography-mass spectrometry (HPLC-MS) provided mechanistic insight into this complex process. The affinity of mixHC[8] for selected anions and the subtle differences in the binding properties of the two chimeric diastereomers were determined by isothermal titration calorimetry (ITC) and characterized by single-crystal X-ray crystallography (SC-XRD) and modeling studies. Furthermore, a practical example of the selective anion capture by silica-immobilized mixHC[8] was demonstrated in the efficient removal of perchlorate from a spiked mineral matrix.

RESULTS AND DISCUSSION

### Covalent assembly of hemicucurbiturils in the solid state

The first attempts to synthesize mono-functionalized mixHC[8] in solution according to the protocol developed for cycHC[8][18] were promising. The condensation of

Cell Reports
Physical Science
Article

CellPress
OPEN ACCESS
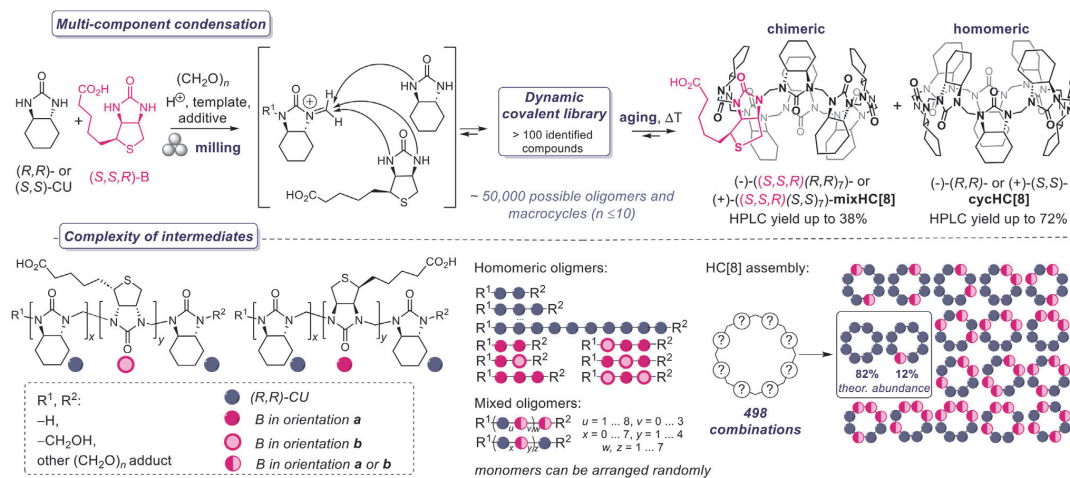
Figure 1. Synthetic scheme and complexity of intermediates during formation of the HC[8]s studied in this work

Multi-component condensation of (S,S,R)-biotin (B) and (R,R)- or (S,S)-cyclohexa-1,2-diylurea (CU) to homomeric cycHC[8]s and chimeric mixHC[8]s. The complexity of the intermediates in the DCL is expressed via possible numbers of oligomers, HC[8]s, and the abundance of major HC[8]s resulting from the 1:7 (B:CU) ratio of starting materials (theoretical number of linear cyclic oligomers in the supplemental experimental procedures; Data S1). The best reaction conditions afford 38% and 34% yields of mixHC[8] and cycHC[8], respectively: 1 equiv B, 7 equiv CU, 8 equiv $(CH_2O)_n$ in the presence of 2 equiv HPF_6 and 1 equiv KPF_6, milled at 30 Hz for 60 min and aged at 60°C for 3 h. (Table S15). The highest yield (72%) of cycHC[8] was observed under the following conditions: 1 equiv B, 15 equiv CU, 16 equiv $(CH_2O)_n$ in the presence of 3 equiv $HClO_4$, milled at 30 Hz for 60 min and aged at 45°C for 24 h (Table S2).

biotin and CU taken in stoichiometric 1:7 molar ratio with paraformaldehyde, mediated by trifluoroacetic acid in acetonitrile, produced mixHC[8] and cycHC[8] in 9% and 38% yields, respectively (see synthesis in solution in the supplemental experimental procedures; Data S1). The ratio of the macrocycles did not reflect the statistical distribution based on the starting monomer ratio, which implied a strong influence of the chemical parameters. In solution-based synthesis, compatibility between the solvent and reagents governs the fast diffusion and mixing of starting materials, intermediates, and products, as well as their reactivity. Poor solubility can obstruct reactions, especially in DCC, due to suppressed exchange between reactants. We envisioned that mixHC[8]s may be assembled with higher efficiency in the solid state, where solubility is not critical, non-covalent interactions are not obstructed by the solvent, and templation is enhanced due to a high concentration of reactants.[3] According to the previous study,[17] covalent self-assembly in the solid state required just a minute amount of a liquid additive[33–35] to facilitate proton transfer and delivery of the anionic template, as well as to promote conformational flexibility. The complexity of the dynamic covalent library (DCL) drastically increases in multi-component reactions; for instance, the incorporation of non-C_2 symmetric (R,S)-CU units resulted in higher stereochemical diversity and the formation of several diastereomeric HC[n]s (i.e., cis-cycHC[6] and inverted-cis-cycHC[6]).[36] Similarly, condensation of chiral CU and non-C_2 symmetric biotin into linear and cyclic oligomers can be realized via various combinations, considering the possibility of different orientations of the biotin unit (Figure 1). For instance, all forms with a length of 2 to 10 monomers result in ca. 50,000 cyclic and linear oligomers. However, the number of possible products can be decreased by templation. Variation of position, orientation, and number of B and CU monomers leads to 498 potential 8-membered macrocycles[31] (Figure 1; theoretical number of linear cyclic oligomers in the
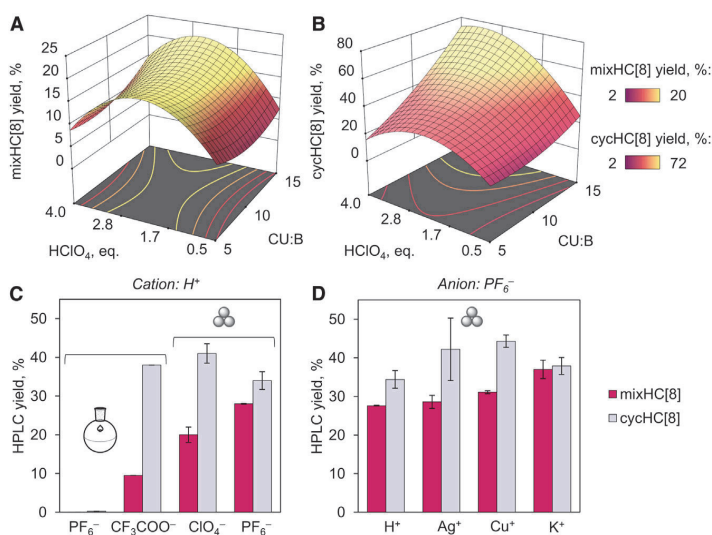
Figure 2. 3D response surfaces and bar charts expressing the formation of HC[8]s

(A and B) 3D response surfaces displaying the influence of the ratio of monomers and loading of aq. $HClO_4$ on the HPLC yields of (A) mixHC[8] and (B) cycHC[8].

(C and D) Bar charts comparing the effect of the acid anions (CF_3COO^-, ClO_4^-, and PF_6^-) in solution and the solid state (C) and hexafluorophosphate salt cations (Ag^+, Cu^+, K^+) in the solid state (D) on the yields of cycHC[8] (gray) and mixHC[8] (magenta). Error bars on HPLC yields express standard deviation between reproduced reactions (n = 2–8). For more details, see Table S7.

supplemental experimental procedures; Data S1). Full conversion of the 1:7 ratio of B and CU into HC[8]s is expected to direct 498 combinations to 12% and 82% of mixHC[8] and cycHC[8], respectively (Figure 1; Table S1).

The fact that solution-phase synthesis did not result in a statistical ratio of more favored HC[8]s encouraged us to study if the selectivity of mono-biotinylated mixHC[8] formation can be increased via tuning the conditions of the mechanosynthesis. To investigate the effect of multiple reaction parameters on the assembly of 8-membered macrocycles, we utilized RSM for experimental design and screening of reaction conditions.[37] The HPLC yields of mixHC[8] and cycHC[8] obtained after the aging step were plotted as 3D response surfaces, highlighting the conditions favorable for the assembly of mixHC[8] compared to cycHC[8] (Figures 2A, 2B, S3, and S4; Tables S2–S6). The ratio of monomers, loading of aqueous mineral acid ($HClO_4$), milling duration, and aging temperature, which affect macrocyclization,[8] were simultaneously explored.

The formation of mixHC[8] and cycHC[8] proved to be sensitive to the monomer ratio and acid loading (Figures 2A and 2B). Variations of the monomer ratios within the range of 1:5 to 1:15 did not significantly affect the yield of chimeric mixHC[8] (Figure 2A; Table S2); however, using an excess of CU clearly resulted in the enhanced generation of cycHC[8] (Figure 2B; Table S2). The quantity of $HClO_4$ appeared to be the vital parameter affecting the formation of mixHC[8]. The highest yields of mixHC [8] were attained within the specific range of $HClO_4$ loadings of 1.2–3.0 equiv (Figure 2A), while cycHC[8] was less dependent on the quantity of acid catalyst. This observation highlights the difference in formation of mixHC[8] and cycHC[8] in

Cell Reports
Physical Science
Article

CellPress
OPEN ACCESS

response to varied reaction conditions. The impacts of milling time and aging temperature appeared to be less significant, and the optimal temperature for ripening mixHC[8] was found to range from 40°C to 65°C. RSM helped to reach a 20% yield of mixHC[8] under standard conditions—3 equiv of template, 1 h ball milling followed by 24 h aging at 60°C—selected for further optimization studies.

It was hypothesized that an alternative template could amplify the formation of the target macrocycle. The binding studies for the cycHC[8] receptor revealed the following ranking of anion affinity: $SbF_6^- > PF_6^- > ReO_4^- > ClO_4^-$.[11] The use of hexafluoroantimonate (SbF_6^-) as a template did not seem practical since $HSbF_6$ mainly exists as the HF/SbF_5 superacid system.[38,39] Hexafluorophosphate (PF_6^-), on the other hand, serves as an efficient template for the synthesis of homomeric cycHC [8] in solution.[18] Due to its advantageous templating potential, HPF_6 was chosen as an alternative reagent to mediate the solid-state synthesis of mixHC[8]. In addition, it is safer to handle than perchlorates, which are known for their undesirable oxidative, flammable, and explosive hazards.[40,41] Interestingly, the use of HPF_6 resulted in decreased formation of homomeric cycHC[8], contrary to an improved yield (28%) of mixHC[8] (Figure 2C; Table S7). Since the mixHC[8] assembly was highly sensitive to the quantity of acid (Figure 2A), we tested three hexafluorophosphate salts ($AgPF_6$, $[Cu(CH_3CN)_4]PF_6$, and KPF_6) as additives to partially substitute the acid while keeping the amount of template anion constant (Figure 2D; Table S7). Additionally, we anticipated that the Ag^+ and Cu^+ cations could serve as potential promoters for the generation of mixHC[8] due to their affinity for biotin.[42–44] As depicted in Figure 2D, the Ag^+ and Cu^+ salts had a negligible effect on the formation of mixHC[8] while improving the yield of homomeric cycHC[8] compared to the reaction with HPF_6. The latter points at the effective decrease in the concentration of antagonistic[45] CU-rich mixed oligomers, which reassembled and provided CU to cyclize into cycHC[8]. The best result was achieved with KPF_6, which afforded the highest yield of mixHC[8] (37%) with the accompanying formation of cycHC[8] (38%) (Figure 2D). Further variation of HPF_6/KPF_6 equivalence by RSM, however, did not improve the formation of mixHC[8] (Tables S8–S12; Figure S8). It was additionally confirmed that the stoichiometric ratio of the starting monomers provided the best mixHC[8] yield (Table S13). Once the key chemical parameters had been identified, the durations of ball milling and aging at moderately elevated temperatures were optimized, leading to the best 38% yield of mixHC[8] in a 4 h total reaction time (Tables S14 and S15; for conditions, see the Figure 1 caption).

The changes in the content of intermediates and products were analyzed by HRMS. Altogether, over 100 reaction species were identified in the crude reaction mixtures during different stages of covalent assembly and mapped based on MS signal intensities (Figures 3A and S9–S13; Tables S16 and S29; MatchMass tool[46]). The results display the dynamic changes in the composition of the reaction mixture during milling and aging. Biotin was found to be incorporated into different linear oligomers $(CU)_x(B)_y$ ($x = 1 \ldots 8$, $y = 1 \ldots 4$), as well as into a number of mono-, di-, tri-, and tetra-biotinylated mixHC[n]s ($n = 6 \ldots 8$). Homomeric CU oligomers dominate at the initial phase of the polycondensation reaction (milling time: 5 min) and are kinetically favored products. Consequently, the milling time must be sufficient (60 min; Tables S14 and S15) to enable the accumulation of the slowly generated mixed biotin-containing chains. The content of the mixed oligomers ($n = 6–8$), which are essential for mixHC[n] formation, significantly increased after 45–60 min milling. This difference in the contents of the short- and long-milled mixtures emphasizes the dynamic shuffling of the monomers, which resulted in an increased random distribution of biotin upon prolonged milling. The low content of macrocycles in DCL

CellPress
OPEN ACCESS

Cell Reports
Physical Science
Article
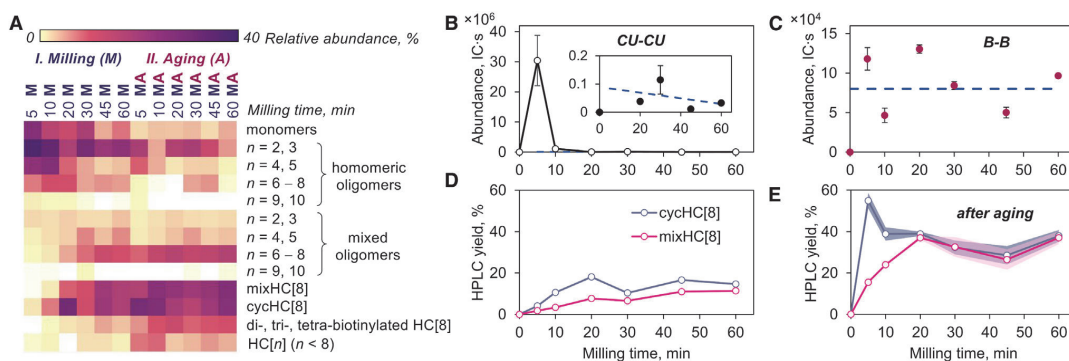
Figure 3. Dynamic covalent library composition and changes in the content of dimers and HC[8]s during mechanosynthesis

DCL composition summarized in a heatmap (A) based on MS abundance of the detected species (Tables S29 and S16; Figure S10); content of homomeric dimers CU-CU (B) and B-B (C) and HPLC yields of macrocycles (D and E) during milling and after aging. The content of the dimers is reported as the MS abundance for triplicate measurements ($n = 3$) $\pm$ standard deviation, and the linear fit is expressed as dashed lines. The yields of macrocycles are presented as mean values obtained in a series of replicated experiments ($2 \leq n \leq 4$) with confidence intervals. More details are provided in Figures S11–S15 and Table S19.

directly after milling can be attributed to the unfavorable complexation with the template,[11,17] most likely due to increased entropy during mechanical agitation. The macrocyclic products predominantly ripened at the aging stage, at which point the mixed and homomeric oligomers underwent additional, although less intense, crossover unit exchange. Moreover, crossover between monomers from macrocycles was observed under similar conditions using cycHC[n]s and biotin as the starting materials for mixHC[8] synthesis (Table S17), which confirms the dynamic character of the covalent self-assembly.

Further understanding of the dynamic processes and interconversion of intermediates occurring at the milling stage was obtained by tracking the fate of selected short oligomers (Figures 3B and 3C; Table S18). The changes in the content of characteristic dimers and trimers prior to and after the aging stage were determined by HPLC-MS analyses. The collected data confirmed that coupling between the CU monomers is kinetically preferred and occurs at the initial phase of the polycondensation reaction. Thus, the quantity of the CU-CU dimer drastically increased after 5 min of milling and subsequently underwent rapid decay (Figure 3B). Such fast dynamics and decay were absent for the biotin units, reflecting a major difference in the condensation between biotin and CU. In contrast to CU, the condensation of the biotin units to the respective dimer, B-B, reached its maximum at the beginning of the reaction and probably acts as a transient intermediate (Figures 3B and 3C). Similar behavior was observed for the respective trimers (Table S18). The yields of the macrocycles generated at the milling stage did not exceed 20% but greatly increased during aging (Figures 3D and 3E). Notably, the macrocyclic content in the aged mixtures is significantly affected by milling duration, when monomer shuffling occurs. Thus, aging of the short-milled (5 min) reaction mixture, which contained mainly homomeric CU oligomers, resulted in the ripening of cycHC[8] as the dominant product (55% yield), along with a minor quantity of mixHC[8] (16% yield). However, fast reversible C–N bond formation and cleavage during milling caused rapid dynamic changes in the oligomeric profile with a random distribution of the biotin units. Upon prolonged milling (60 min; Tables S14 and S15), the yield of mixHC[8] notably increased from 16% to 37%, with a concurrent decrease in the yield of cycHC[8] to 38%, resulting

Cell Reports
Physical Science
Article

CellPress
OPEN ACCESS
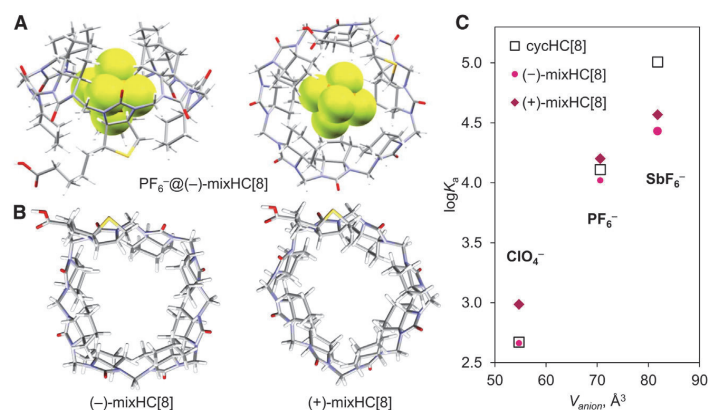
Figure 4. Structures of mixHC[8]s and data on anion binding

PF_6^-@(−)-mixHC[8] inclusion complex from SC-XRD (A) (CCDC: 2251913). DFT low-energy structures of (−)- and (+)-mixHC[8] diastereomers (B) (see the computational study in the supplemental experimental procedures; Data S2). Correlation between anion volumes (V_{anion}) and association constants ($\log K_a$) was determined by ITC for complexes with (TBA)ClO$_4$, (TBA)PF$_6$ (TBA = tetrabutylammonium), and NaSbF$_6$ salts in methanol using one-to-one binding model (C) (Table S6.1).

in a 1:1 product ratio. Finally, a close examination of the aging duration (Table S15) revealed that the maximum content of mixHC[8] was achieved in 3 h, when the templated self-assembly process was essentially complete.

The developed mechanochemical procedure significantly surpassed mixHC[8] synthesis in solution, yielding superior selectivity and conversion rates (Table S30). Solution-state processes are affected by diffusion, with diffusion constants varying for monomers, aggregates, and oligomeric intermediates due to size differences. In mechanochemistry, reaction rates do not directly depend on the molecular size of the intermediates but rather on the number of molecular collisions.[47] In addition to the chemical advantages, solvent-free synthesis produces less waste (PMI = 4) compared to the reaction in solution (PMI = 306) and is more sustainable based on the respective green metrics (Table S30).[32]

Diastereoisomeric (−)- and (+)-mixHC[8]s were synthesized via condensation of either (R,R)-CU or (S,S)-CU with (S,S,R)-B, isolated in 16% and 11% yields with high purity (88% and 90%, respectively), and characterized by nuclear magnetic resonance (NMR) and infrared spectroscopy (Figures S16–S32).

Anion binding properties

The encapsulation of suitably sized anionic guests by HC[n]s is likely governed by electrostatic and orbital interactions.[48] In addition, the anions form weak interactions with C-H groups of HC[n]s pointing inside the cavity.[49] Efficient anion recognition has been reported for bambusurils,[22,50–53] heterobambusurils,[54] biotinurils,[55,56] and cycHC[n]s.[11] We were fortunate to obtain single crystals of the PF_6^- inclusion complex with (−)-mixHC[8] (Figures 4A and S33–S39; Tables S19 and S20). A DFT modeling study of the mixHC[8] diastereomers (Figure S40; Tables S21–S24; Data S2) revealed clear differences in their conformations (Figure 4B; Data S2). The cavity, which is mainly surrounded by CU units, is mostly

CellPress
OPEN ACCESS

**Cell Reports
Physical Science**
Article

distorted by the biotin position. Therefore, its influence on the anion binding properties was evaluated via comparison of the three HC[8] hosts.

Encapsulation of the selected anions by the mixHC[8]s was studied by ITC (Figures 4C and S51–S54; Table S25); the data for cycHC[8] were available from a previous work.[11] Complexation between the mono-biotinylated macrocycles and chaotropic anions (ClO_4^-, PF_6^-, and SbF_6^-) in methanol and a methanol-water mixture (1:1) occurred as an exothermic enthalpy-driven process. The association constants for PF_6^- were greater than that of ClO_4^- in both media, which explains the better templating properties of PF_6^-. Noticeably, the differences between the affinities of the three HC[8] derivatives are the smallest for the templating PF_6^- anion, while for ClO_4^- and SbF_6^-, either (+)-mixHC[8] or cycHC[8], respectively, exhibit stronger binding. The noted dissimilarities highlight distinctions in the cavities and point to the steric differences of these host compounds, which have potential in a diverse array of applications and unique guest-binding properties.

Selective capture of perchlorate by immobilized mixHC[8]

The mixHC[8] can be utilized to afford functional materials, which was showcased by the selective removal of perchlorates from contaminated soil samples. Perchlorate is a persistent pollutant that adversely affects human health by interfering with thyroid hormone production and occurs in soil, ground water, and food.[40,41] The accumulation of perchlorate in fertilizers, soil, and irrigation water leads to increased plant uptake and subsequent food-chain transfer.[57,58] This pollutant has been found in various environmental matrices and typically originates from human activities.

The carboxylate side chain of mixHC[8] enabled its facile covalent immobilization on the surface of 3-aminopropyl silica gel (APS; Figure 5A).[59] The resulting solid perchlorate-extracting material (mixHC[8]-APS) contained ca. 12% (w/w) of mixHC [8], based on infrared spectroscopic analysis (Figures 5B and S55). Once covalently attached to APS, the macrocycle remains in the solid phase even in the solvents where it is commonly soluble (i.e., dichloromethane, methanol) and can, therefore, be applied in solid-phase extraction. To prove the removal of perchlorate in the presence of other minerals, a regolith simulant[60] was employed as the matrix of the known composition and spiked with (TBA)ClO_4, imitating contamination with perchlorate (1% w/w). The obtained model mixture contained cations (Ca^{2+}, Mg^{2+}, Fe^{2+}, Fe^{3+}), oxides, and kosmotropic anions (SO_4^{2-}, CO_3^{2-}) but was essentially free of the organic matter (Table S26). According to ion chromatography analysis (Tables S27 and S28; Figures S56–S59), the methanolic extract of the contaminated matrix contained primarily perchlorate and sulfate, the latter arising from the $MgSO_4$ component (Table S26). Treatment of the methanolic extract with solid mixHC[8]-APS resulted in the complete removal of ClO_4^-, in contrast to non-modified APS, which adsorbed ca. 15% ClO_4^- (Figures 5C and S59; Table S28).

The extraction of sulfate occurred with similar efficiency (ca. 85%–97%) using both APS and mixHC[8]-APS materials, demonstrating that mixHC[8] is not the main contributor responsible for the capture of SO_4^{2-}. The absence of mixHC[8] affinity toward sulfate was additionally confirmed by an ITC experiment (Table S25; Figures S47 and S54).

The captured perchlorate was easily removed by washing mixHC[8]-APS material with water, taking advantage of the weaker binding in the aqueous medium, which demonstrates the potential for the material's reusability.[61]

Cell Reports
Physical Science
Article

CellPress
OPEN ACCESS
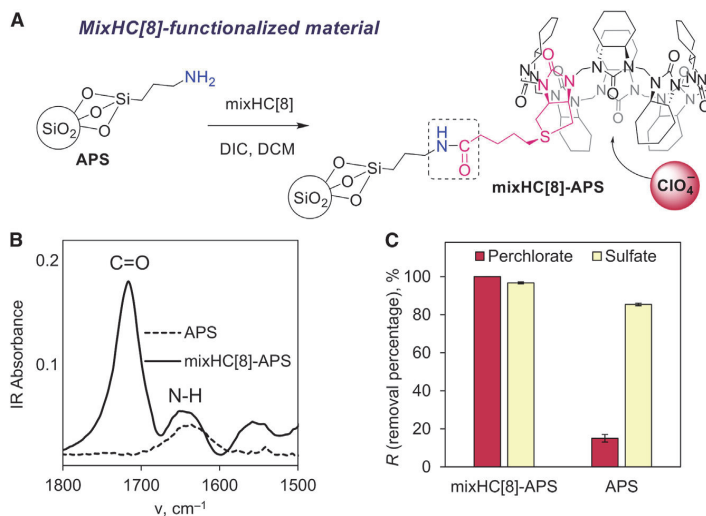
Figure 5. Derivatization of aminated silica by mixHC[8] and perchlorate removal efficiency of the obtained material
Immobilization of mixHC[8] on APS (A), DIC – N,N'-diisopropylcarbodiimide, and DCM (dichloromethane); characterization of material by infrared (IR) (B) and perchlorate removal from spiked mineral matrix using mixHC[8]-APS and non-modified APS, determined by ion chromatography (C). The error bars represent the standard deviation between the parallel experiments ($n \geq 2$) (isothermal calorimetric titration and immobilization of mixHC[8] on APS in the supplemental experimental procedures).

In conclusion, an efficient mechanochemical protocol for the synthesis of enantio-pure mono-biotinylated HC[8]s was developed. The process involves two stages: (1) the mechanochemically assisted and acid-catalyzed polycondensation of D-biotin, (R,R)- or (S,S)-CU, and formaldehyde and (2) the aging step, in which the template-driven covalent self-assembly of oligomers into macrocycles takes place. Screening experiments uncovered the key process and chemical parameters affecting the assembly: the ratio of the monomers, the loading of the acid catalyst, and the nature of the templating anion. The present study offers insight into the complex mixture of oligomeric intermediates, including their interconversion and self-organization processes en route to the macrocyclic products. HPLC-MS analysis of short oligomers revealed differences in condensation kinetics of paraformaldehyde with biotin and CU into homomeric dimers and trimers under mechanochemical agitation. The faster condensation of CU led to amplification of the homomeric cycHC[8] during the aging of shortly agitated reaction mixtures. On the contrary, upon prolonged ball milling, which ensures sufficient shuffling of monomers, higher efficiency in the formation of the chimeric mixHC[8] in 38% yield was achieved. The mechanochemically driven solid-state approach allowed for the fine-tuning of the composition of the rich DCL and directing covalent self-assembly processes beyond statistical distribution. Diastereomeric (−)- and (+)-mixHC[8]s were isolated and their structures characterized by DFT, NMR, and SC-XRD methods. Furthermore, the comparison of their affinities toward chaotropic anions pointed at specific binding differences, which makes the chimeric family of HC[8] appealing for host-guest chemistry. The biotin carboxylate group of the mixHC[8] enabled its facile covalent immobilization on aminated silica. The functional material obtained was employed in the selective capture of anions, as

CellPress
OPEN ACCESS

Cell Reports
Physical Science

Article

demonstrated by the complete removal of perchlorate from an extract of a mineral model mixture. Further applications of these chiral chimeric hemicucurbiturils are currently being studied.

EXPERIMENTAL PROCEDURES

Resource availability

Lead contact

Further information and requests for resources should be directed to and will be fulfilled by the lead contact, Riina Aav (riina.aav@taltech.ee).

Materials availability

All materials generated in this study are available from the lead contact without restrictions for research purposes.

Data and code availability

All data supporting this study's findings are included in the article and its supplemental information and are also available from the authors upon request. Crystallographic data for the structures reported in this paper have been deposited at the Cambridge Crystallographic Data Center under CCDC: 2251913. Copies of these data can be obtained free of charge via www.ccdc.cam.ac.uk/data_request/cif.

SUPPLEMENTAL INFORMATION

Supplemental information can be found online at https://doi.org/10.1016/j.xcrp. 2024.102161.

AUTHOR CONTRIBUTIONS

All authors contributed to the manuscript's preparation and have provided their approval for the final version of the manuscript. The authors' specific contributions are as follows: E.S.-T. was the main contributor for the development of the synthesis and mixHC[8] characterization and participated in binding studies; T.J. was the main contributor of the chemical analysis, binding, immobilization, and perchlorate removal studies; P.T. and S.P. contributed to perchlorate removal; K.-M.L., K.S., and J.V.N. contributed to the synthesis; J.M., J.S.W., and K.R. contributed to SC-XRD analysis; R.R. and M.Ö. contributed to computational studies; L.U. contributed to the script for MS data analysis and binding studies; M.V. contributed to the assessment of combinatorics; V.R. contributed to NMR analysis; D.K. contributed to conceptualization of the synthesis, perchlorate removal, and assessment of green metrics; and R.A. contributed to conceptualization of the overall research, data analysis, writing, and supervision.

Cell Reports
Physical Science
Article

CellPress
OPEN ACCESS

REFERENCES

1. Schnitzer, T., Preuss, M.D., van Basten, J., Schoenmakers, S.M.C., Spiering, A.J.H., Van-tomme, G., and Meijer, E.W. (2022). How subtle changes can make a difference: Reproducibility in complex supramolecular systems. Angew. Chem. *61*, e202206738. https://doi.org/10.1002/ange.202206738.

2. Yamaoki, Y., Nagata, T., Kondo, K., Sakamoto, T., Takami, S., and Katahira, M. (2022). Shedding light on the base-pair opening dynamics of nucleic acids in living human cells. Nat. Commun. *13*, 7143. https://doi.org/10.1038/s41467-022-34822-4.

3. Kwon, T.W., Song, B., Nam, K.W., and Stoddart, J.F. (2022). Mechanochemical enhancement of the structural stability of pseudorotaxane intermediates in the synthesis of rotaxanes. J. Am. Chem. Soc. *144*, 12595–12601. https://doi.org/10.1021/jacs.2c00515.

4. Dračínský, M., Hurtado, C.S., Masson, E., and Kaleta, J. (2021). Stuffed pumpkins: Mechanochemical synthesis of host–guest complexes with cucurbit[7]uril. Chem. Commun. *57*, 2132–2135. https://doi.org/10.1039/D1CC00240F.

5. Friščić, T., Mottillo, C., and Titi, H.M. (2020). Mechanochemistry for synthesis. Angew. Chem. *132*, 1030–1041. https://doi.org/10.1002/ange.201906755.

6. Cuccu, F., De Luca, L., Delogu, F., Colacino, E., Solin, N., Mocci, R., and Porcheddu, A. (2022). Mechanochemistry: New tools to navigate the uncharted territory of "impossible" reactions. ChemSusChem *15*, e202200362. https://doi.org/10.1002/cssc.202200362.

7. Reynes, J.F., Isoni, V., and García, F. (2023). Tinkering with mechanochemical tools for scale-up. Angew. Chem., Int. Ed. Engl. *62*, e202300819. https://doi.org/10.1002/anie.202300819.

8. Kaabel, S., and Aav, R. (2018). Templating effects in the dynamic chemistry of cucurbiturils and hemicucurbiturils. Isr. J. Chem. *58*, 296–313. https://doi.org/10.1002/ijch.201700106.

9. Lehn, J.-M. (1999). Dynamic combinatorial chemistry and virtual combinatorial libraries. Chem. Eur. J. *5*, 2455–2463. https://doi.org/10.1002/(SICI)1521-3765(19990903)5:9<2455::AID-CHEM2455>3.0.CO;2-H.

10. Corbett, P.T., Leclaire, J., Vial, L., West, K.R., Wietor, J.-L., Sanders, J.K.M., and Otto, S. (2006). Dynamic combinatorial chemistry. Chem. Rev. *106*, 3652–3711. https://doi.org/10.1021/cr020452p.

11. Kaabel, S., Adamson, J., Topić, F., Kiesilä, A., Kalenius, E., Öeren, M., Reimund, M., Prigorchenko, E., Lõokene, A., Reich, H.J., et al. (2017). Chiral hemicucurbit[8]uril as an anion receptor: Selectivity to size, shape and charge distribution. Chem. Sci. *8*, 2184–2190. https://doi.org/10.1039/C6SC05058A.

12. Andersen, N.N., Lisbjerg, M., Eriksen, K., and Pittelkow, M. (2018). Hemicucurbit[n]urils and their derivatives – Synthesis and applications. Isr. J. Chem. *58*, 435–448. https://doi.org/10.1002/ijch.201700129.

13. Lisbjerg, M., Jessen, B.M., Rasmussen, B., Nielsen, B.E., Madsen, A.Ø., and Pittelkow, M. (2014). Discovery of a cyclic 6 + 6 hexamer of D-biotin and formaldehyde. Chem. Sci. *5*, 2647–2650. https://doi.org/10.1039/C4SC00990H.

14. Havel, V., Yawer, M.A., and Sindelar, V. (2015). Real-time analysis of multiple anion mixtures in aqueous media using a single receptor. Chem. Commun. *51*, 4666–4669. https://doi.org/10.1039/C4CC10108A.

15. Yawer, M.A., Havel, V., and Sindelar, V. (2015). A bambusuril macrocycle that binds anions in water with high affinity and selectivity. Angew. Chem., Int. Ed. Engl. *54*, 276–279. https://doi.org/10.1002/anie.201409895.

16. Lizal, T., and Sindelar, V. (2018). Bambusuril anion receptors. Isr. J. Chem. *58*, 326–333. https://doi.org/10.1002/ijch.201700111.

17. Kaabel, S., Stein, R.S., Fomitšenko, M., Järving, I., Friščić, T., and Aav, R. (2019). Size-control by anion templating in mechanochemical synthesis of hemicucurbiturils in the solid state. Angew. Chem., Int. Ed. Engl. *58*, 6230–6234. https://doi.org/10.1002/anie.201813431.

18. Prigorchenko, E., Öeren, M., Kaabel, S., Fomitšenko, M., Reile, I., Järving, I., Tamm, T., Topić, F., Rissanen, K., and Aav, R. (2015). Template-controlled synthesis of chiral cyclohexylhemicucurbit[8]uril. Chem. Commun. *51*, 10921–10924. https://doi.org/10.1039/C5CC04101E.

19. Zeng, Q., Long, Q., Lu, J., Wang, L., You, Y., Yuan, X., Zhang, Q., Ge, Q., Cong, H., and Liu, M. (2021). Synthesis of a novel aminobenzene-containing hemicucurbituril and its fluorescence spectral properties with ions.

Beilstein J. Org. Chem. *17*, 2840–2847. https://doi.org/10.3762/bjoc.17.195.

20. Wang, L., Han, J., Pan, R., Yuan, X., You, Y., Cen, X., Zhang, Q., Ge, Q., Cong, H., and Liu, M. (2022). Synthesis of hybrid thiohemicucurbiturils. Tetrahedron Lett. *101*, 153918. https://doi.org/10.1016/j.tetlet.2022.153918.

21. Maršálek, K., and Šindelář, V. (2020). Monofunctionalized bambus[6]urils and their conjugates with crown ethers for liquid–liquid extraction of inorganic salts. Org. Lett. *22*, 1633–1637. https://doi.org/10.1021/acs.orglett.0c00216.

22. De Simone, N.A., Chvojka, M., Lapešová, J., Martínez-Crespo, L., Slávik, P., Sokolov, J., Butler, S.J., Valkenier, H., and Šindelář, V. (2022). Monofunctionalized fluorinated bambusurils and their conjugates for anion transport and extraction. J. Org. Chem. *87*, 9829–9838. https://doi.org/10.1021/acs.joc.2c00870.

23. Del Mauro, A., Lapešová, J., Rando, C., and Šindelář, V. (2024). Merging bambus[6]uril and biotin[6]uril into an enantiomerically pure monofunctionalized hybrid macrocycle. Org. Lett. *26*, 106–109. https://doi.org/10.1021/acs.orglett.3c03715.

24. Langerreiter, D., Kostiainen, M.A., Kaabel, S., and Anaya-Plaza, E. (2022). A greener route to blue: Solid-state synthesis of phthalocyanines. Angew. Chem., Int. Ed. Engl. *61*, e202209033. https://doi.org/10.1002/anie.202209033.

25. Pascu, M., Ruggi, A., Scopelliti, R., and Severin, K. (2013). Synthesis of borasiloxane-based macrocycles by multicomponent condensation reactions in solution or in a ball mill. Chem. Commun. *49*, 45–47. https://doi.org/10.1039/C2CC37538A.

26. Sim, Y., Shi, Y.X., Ganguly, R., Li, Y., and García, F. (2017). Mechanochemical synthesis of phosphazane-based frameworks. Chem. Eur. J. *23*, 11279–11285. https://doi.org/10.1002/chem.201701619.

27. Xi, H.-T., Zhao, T., Sun, X.-Q., Miao, C.-B., Zong, T., and Meng, Q. (2013). Rapid and efficient solvent-free synthesis of cyclophanes based on bipyridinium under mechanical ball milling. RSC Adv. *3*, 691–694. https://doi.org/10.1039/C2RA22802E.

28. Kunde, T., Pausch, T., Guńka, P.A., Krzyżanowski, M., Kasprzak, A., and Schmidt,

B.M. (2022). Fast, solvent-free synthesis of ferrocene-containing organic cages via dynamic covalent chemistry in the solid state. Chem. Sci. *13*, 2877–2883. https://doi.org/10.1039/D1SC06372C.

29. Shy, H., Mackin, P., Orvieto, A.S., Gharbharan, D., Peterson, G.R., Bampos, N., and Hamilton, T.D. (2014). The two-step mechanochemical synthesis of porphyrins. Faraday Discuss *170*, 59–69. https://doi.org/10.1039/C3FD00140G.

30. Su, Q., and Hamilton, T.D. (2019). Extending mechanochemical porphyrin synthesis to bulkier aromatics: Tetramesitylporphyrin. Beilstein J. Org. Chem. *15*, 1149–1153. https://doi.org/10.3762/bjoc.15.111.

31. MathWorld–A Wolfram Web Resource. Weisstein, E. W. Necklace. https://mathworld.wolfram.com/Necklace.html.

32. McElroy, C.R., Constantinou, A., Jones, L.C., Summerton, L., and Clark, J.H. (2015). Towards a holistic approach to metrics for the 21st century pharmaceutical industry. Green Chem. *17*, 3111–3121. https://doi.org/10.1039/C5GC00340G.

33. Friščić, T., Childs, S.L., Rizvi, S.A.A., and Jones, W. (2009). The role of solvent in mechanochemical and sonochemical cocrystal formation: A solubility-based approach for predicting cocrystallisation outcome. CrystEngComm *11*, 418–426. https://doi.org/10.1039/B815174A.

34. Do, J.-L., and Friščić, T. (2017). Chemistry 2.0: Developing a new, solvent-free system of chemical synthesis based on mechanochemistry. Synlett *28*, 2066–2092. https://doi.org/10.1055/s-0036-1590854.

35. Belenguer, A.M., Lampronti, G.I., De Mitri, N., Driver, M., Hunter, C.A., and Sanders, J.K.M. (2018). Understanding the influence of surface solvation and structure on polymorph stability: A combined mechanochemical and theoretical approach. J. Am. Chem. Soc. *140*, 17051–17059. https://doi.org/10.1021/jacs.8b08549.

36. Prigorchenko, E., Kaabel, S., Narva, T., Baškir, A., Fomitšenko, M., Adamson, J., Järving, I., Rissanen, K., Tamm, T., and Aav, R. (2019). Formation and trapping of the thermodynamically unfavoured inverted-hemicucurbit[6]uril. Chem. Commun. *55*, 9307–9310. https://doi.org/10.1039/C9CC04990H.

37. Myers, R.H., Montgomery, D.C., and Anderson-Cook, C.M. (2016). Response Surface Methodology: Process and Product Optimization Using Designed Experiments (John Wiley & Sons).

38. Czapla, M., and Skurski, P. (2015). Strength of the Lewis–Brønsted superacids containing In, Sn, and Sb and the electron binding energies of their corresponding superhalogen anions. J. Phys. Chem. A *119*, 12868–12875. https://doi.org/10.1021/acs.jpca.5b10205.

39. Bour, C., Guillot, R., and Gandon, V. (2015). First evidence for the existence of hexafluoroantimonic(V) acid. Chem. Eur J. *21*, 6066–6069. https://doi.org/10.1002/chem.201500334.

40. Urbansky, E.T. (2002). Perchlorate as an environmental contaminant. Environ. Sci. Pollut. Res. Int. *9*, 187–192. https://doi.org/10.1007/BF02987487.

41. Kumarathilaka, P., Oze, C., Indraratne, S.P., and Vithanage, M. (2016). Perchlorate as an emerging contaminant in soil, water and food. Chemosphere *150*, 667–677. https://doi.org/10.1016/j.chemosphere.2016.01.109.

42. Sigel, H., and Scheller, K.H. (1982). Metal ion complexes of D-biotin in solution. Stability of the stereoselective thioether coordination. J. Inorg. Biochem. *16*, 297–310. https://doi.org/10.1016/S0162-0134(00)80266-4.

43. Aoki, K., and Saenger, W. (1983). Interactions of biotin with metal ions. X-ray crystal structure of the polymeric biotin-silver(i) nitrate complex: metal bonding to thioether and ureido carbonyl groups. J. Inorg. Biochem. *19*, 269–273. https://doi.org/10.1016/0162-0134(83)85031-4.

44. Altaf, M., and Stoeckli-Evans, H. (2013). Chiral one- and two-dimensional silver(I)–biotin coordination polymers. Acta Crystallogr. C *69*, 127–137. https://doi.org/10.1107/S0108270113000322.

45. Lehn, J.-M. (2013). Perspectives in chemistry—steps towards complex matter. Angew. Chem., Int. Ed. Engl. *52*, 2836–2850. https://doi.org/10.1002/anie.201208397.

46. Ustrnul, L., Jarg, T., Jantson, M., Osadchuk, I., Anton, L., and Aav, R. (2024). MatchMass: A web-based tool for efficient mass spectrometry data analysis. Preprint at ChemRxiv. https://doi.org/10.26434/chemrxiv-2024-7j8n7.

47. Ma, X., Yuan, W., Bell, S.E.J., and James, S.L. (2014). Better understanding of mechanochemical reactions: Raman monitoring reveals surprisingly simple 'pseudo-fluid' model for a ball milling reaction. Chem. Commun. *50*, 1585–1587. https://doi.org/10.1039/C3CC47898J.

48. Ortolan, A.O., Madureira, L., Rodríguez-Kessler, P.L., Maturana, R.G., Olea Ulloa, C., Caramori, G.F., Parreira, R.L., and Muñoz-Castro, A. (2023). The nature of the central halide encapsulation in bambusuril hosts (BU [6]). Structural and interaction energy insights in BU[6]·X− (X = Cl, Br, I) from relativistic DFT calculations. Inorg. Chim. Acta. *555*, 121596. https://doi.org/10.1016/j.ica.2023.121596.

49. Öeren, M., Shmatova, E., Tamm, T., and Aav, R. (2014). Computational and ion mobility MS study of (All-S)-Cyclohexylhemicucurbit[6]uril structure and complexes. Phys. Chem. Chem. Phys. *16*, 19198–19205. https://doi.org/10.1039/C4CP02202E.

50. Jašíková, L., Rodrigues, M., Lapešová, J., Lízal, T., Šindelář, V., and Roithová, J. (2019). Bambusurils as a mechanistic tool for probing anion effects. Faraday Discuss *220*, 58–70. https://doi.org/10.1039/C9FD00038K.

51. Sokolov, J., Štefek, A., and Šindelář, V. (2020). Functionalized chiral bambusurils: Synthesis and host-guest interactions with chiral

carboxylates. ChemPlusChem *85*, 1307–1314. https://doi.org/10.1002/cplu.202000261.

52. Itterheimová, P., Bobacka, J., Šindelář, V., and Lubal, P. (2022). Perchlorate solid-contact ion-selective electrode based on dodecabenzylbambus[6]uril. Chemosensors *10*, 115. https://doi.org/10.3390/chemosensors10030115.

53. Rando, C., Vázquez, J., Sokolov, J., Kokan, Z., Nečas, M., and Šindelář, V. (2022). Highly efficient and selective recognition of dicyanoaurate(I) by a bambusuril macrocycle in water. Angew. Chem., Int. Ed. Engl. *61*, e202210184. https://doi.org/10.1002/anie.202210184.

54. Reany, O., Mohite, A., and Keinan, E. (2018). Hetero-bambusurils. Isr. J. Chem. *58*, 449–460. https://doi.org/10.1002/ijch.201700138.

55. Lisbjerg, M., Nielsen, B.E., Milhøj, B.O., Sauer, S.P.A., and Pittelkow, M. (2015). Anion binding by biotin[6]uril in water. Org. Biomol. Chem. *13*, 369–373. https://doi.org/10.1039/C4OB02211D.

56. Andersen, N.N., Eriksen, K., Lisbjerg, M., Ottesen, M.E., Milhøj, B.O., Sauer, S.P.A., and Pittelkow, M. (2019). Entropy/enthalpy compensation in anion binding: Biotin[6]uril and biotin-l-sulfoxide[6]uril reveal strong solvent dependency. J. Org. Chem. *84*, 2577–2584. https://doi.org/10.1021/acs.joc.8b02797.

57. Calderón, R., Palma, P., Arancibia-Miranda, N., Kim, U.-J., Silva-Moreno, E., and Kannan, K. (2022). Occurrence, distribution and dynamics of perchlorate in soil, water, fertilizers, vegetables and fruits and associated human exposure in Chile. Environ. Geochem. Health *44*, 527–535. https://doi.org/10.1007/s10653-020-00680-6.

58. Chen, Y., Zhu, Z., Wu, X., Zhang, D., Tong, J., Lin, Y., Yin, L., Li, X., Zheng, Q., and Lu, S. (2022). A nationwide investigation of perchlorate levels in staple foods from China: Implications for human exposure and risk assessment. J. Hazard Mater. *439*, 129629. https://doi.org/10.1016/j.jhazmat.2022.129629.

59. Tabakci, M. (2008). Immobilization of calix[6] arene bearing carboxylic acid and amide groups on aminopropyl silica gel and its sorption properties for Cr(VI). J. Inclusion Phenom. Macrocycl. Chem. *61*, 53–60. https://doi.org/10.1007/s10847-007-9392-2.

60. Cannon, K.M., Britt, D.T., Smith, T.M., Fritsche, R.F., and Batcheldor, D. (2019). Mars global simulant MGS-1: A rocknest-based open standard for basaltic Martian regolith simulants. Icarus *317*, 470–478. https://doi.org/10.1016/j.icarus.2018.08.019.

61. Shalima, T., Mishra, K.A., Kaabel, S., Ustrnul, L., Bartkova, S., Tõnsuaadu, K., Heinmaa, I., and Aav, R. (2021). Cyclohexanohemicucurbit[8]uril inclusion complexes with heterocycles and selective extraction of sulfur compounds from water. Front. Chem. *9*, 786746. https://doi.org/10.3389/fchem.2021.786746.

Curriculum vitae

Personal data
Name: Tatsiana Jarg (Shalima)
Date of birth: 16.01.1991
Place of birth: Minsk, Belarus
Citizenship: Belarusian

Contact data
E-mail: tatsiana.jarg@taltech.ee

Education
2019 – 2024   Tallinn University of Technology, Chemistry and Biotechnology, PhD
2016 – 2018   Belarusian State Technological University, Chemistry, MSc
2009 – 2014   Belarusian State University, Pharmaceutical Chemistry, Specialist
1998 – 2009   Minsk Gymnasium №11

Language competence
Belarusian   Native
Russian   Native
English   Fluent

Professional employment
2020 – 2024   Tallinn University of Technology, Department of Chemistry and Biotechnology, Early Stage Researcher (0.1 – 0.6)
2017 – 2019   Institute of Bioorganic Chemistry, National Academy of Sciences of Belarus (NASB), Deputy Supervisor of Testing Laboratory (1.0)
2014 – 2017   Institute of Bioorganic Chemistry NASB, Pharmaceutical Chemist (1.0)

Honours and awards
2024   Best research paper in natural, exact and health sciences: Nallaparaju *et al., Angew. Chem. Int. Ed.* 2023, 63, e202319449 (Tallinn University of Technology)
2023   Erasmus+ short-term mobility grant (Tallinn University of Technology)
2022   Dora Plus short-term mobility grant (Archimedes Foundation)
2022   Graduate School of Functional Materials and Technology travel award (Tallinn University of Technology)
2021   Dora Plus. short-term mobility grant (Archimedes Foundation)
2020   Best research paper in natural, exact and health sciences: Dalidovich *et al., ACS Sustain. Chem. Eng.* 2020, 8, 15703–15715 (Tallinn University of Technology)
2020   Dora Plus short-term mobility grant (Archimedes Foundation)

Supervised theses
2023   Ketren-Marlein Lootus, BSc. *Interactions of cyclohexano-hemicucurbit[8]uril with halogenoalkanes and its application for bromoform removal from water*

Elulookirjeldus

Isikuandmed

Nimi: Tatsiana Jarg (Shalima)
Sünniaeg: 16.01.1991
Sünnikoht: Minsk, Valgevene
Kodakondsus: Valgevene

Kontaktandmed

E-post: tatsiana.jarg@taltech.ee

Hariduskäik

2019 – 2024   Tallinna Tehnikaülikool, Keemia ja biotehnoloogia, PhD
2016 – 2018   Valgevene Riiklik Tehnoloogia Ülikool, Keemia, MSc
2009 – 2014   Valgevene Riiklik Ülikool, Farmatseutiline keemia, spetsialist
1998 – 2009   Minski gümnaasium №11

Keelteoskus

Valgevene   emakeel
Vene   emakeel
Inglise   kõrgtase

Teenistuskäik

2020 – 2024   Tallinna Tehnikaülikool, Keemia ja biotehnoloogia Instituut, nooremteadur
               (0.1 – 0.6)
2017 – 2019   Valgevene Teaduste Akadeemia (VTA) Bioorgaanilise keemia Instituut,
               laborijuhataja asetäitja (1.0)
2014 – 2017   VTA Bioorgaanilise keemia Instituut, keemik-farmatseut (1.0)

Teaduspreemiad ja tunnustused

2024   Tallinna Tehnikaülikooli parim teadusartikkel loodus-, täppis- ja
               terviseteaduste valdkonnas: Nallaparaju *et al., Angew. Chem. Int. Ed.*
               2023, 63, e202319449
2023   Erasmus+ lühiajalise õpirände stipendium (Tallinna Tehnikaülikool)
2022   Dora Pluss lühiajalise õpirände stipendium (Sihtasutus Archimedes)
2022   Funktsionaalsete materjalide ja tehnoloogiate doktorikooli stipendium
               (Tallinna Tehnikaülikool)
2021   Dora Pluss lühiajalise õpirände stipendium (Sihtasutus Archimedes)
2020   Tallinna Tehnikaülikooli parim teadusartikkel loodus-, täppis- ja
               terviseteaduste valdkonnas: Dalidovich *et al., ACS Sustain. Chem. Eng.*
               2020, 8, 15703–15715
2020   Dora Pluss lühiajalise õpirände stipendium (Sihtasutus Archimedes)

Juhendatud lõputööd

2023   Ketren-Marlein Lootus, BSc. *Tsükloheksanohemikukurbit[8]uriili
               interaktsioonid halogenoalkaanidega ja selle rakendamine bromoformi
               eraldamiseks veest*